



Helmholtz-Zentrum für Ozeanforschung Kiel

## **RV MARIA S. MERIAN Fahrbericht / Cruise Report MSM71**

**LOBSTER: Ligurian Ocean Bottom Seismology  
and Tectonics Research**

Las Palmas (Spain) – Heraklion (Greece)  
07.02.-27.02.2018



Berichte aus dem GEOMAR  
Helmholtz-Zentrum für Ozeanforschung Kiel

**Nr. 41 (N. Ser.)**

February 2018





Helmholtz-Zentrum für Ozeanforschung Kiel

# **RV MARIA S. MERIAN Fahrtbericht / Cruise Report MSM71**

**LOBSTER: Ligurian Ocean Bottom Seismology  
and Tectonics Research**

Las Palmas (Spain) – Heraklion (Greece)  
07.02.-27.02.2018



Berichte aus dem GEOMAR  
Helmholtz-Zentrum für Ozeanforschung Kiel

**Nr. 41 (N. Ser.)**

February 2018

Das GEOMAR Helmholtz-Zentrum für Ozeanforschung Kiel  
ist Mitglied der Helmholtz-Gemeinschaft  
Deutscher Forschungszentren e.V.

The GEOMAR Helmholtz Centre for Ocean Research Kiel  
is a member of the Helmholtz Association of  
German Research Centres

**Herausgeber / Editors:**

H. Kopp, D. Lange, M. Thorwart, A. Paul, A. Dannowski, F. Petersen, C. Aubert, F. Beek, A. Beniest,  
S. Besançon, A. Brotzer, G. Caielli, W. Crawford, M. Deen, C. Lehmann, K. Marquardt, M. Neckel, L.  
Papanagnou, B. Schramm, P. Schröder, K.-P. Steffen, F. Wolf, Y. Xia

**GEOMAR Report**

ISSN Nr. 2193-8113, DOI 10.3289/GEOMAR\_REP\_NS\_41\_2018

**Helmholtz-Zentrum für Ozeanforschung Kiel / Helmholtz Centre for Ocean Research Kiel**

GEOMAR  
Dienstgebäude Westufer / West Shore Building  
Düsternbrooker Weg 20  
D-24105 Kiel  
Germany

**Helmholtz-Zentrum für Ozeanforschung Kiel / Helmholtz Centre for Ocean Research Kiel**

GEOMAR  
Dienstgebäude Ostufer / East Shore Building  
Wischhofstr. 1-3  
D-24148 Kiel  
Germany

Tel.: +49 431 600-0  
Fax: +49 431 600-2805  
[www.geomar.de](http://www.geomar.de)

# **RV MARIA S. MERIAN**

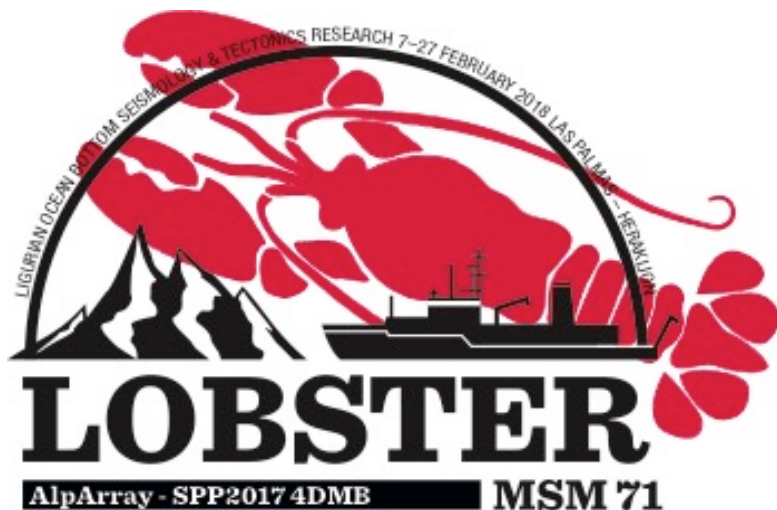
## **Cruise Report**

Las Palmas de Gran Canaria, 07.02.2018 – Heraklion, 27.02.2018

### **MSM 71 - LOBSTER**

### **Ligurian Ocean Bottom Seismology & Tectonics**

### **Research**



Heidrun Kopp, Dietrich Lange, Martin Thorwart, Anne Paul, Anke Dannowski, Florian Petersen,  
Coralie Aubert, Florian Beek, Anouk Beniest, Simon Besançon, Andreas Brotzer, Grazia Caielli,  
Wayne Crawford, Martha Deen, Carsten Lehmann, Kevin Marquardt, Morlin Neckel, Leonie Papanagnou,  
Bettina Schramm, Patrick Schröder, Klaus-Peter Steffen, Felix Wolf, Yueyang Xia

GEOMAR Helmholtz Centre for Ocean Research Kiel

February 2018

**Chief Scientist MSM 71:**

Prof. Dr. habil. Heidrun Kopp

GEOMAR Helmholtz Centre for Ocean Research Kiel

Wischhofstr. 1-3, 24148 Kiel, Germany

P: +49 431 600 2334

F: +49 431 600 2922

[hkopp@geomar.de](mailto:hkopp@geomar.de)

**Co-Chief Scientist MSM 71:**

Dr. Dietrich Lange

GEOMAR Helmholtz Centre for Ocean Research Kiel

Wischhofstr. 1-3, 24148 Kiel, Germany

P: +49 431 600 2334

F: +49 431 600 2922

[dlange@geomar.de](mailto:dlange@geomar.de)

**Master RV MARIA S. MERIAN:**

Ralf Schmidt

RV MARIA S MERIAN

P: +870 764 354 964

F: +870 764 354 966

[master@merian.briese-research.de](mailto:master@merian.briese-research.de)

## Table of Content

1.	Cruise Summary.....	5
1.1	German .....	5
1.2	English .....	5
2.	Participants.....	6
2.1	Principal Investigators .....	6
2.2	Scientific Party .....	6
2.2	Affiliations .....	7
2.3	Crew.....	8
3.	Research Program.....	9
3.1	Motivation.....	9
3.2	Aims of the Cruise.....	14
4.	Narrative of the Cruise.....	18
5.	Preliminary Results .....	22
5.1	Instrumentation .....	22
5.1.1	Seismology.....	22
5.1.2	Refraction and Reflection Seismics .....	24
5.2	The AlpArray Broadband Station Network .....	28
5.2.1	Recovery Operations .....	28
5.2.2	First Results of OBS Deployment June 2017 – February 2018.....	29
5.3	Seismic Refraction and Reflection Lines .....	33
5.3.1	Refraction / Reflection Profile P01 .....	34
5.3.2	Refraction / Reflection Profile P02 .....	37
5.4	Multibeam Bathymetry.....	40
5.4.1	The Kongsberg EM122 and EM710 systems .....	40
5.4.2	Multibeam Bathymetry Data.....	42
6.	Ship's Meterological Station.....	43
7.	Station List MSM 71 .....	43
8.	Data and Sample Storage and Availability .....	43
9.	Acknowledgements .....	44
10.	References.....	44
	Appendices .....	47
	Appendix A: XSV Sound velocity profiles.....	47
	Appendix B: OBS Record Sections (Profiles P01, P02).....	48
	Appendix C: Station Lists Cruise MSM 71.....	71



## 1. Cruise Summary

(H. Kopp)

### 1.1 German

Die Reise MSM 71 des FS MARIA S MERIAN fand vom 07. Februar bis 27. Februar 2018 in der Ligurischen See statt. Ziel der Ausfahrt war die Bergung eines Langzeitnetzwerkes von Ozeanbodenseismometern (OBS), das im Juni 2017 installiert wurde, sowie die Aufzeichnung refraktionsseismischer Daten mittels kurzperiodischer OBS entlang zweier Profile. Das Langzeitnetzwerk bestehend aus 30 Breitbandseismometern ist integraler Teil der europäischen AlpArray-Initiative sowie des DFG-Schwerpunktprogrammes SPP ‚Mountain Building in 4 Dimensions‘ MB 4D (<http://www.spp-mountainbuilding.de/>). Das Netzwerk besteht aus Geräten des DEPAS-Pools sowie der Institute IPGP, GEOMAR und GeoAzur; im Rahmen von MSM 71 sollen 29 der Stationen geborgen werden. Die Geräte liegen mit einem durchschnittlichen Abstand von 25 nm (46km) zum nächsten Gerät (bzw. 28 nm (51 km) zu den benachbarten 3 Geräten) westlich und nördlich der Insel Korsika, wobei die westlichen Geräte am Rande des Golf von Lyon installiert sind und die nördlichsten vor der ligurischen Küste ausgebracht wurden. Das Gebiet liegt sowohl in französischen als auch in italienischen Hoheitsgewässern und überdeckt mit einer Fläche von ca. 85.000 km<sup>2</sup> in etwa die Fläche der norddeutschen Bundesländer. Die refraktionsseismischen Profile mit einer Länge von 147 nm (272 km) und 136 km (73 nm) wurden mit einem 84 1 G-Gun Array überschossen. Hierbei kam ebenfalls ein Mehrkanalstreamer zum Einsatz, der die Sedimentabfolgen unter dem Meeresboden aufzeichnete, die als *a priori* Information in die Analyse der Refraktionsdaten mit einfließen sollen. Die Signale der Luftpulserkanonen sollten dabei ebenfalls von den Stationen des Langzeitnetzwerkes registriert werden, um eine nachträgliche Lokation und Rotation der Stationen mit Hilfe der Schüsse zu ermöglichen. Daher wurde ein zusätzliches Schussprofil in das Netzwerk hinein gefahren. Die Stationen des Langzeitnetzwerkes haben diese Signale über Distanzen von 290 km (157 nm) registriert. Das Hauptprofil mit 35 Ozeanbodenstationen wurde durch Landstationen auf der Insel Korsika verlängert, um so den Küstenübergang abdecken zu können. Zu Beginn der Fahrt zeigte sich, dass die Sender und Blitzer an einigen der Langzeit-OBS nicht zuverlässig arbeiteten, so dass diese Geräte nur tagsüber geborgen werden konnten. Aufgrund sich ändernder Auflagen und Sperrungen bestimmter Seengebiete durch die französische Marine musste der Arbeitsplan entsprechend wiederholt angepasst werden. Zwei Breitband-Stationen (A406A, A408A) sowie ein Ozeanbodenhydrophon (OBH134) konnten nicht geborgen werden. Die Datenqualität der Langzeitstationen sind von herausragender Qualität und die Refraktionsstationen haben auf der Mehrzahl der Geräte die ozeanische Moho aufgezeichnet, so dass anhand dieser Daten zum ersten Mal eine regionale Bestimmung der Krustenmächtigkeit in der Ligurischen See möglich sein wird.

### 1.2 English

RV MARIA S MERIAN cruise MSM 71 sailed in the Ligurian Sea from Feb 07 to Feb 27, 2018 to de-install a network of broadband ocean bottom seismometers (OBS) deployed in June 2017 and to acquire two refraction seismic profiles using short period OBS. The long-term network comprising 30 broadband seismometers forms an integral part of the European AlpArray initiative and the German DFG Priority Programme SPP ‚Mountain Building in 4 Dimensions‘ MB 4D (<http://www.spp-mountainbuilding.de/>). The network consists of stations provided by the DEPAS-

Pool as well as the institutes IPGP, GEOMAR, and GeoAzur. The aim of MSM 71 was to recover 29 of the stations. The instruments are deployed with a mean distance of 25 nm (46km) to the neighboring station (28 nm (51 km) to neighboring three stations) west and north of the island of Corsica. The westernmost instruments are located near the Gulf of Lions and the northernmost instruments were installed off the Ligurian coast. The working area lies in French and Italian territorial waters and covers an area of around 85.000 km<sup>2</sup>, hence almost equaling the area of the northern German states. The refraction seismic profiles with a length of 270 km (147 nm) and 136 km (73 nm) were shot with a 84 l G-gun array. A multi channel seismic streamer was deployed along both profiles to record the upper sedimentary sequences in the subsurface. These data will be used as *a priori* information during refraction data analysis. Shot signals were also recorded by the broadband stations in the network in order to facilitate the exact positioning and orientation of the stations on the sea floor during post-cruise processing. Therefore an additional shot profile into the network was acquired. The stations in the array recorded the shot signals over distances of 290 km (172 nm). The main refraction profile consisting of 35 ocean bottom seismometers and ocean bottom hydrophones was extended by land stations on the island of Corsica in a shoreline crossing mode. At the beginning of the cruise it became clear that the flash lights and radio beacons on a number of broadband stations did not work reliably so that these instruments could only be recovered during daylight hours. Due to military operations of the French navy and the concurrent closure of marine areas we were forced to re-schedule our working plan a number of times. Unfortunately, two broadband stations (A406A, A408A) as well as an ocean bottom hydrophone (OBSH134) could not be recovered. The data quality on the broadband stations is superb and the majority of stations along the refraction profiles recorded the oceanic Moho. These data will for the first time allow the determination of the Moho depth and the reconstruction of the oceanic crust in the Ligurian Sea on a regional basis.

## 2. Participants

(H. Kopp and all Cruise Participants)

### 2.1 Principal Investigators

Name		Institution
Prof. Dr. Heidrun Kopp	Chief Scientist	GEOMAR
Dr. Dietrich Lange	Co-Chief Scientist	GEOMAR

### 2.2 Scientific Party

Name		Institution
Prof. Dr. Anne Paul	Seismology	ISTerre
Dr. Anke Dannowski	OBS/MCS	GEOMAR
Dr. Martin Thorwart	Seismology	CAU
Florian Petersen	OBS/MCS	GEOMAR
Felix Wolf	Seismics	GEOMAR
Yueyang Xia	Seismics	GEOMAR
Kevin Marquardt	Watch Keeper	CAU
Andreas Brotzer	Watch Keeper	KIT

---

Carsten Lehmann	Seismics	GEOMAR
Morlin Neckel	Watch Keeper	CAU
Leonie Papanagnou	Watch keeper	CAU
Bettina Schramm	Seismics	GEOMAR
Coralie Aubert	OBS	ISTerre
Simon Besançon	OBS	IPGP
Dr. Martha Deen	Seismics	IPGP
Dr. Anouk Beniest	Seismics	UPMC
Klaus-Peter Steffen	Air guns	GEOMAR
Florian Beek	Air guns	GEOMAR
Patrick Schröder	Air guns	GEOMAR

---

## 2.2 Affiliations

**GEOMAR**

**Helmholtz-Zentrum für Ozeanforschung Kiel**  
Wischhofstr .1-3  
24148 Kiel, Germany  
[www.geomar.de](http://www.geomar.de)

**CAU**

**Christian-Albrechts-Universität zu Kiel**  
Christian-Albrechts-Platz 4  
24188 Kiel, Germany  
[www.uni-kiel.de](http://www.uni-kiel.de)

**ISTerre**

**Institut des Sciences de la Terre**  
Université Grenoble Alpes  
CS 40700  
38058 GRENOBLE Cedex 9, France

**IPGP**

**Institut de Physique du Globe de Paris**  
Laboratoire de Géosciences Marines  
4 Place Jussieu  
75252 Paris Cedex 5

**KIT**

**Karlsruher Institut für Technologie**  
Geophysikalisches Institut (GPI)  
Hertzstrasse 16  
76187 Karlsruhe, Germany

Cruise MSM 71 was conducted in the framework of the European initiative AlpArray  
[www.alparray.ethz.ch](http://www.alparray.ethz.ch)

and the DFG Priority Program ‘Mountain Building in 4 Dimensions’ MB 4D  
<http://www.spp-mountainbuilding.de>



Figure 2.1: Group photo of the MSM 71 scientific party.

### 2.3 Crew

Name	
Ralf Schmidt	Master
Björn Maaß	Chiefmate
Sören Janssen	2. Mate
Sandra Schilling	2. Mate
Dr. Gabriele Wolters	Surgeon
Benjamin Rogers	Chief Engineer
Phillip Schwieger	2 <sup>nd</sup> Engineer
Stefanie Liedtke	2 <sup>nd</sup> Engineer
Thomas Beyer	Chief Electrician
Emmerich Reize	System Operator
Jörg Walter	Electro Eng.
Olaf Wiechert	Fitter
Jürgen Sauer	Motorman
Norbert Bosselmann	Bosun
Enno Vredenborg	Ship Mechanic
Andreas Wolff	Ship Mechanic.
Detlef Altmann	Ship Mechanic
Sebastian Plink	Ship Mechanic
Olaf Bischeck	Ship Mechanic
Andre Werner	Ship Mechanic
Tobias Siefken	Ship Mechanic
Sebastian Matter	Chief Cook
Mario Becker	Cook' Assist.
Iris Seidel	Chief Steward

### 3. Research Program

(H. Kopp and all Cruise Participants)

#### 3.1 Motivation

A significant proportion of Europeans inhabit the greater Alpine area and their lives are directly impacted by the Alpine topography and its potential geohazards, including mass wasting events, the retreat of glaciers (which pose a hazard to income from tourism) and changing landscapes. Despite the central location of the Alps within Europe and their national and cultural relevance to a number of European countries, we still do not understand basic principles of mountain building. Cruise MSM 71 LOBSTER is motivated by the unresolved tectonic-geologic issues pertaining to the Alpine orogeny in particular and mountain building over time in general by challenging conventional wisdom that the formation of mountain belts is primarily driven by shallow processes. The cruise forms an integral part of two interdisciplinary projects (AlpArray, SPP MB 4D) that test the hypothesis that re-organizations of Earth's mantle during the collision of tectonic plates have both immediate and long-lasting effects on crustal motion, fault kinematics, earthquake distribution and surface evolution (<http://www.spp-mountainbuilding.de/>). The geodynamic setting of the Ligurian Basin is unique owing to its position at the transition from the western Alpine orogen to the Apennine system (Fig. 3.1). The region is characterized by a change in subduction polarity (e.g. Jolivet and Faccenna, 2000; Handy et al., 2010) between the two orogens.

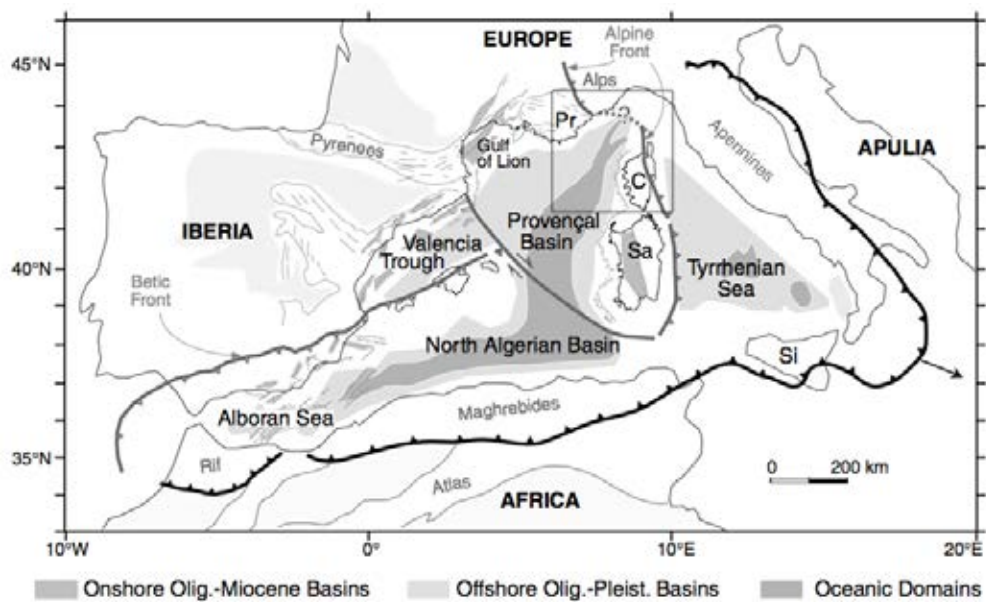


Figure 3.1: Tectonic sketch from Rollet et al. (2002) displaying the major tectonic domains. The proposed study area in the Ligurian Sea is marked by the square. Dashed line indicates poorly known prolongation of the Alpine front offshore.

The kinematic boundaries around the Ligurian Basin are poorly resolved, in particular the transition from the oceanic domain to the continental domain at its north-northeastern termination, where the nature of the offshore prolongation of the Alpine front remains unknown (Rollet et al., 2002; Nocquet, 2012) (Fig. 3.1). Specifically, in the Alps-Apennines transition zone, geophysical imaging of the deep structure is clearly insufficient in the sense that based on existing data it remains unclear if the change in subduction polarity between the two orogens (Fig. 3.2) is a lateral one that existed since at least 50 Ma ago (e.g. Faccenna et al., 2001; Vignaroli et al., 2008).

Alternatively, there could be a temporal change related to a more recent (post-35 Ma) reversal of subduction polarity entirely triggered by slab retreat, which also caused the opening of the Ligurian Basin (e.g. Handy et al., 2010) and is thus intricately related to the basin structure (Fig. 3.3).

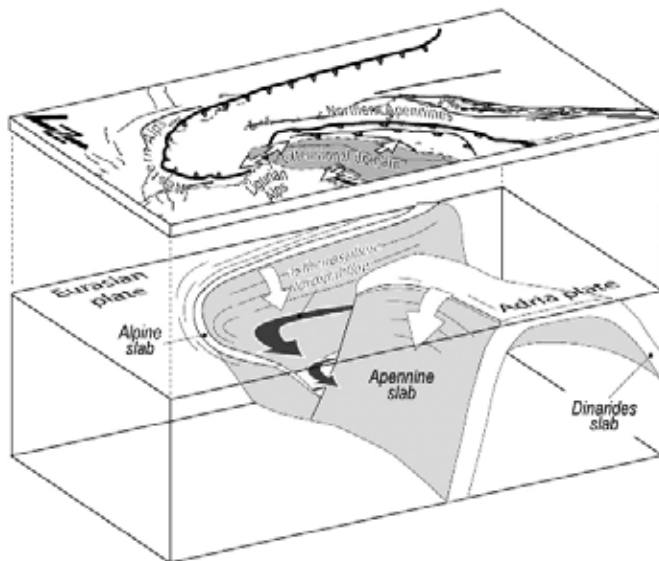


Figure 3.2: 3D block diagram depicting the subduction geometry below the Alps-Apennines system characterized by a reversal of subduction polarity (from Vignaroli et al., 2008).

Improved seismic imaging of the deep crustal and lithospheric structure of the junction between the Alpine and the Apennine system in the Ligurian Basin is hence mandatory to address these open issues on regional kinematics, strain distribution and surface response. This was the catalyst for AlpArray, a European-wide initiative aiming to foster our knowledge on the orogenesis in relation to deep geodynamic processes in the Alps- Apennines-Carpathians-Dinarides system.

The Ligurian Sea is located north of the island of Corsica and the Tyrrhenian Sea and east of the Gulf of Lions. The junction from the Alpine orogen to the Apennines has been termed the 'Ligurian Knot' (Laubscher, 1992) because of its complex geodynamic setting manifested in pronounced variations in crustal nature and thickness and in subducting lithospheric slabs of opposite dip. The geodynamic regime of the region is dominated by the African-European convergence and by subduction rollback below the Apennines (Jolivet and Faccenna, 2000) advancing to the NE. The Ligurian Basin is a back-arc basin generated by the southeastward trench retreat of the Apennines-Calabria-Maghrebides subduction zone (e.g. Rollet et al., 2002), which also triggered the opening of the adjacent western Mediterranean basins (e.g. Doglioni et al., 1997). The opening of the basin occurred from late Oligocene to Miocene times during the initial stage of subduction roll-back (Rehault et al., 1984). Back-arc extension led to continental thinning and subsidence and eventually to the formation of oceanic domains. For the Ligurian Sea, crustal thinning has been proposed to be as large as ~18 km (Chamot-Rooke et al., 1999), but local refraction studies to confirm crustal thickness in the central Ligurian Basin were not available prior to LOBSTER. Topographic gradients in the area are the largest for the entire Alpine-Mediterranean domain, rising from -2500 m in the Ligurian basin to >3000 m in the Alpine-Apennine orogen over a distance of less than 100 km.

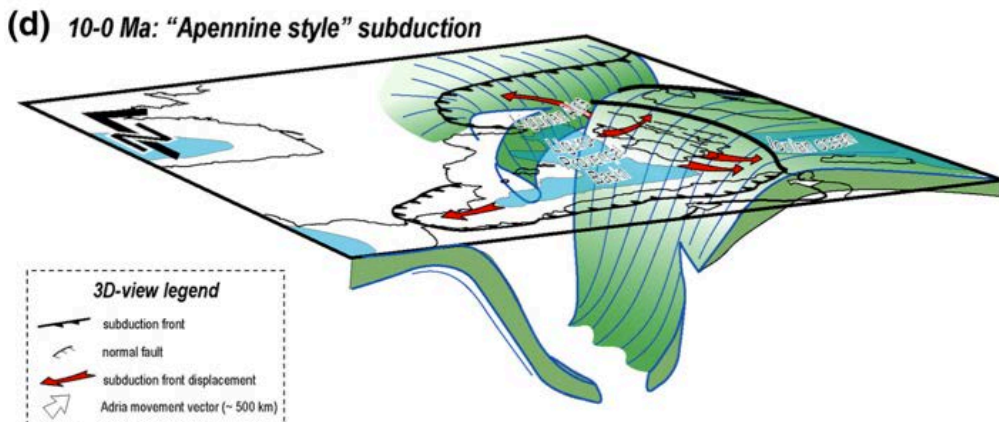


Figure 3.3: 3D view of current Apennine style subduction. Slab polarity reversal is proposed by a number of authors (see text) to occur at the transition from the Alps to the Apennines, but details regarding the kinematic evolution of slab reversal remain enigmatic due to a lack of geophysical imaging in the area (from Vignaroli et al., 2008).

The distinct onshore/offshore transitions of the Ligurian Basin with their steep topographic slopes correspond to strong heterogeneities at depth at crustal and lithospheric scales (Béthoux et al., 2008) (Fig. 3.4). Crustal structures of the continental slope at the northern Ligurian margin along the French Riviera coastline have been analyzed by Sage et al. (2011) who studied the influence of a compressive regime on the evolution of a passive margin. The North-Ligurian margin was also the target of the GROSMARIN project, where 21 OBS were deployed offshore the French Riviera in 2009 (Dessa et al., 2011). The Moho deepens from ~12.5 km underneath the basin to more than 50 km underneath the Alps (Waldhauser et al., 1998; Thouvenot et al., 2007) and a large-scale high of the asthenosphere, reaching a depth of 70 km in the southern central Ligurian Sea dominates the deeper structure (Solarino et al., 1996).

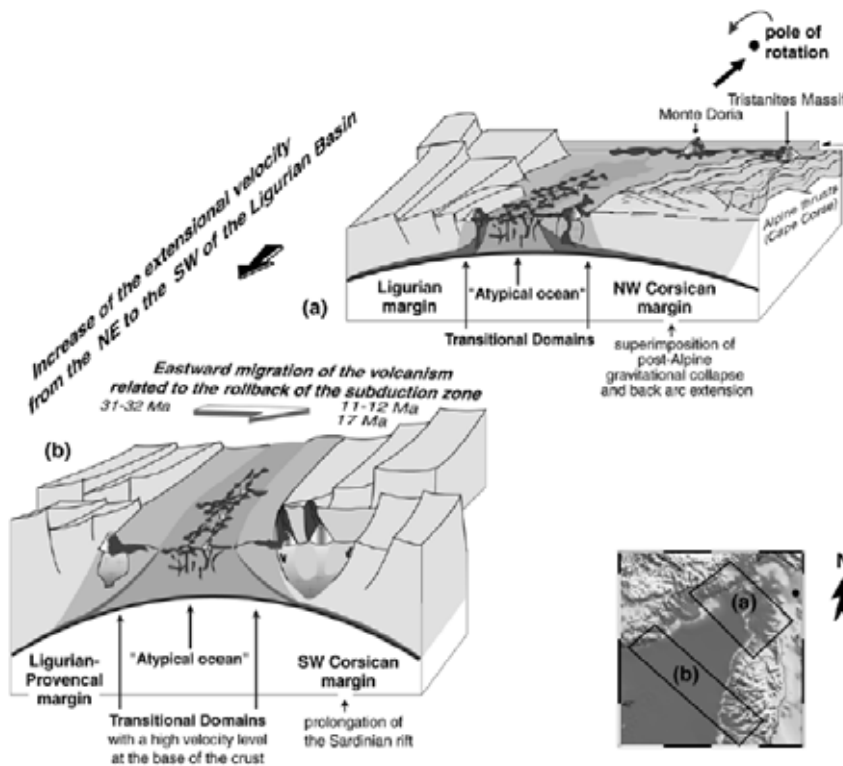


Figure 3.4:  
Structural overview of the  
Ligurian seafloor based on  
multichannel seismic profiling.  
Deeper structures and crustal  
thickness are not resolved (from  
Rollet et al., 2002).

However, the precise Moho geometry and deeper structure of the basin as well as the transition from oceanic to continental domains are still poorly established due to a lack of modern refraction and seismology data resolving the structure at crustal and lithospheric scales. Different geological domains have been identified from the dense coverage of the basin with multichannel reflection seismic data (Fig. 3.4): continental thinned crust offshore the French Riviera and Corsica is found bordering a ‘transitional domain’, which forms the rim around a narrow region of atypical oceanic crust (e.g. Contrucci et al., 2001; Rollet et al., 2002; Larroque et al., 2009).

The nature of this ‘atypical’ (unusually thin?) oceanic crust is poorly constrained due to a lack of deep drilling data as well as deep-penetration refraction data. The deeper (lithospheric) structure and variations in Moho depth as well as the architecture of the northern part of the basin, where the above mentioned transition from oceanic to continental crust and the junction from the Alpine to the Apennine system must exist, are still a matter of debate. Magnetic anomalies are ambiguous and too complex and discontinuous to correlate with isochrons (e.g. Burrus, 1984). An overview of magnetic anomalies determined by reduction to the pole is shown in Figure 3.5. Magnetic anomalies are distributed in distinct areas correlating to magmatic fields resulting from the space-time migration of volcanism during rifting (Rollet et al., 2002).

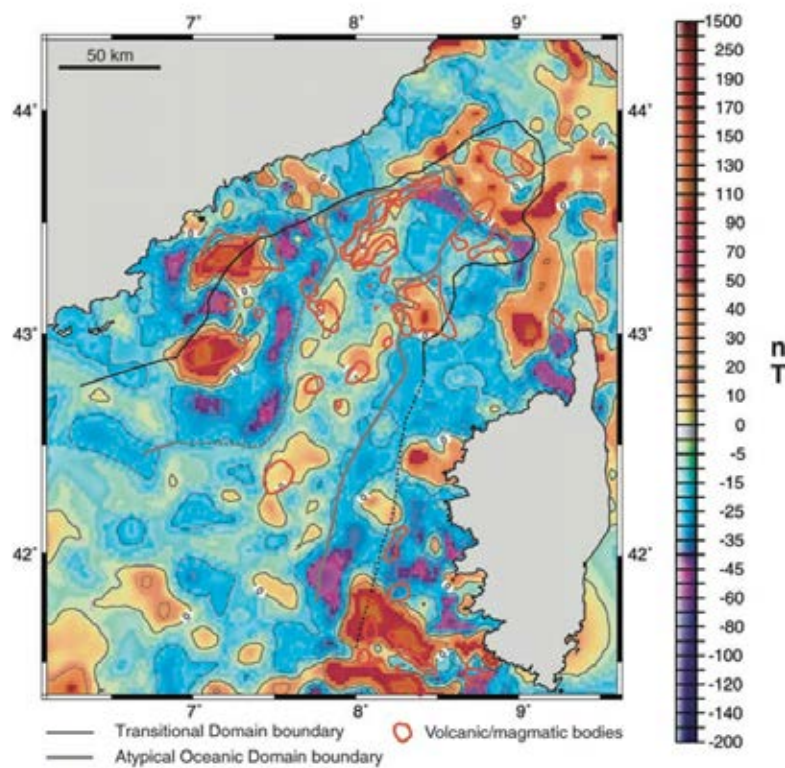


Figure 3.5:  
Magnetic anomalies in the Ligurian Sea  
and adjacent regions overlain by volcanic  
and magmatic bodies determined from  
seismic data (red contours) (from Rollet  
et al., 2002).

Refraction seismic lines in the Ligurian Sea include coverage with 10 OBS of the European Geotraverse, which runs N-S from the Gulf of Genoa to Corsica approximately along 9°E (Ginzburg et al., 1986). This section is part of the southern segment of the Geotraverse (EGT-S) described by Morelli and Nicolich (1990). Velocity-depth models along the EGT in the Ligurian Sea are shown in Morelli and Nicolich (1990; their Fig. 4) and Ginzburg et al. (1986; their Fig. 8) and are of limited resolution compared to modern lines.

A shoreline crossing refraction profile was analyzed by Makris et al. (1999) using 25 OBS and 45 explosive shots. A data example and the resulting velocity model are provided in Figure 3.6.

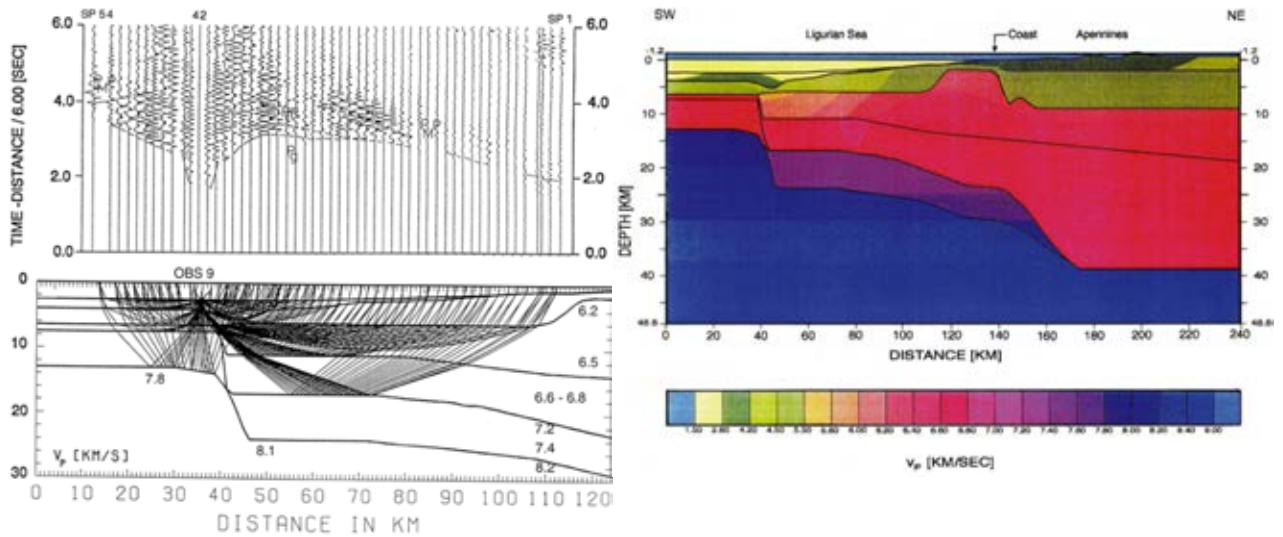


Figure 3.6: Data example from Makris et al. (1999) displaying an OBS record section and modeled ray paths across the ocean-continent transition in the northern Ligurian Sea (left panel). The right section shows the velocity-depth model obtained from 45 shots recorded by 25 OBS.

This profile covers the northern Ligurian Basin trending SE-NW where it crosses the ocean-continent transition (Fig. 3.7). The change from oceanic-type crust to continental crust is marked by a sudden deepening of the Moho by app. 10 km (Fig. 3.6). More recently, a refraction seismic profile was acquired in the Gulf of Lions trending towards Sardinia (Fig. 3.7), covered by 41 ocean bottom stations (Gailler et al., 2009). The SARDINIA profile imaged the crustal structure to a depth of up to 25 km. The gap in the Ligurian Basin between these two profiles was the target of our refraction experiment.

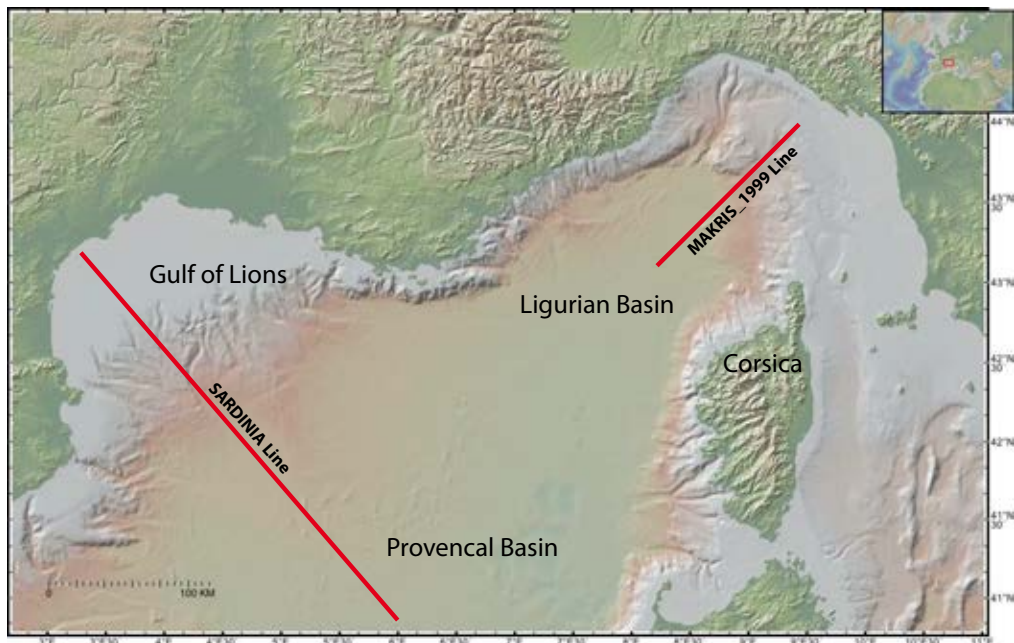


Figure 3.7: Location map of refraction profile presented by Makris et al. (1999) (Fig. 3.6) and refraction line acquired during the SARDINIA experiment (Gailler et al., 2009) trending from the Gulf of Lions towards Sardinia.

### 3.2 Aims of the Cruise

Under the AlpArray framework, 280+ temporary broadband seismometers complement the 400+ permanent stations located within 250 km of the Alps at a spacing of ~40 km throughout the greater Alpine region (Hetényi et al., 2018) (Fig. 3.8). To cover the Ligurian Sea, an additional 30 broadband OBS were deployed at 22 nm spacing on average in June 2017 using the RV POURQUOI PAS? In Germany, AlpArray is complemented by the DFG priority programme ‘Mountain Building Processes in Four Dimensions’ (MB-4D SPP2017).

**Cruise MSM 71 LOBSTER focuses on the following specific aims related to the unresolved tectonic-geologic issues discussed above:**

- The subduction polarity change occurring at the transition from the Alps to the Apennines ('Ligurian Knot') poses a central theme in the greater Alpine orogeny. However, the causes and evolution of polarity flip remain enigmatic due to a lack of high-resolution data. Understanding the deep 3D geometry of this complex lithospheric system requires imaging with a high-end seismic array covering the onshore as well as offshore domain at high density. The offshore deployment of broadband OBS was shared by Germany and France with regards to instrumentation (Crawford et al., 2017) and ship time (June 2017 cruise of RV POURQUOI PAS? for deployment and Feb 2018 cruise of RV MARIA S MERIAN for recovery). IPGP in France contributed seven broadband OBS (Crawford et al., 2012) dedicated to LOBSTER and GEOMAR in Germany secured 22 broadband OBS (partially from the DEPAS instrument pool at AWI in Bremerhaven). The station spacing onshore as well as in the Ligurian Sea as displayed in Figure 3.8 is sufficient to realize an array with the required aperture and resolution for the multiple seismologic methodologies to address the main scientific questions of Alpine orogeny outlined.

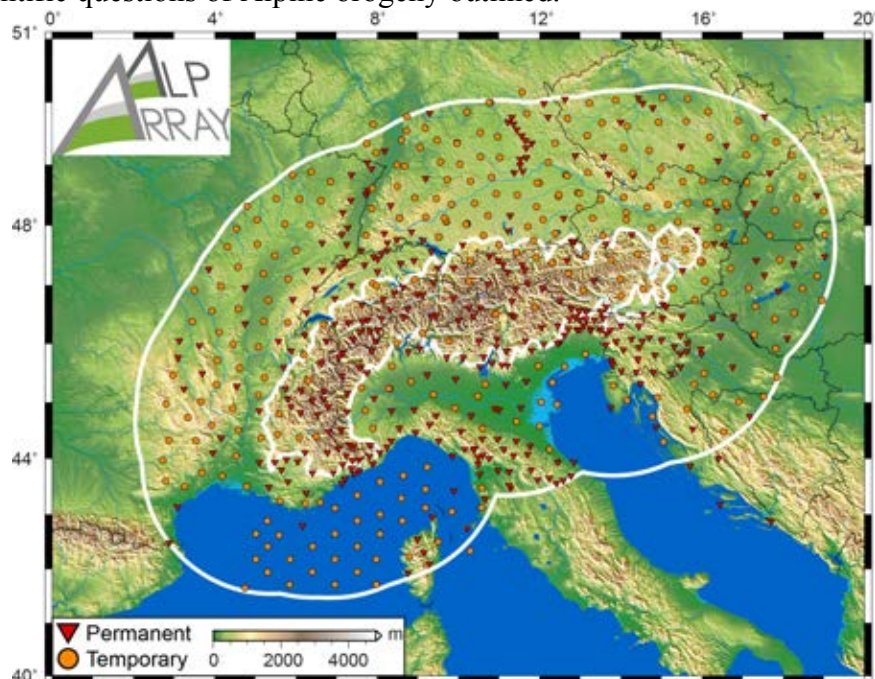


Figure 3.8: Map of the station distribution achieved in the framework of AlpArray (as of February 2018).  
From: <http://www.alparray.ethz.ch/en/home/>.

- The transition from the oceanic domain to the continental domain in the Ligurian Sea remains poorly resolved (Makris et al., 1999). This transition zone represents the continuation of the Alpine front and is hence crucial to the understanding of regional tectonics (Fig. 3.9). While the Ligurian margin offshore the French Riviera has been studied intensely, the basin center and its continuation into the neighboring Gulf of Lions/Provencal basin are not well resolved by previous studies. The refraction seismic line of Makris et al. (1999) shows clear indications for the ocean-continent transition, however, the crustal structure further to the southwest remains unknown. This northeastern part of the Ligurian Basin is situated at the transition from the Alpine orogen to the Apennines and resolving its inner structure at lithospheric scales by passive seismology and refraction seismics as conducted for LOBSTER is essential to understanding local to regional kinematics. In addition, the refraction seismic lines acquired during LOBSTER will provide missing information on the structure and nature of the ‘oceanic-type’ crust found in the basin center, which is yet enigmatic due to a lack of modern refraction data. Our seismic refraction profile extends the Makris Line to the SW. This information will offer important insight into the formation of back-arc basins found in the Mediterranean and globally. Back-arc basin formation is an important geodynamic process observed at locations around the globe and is intricately linked to fundamental plate tectonic processes, so that findings from the Ligurian Basin will likely be applicable to a number of back-arc basins in different domains.

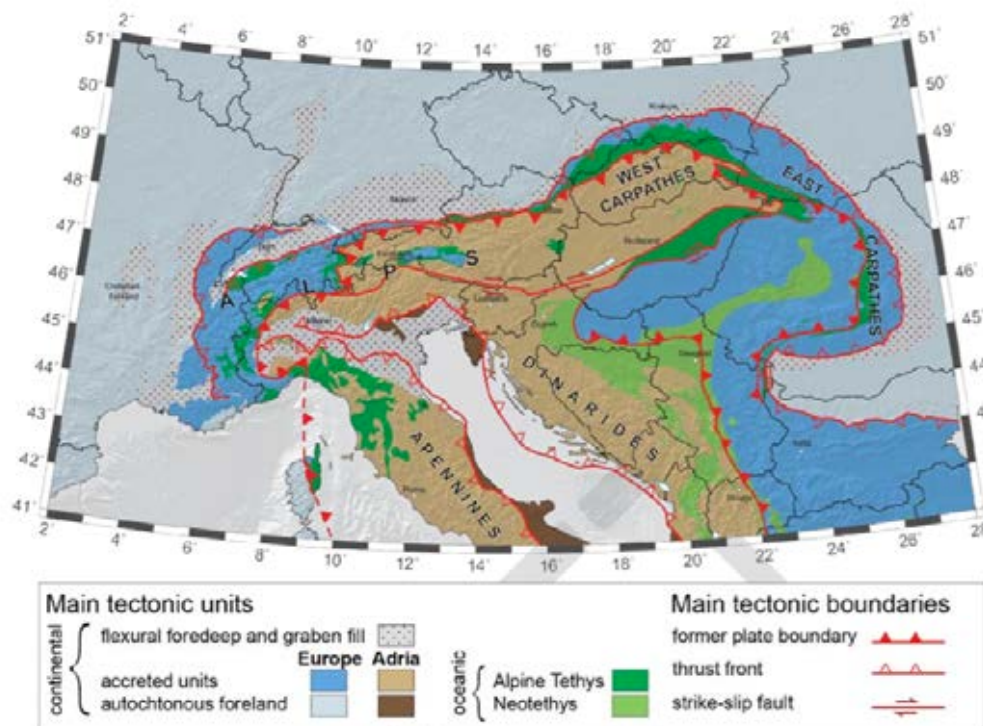


Figure 3.9: Tectonic map of the greater Alpine region. The very major units are coloured according to their overall provenance. Red colours mark the main tectonic boundaries that outline the complex geometry and geological history of the Alps, including the N-S trending continuation of the Alpine front into the Ligurian Sea which is marked by the ocean-continent transition and is poorly resolved to date (stippled line) (from AlpArray Science Plan, 2013).

- Despite negligible present-day horizontal shortening, the Western Alps and their junction with the Mediterranean Sea are among the most seismically active areas in Western Europe. Recent deformation in the Ligurian Sea results from compression along its northern margin (0.3 - 1.5

mm/year shortening) (Larroque et al., 2009; Nocquet, 2012), but no significant convergence is evident from GPS data, and rates of deformation are very low. In the offshore domain of the Ligurian Basin, seismic activity is at a modest level, however, larger than would be expected by comparison with the surrounding regions, which predominantly show microseismic activity (Eva et al., 2001, Courboulex et al., 2007). Destructive earthquakes are known to have occurred in the region in historical times (Boschi et al., 1995) and future events can be disastrous because the coastlines are densely populated and characterized by large site effects (Larroque et al., 2001; Courboulex et al., 2007). Furthermore, the steep topography from the 2500 m deep basin to the adjacent Alpine and Apennine mountain belts is prone to tsunamigenesis. Hence, the historical Ligurian earthquake/tsunami (Imperia earthquake of February 23, 1887; Mw 6.5 (Ferrari, 1991)) and the recent Ajaccio earthquakes (July 7, 2011 and March 24, 2012; Mw 5.1 and 4.4, respectively) attest to an active deformation zone, able to produce significant and potentially destructive earthquakes. Events of magnitude 4-4.5 occur on a regular basis with an approximate period of 2-3 years (Fig. 3.10) (Béthoux et al., 2008). Most seismic activity is focused along the basin's northern rim (Fig. 3.11), however, the Ajaccio earthquakes of 2011 and 2012 are a reminder that also the southern margin and Corsica are capable of producing significant seismic activity.

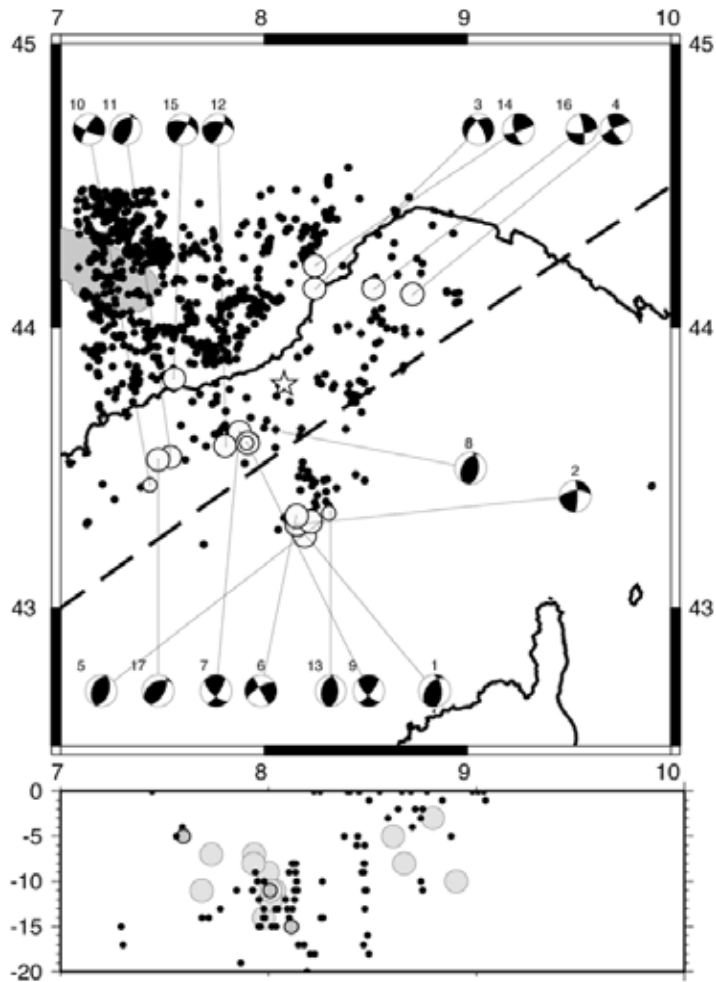


Figure 3.10:  
Relocated seismicity and selected focal mechanisms for the Ligurian Sea (from Béthoux et al., 2008). Dashed line indicates location of cross section shown in lower part of the figure, where hypocenters in a 25 km wide stripe have been projected orthogonally onto the section.

Focal depth of most seismic events concentrate between 2-20 km (Eva et al., 2001; Courboulex et al., 2007) and most events are likely focused along transform faults perpendicular to the spreading axis, as their focal mechanisms (Fig. 3.10) indicate reverse or transpressive faulting (Béthoux et al., 2008). However, a link between deeper tectonic structures and surface deformation could not be established yet due to a lack of long-term local seismicity recordings. The major structures, which can generate a strong earthquake, are yet unknown in the offshore domain.

However, offshore recordings of the seismic activity are necessary in order to establish a link between deeper tectonic structures and surface deformation. The major structures, which can generate a strong earthquake, are yet unknown in the offshore domain. The installation of the AlpArray ocean bottom seismometers addresses this major lack of structural insight and will improve the threshold of detection at the scale of the Western Alps and their forelands including the highly populated Mediterranean border, which is a prerequisite to improve hazard assessment for the entire region. Additionally, far-field recordings by the OBS aim to yield an image of the deep lithosphere-asthenosphere system in the Ligurian basin and aims to furthermore provide information on the elastic properties. In particular, the offshore data in combination with the onshore seismology data will be integral to define the subsurface structures at the transition from the Western Alps to the Apennines to improve our understanding of the 3D-geometry of the system and its kinematics.

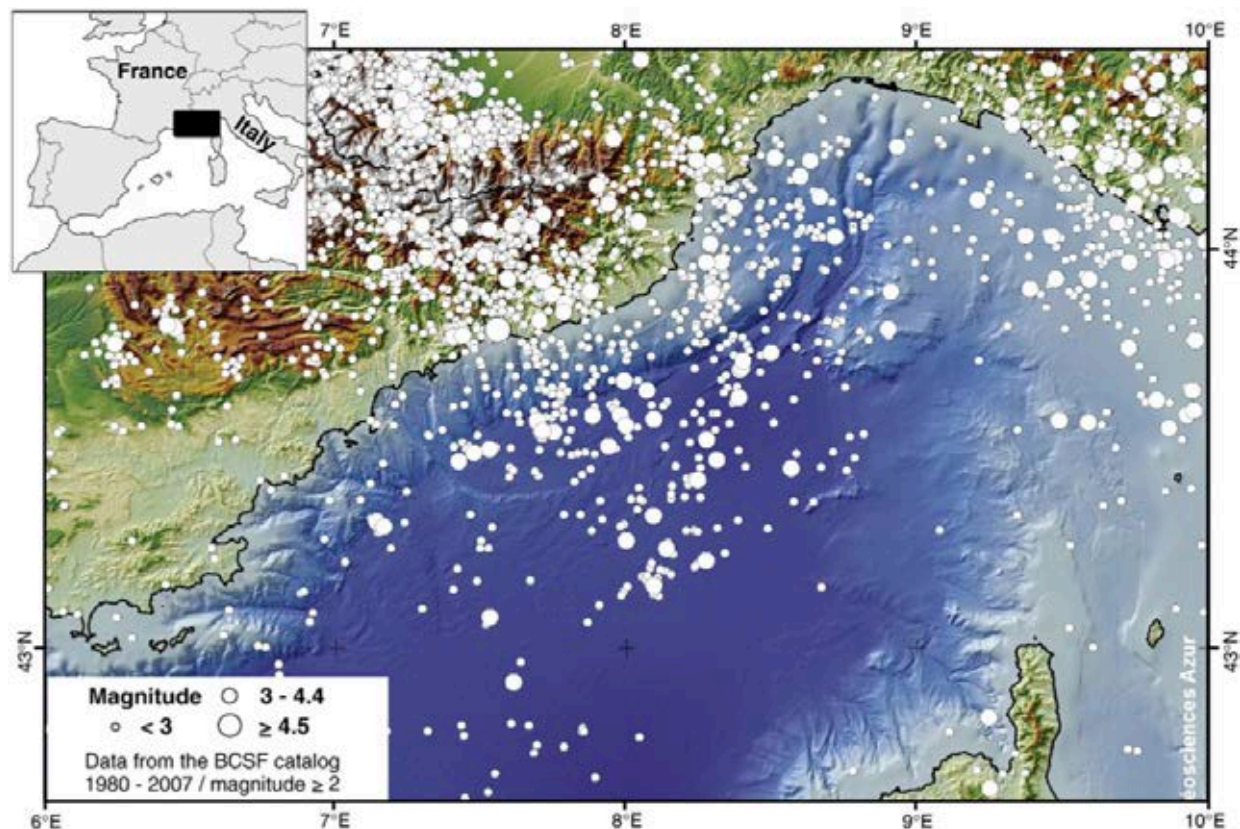


Figure 3.11: Distribution of recent seismicity (magnitude down to 2) of the Alps-Ligurian basin junction recorded from 1980-2007 (B.C.S.F. catalog) (from Larroque et al., 2009).

**The scientific goals outlined above will be met based on the data acquired during cruise MSM 71 LOBSTER in the scope of the AlpArray initiative.**

In the original working plan of the cruise from 2014 it was foreseen that the LOBSTER cruise would install the AlpArray offshore network while a French vessel would recover the stations. Due to a major re-scheduling of the AlpArray initiative the work programs were swapped, i.e. the French RV POURQUOI PAS? installed the network while recovery was conducted from RV MARIA S MERIAN. As a French cruise will target the northern Ligurian Basin in Nov. 2018 (J. X. Dessa, pers. communication), we focused our refraction work on the central part of the basin, acquiring two refraction lines instead of the originally proposed single profile. The seismic refraction data from profiles P01 and P02 and the earthquake data recorded by the passive seismology network are an integral part to realize the scientific targets, as described in the following:

1. Obtain an image of the present day crustal and lithospheric architecture of the Ligurian Basin. In particular, the geometry of the Moho in the basin is of special interest in relation with the major geodynamic events that shaped it. The onshore-offshore refraction seismic profiles will yield information on crustal and upper mantle structures that may be used as a priori information in the tomographic imaging of the broadband data. In addition, the wide-angle lines provide data on the nature of the atypical oceanic domain in the basin center, which is relevant to the understanding of back-arc basin formation.
2. Within the scope of AlpArray, the offshore broadband seismology study recorded teleseismic waves from distance seismic events to image the lithospheric asthenospheric anatomy of the 'Ligurian Knot' at the transition from the Alpine to the Apennine systems and thus contribute to a high-resolution 3D-image of the subduction polarity change expected here.
3. To date, a 3D model for the seismically active zones in the Ligurian Sea is not available and the locations and properties of active faults are poorly known. A thorough analysis of the local seismicity will enlighten the shallow geology for investigating their influence on seismic hazard and will furthermore improve our understanding of the interaction of inherited fault geometry and kinematics with today's stress field, which is important for refining seismic hazard. Specifically, the recordings of the OBS array will contribute to seismic hazard assessment by evaluating the earthquake sources, the wave propagation characteristics and site response in the Ligurian Sea with a high level of detail.

#### **4. Narrative of the Cruise**

(H. Kopp and all Cruise Participants)

Cruise MSM 71 commenced in Las Palmas de Gran Canaria, Spain, on Feb 7, 2018, where 21 scientists from France, Germany, the Netherlands and China embarked on RV MARIA S MERIAN. The vessel left port at 16:30h local time with some hours delay after a last provisions container was loaded to start on the transit north towards the Strait of Gibraltar. The previous days in port as well as the transit were used to prepare our equipment, in particular to set up the air guns, the streamer and the short period ocean bottom hydrophones and ocean bottom seismometers. After five days of transit we arrived at the first OBS site on Feb 12, 2018 at 09:00h to release the first station of the broadband OBS AlpArray network (OBS A412A), which is positioned at the southwestern extremity of the working area at 41°38,85'N/04°44,69'E (Fig. 4.1).

The instrument had been continuously recording since June 2017. We continued on a short transit north to the NW starting point of the 147 nm long refraction line P01 at 42°33,00'N/05°30,00'E. During this time, weather conditions deteriorated and we could only deploy two short-period stations before wind conditions of up to 11 Bft forced us to wait for calmer conditions. An XSV probe was launched at 42°32,44'N/05°35,33'E, reaching a depth of 1956 m. We re-commenced OBS deployment after a two hour break, when conditions had calmed to around 8 Bft. The deployment of a total of 35 short period stations at 4 nm spacing was completed at 13:45h on Feb 13 at 42°12,00'N/08°30,00'E. Simultaneously, colleagues from IDPA-CNR of Milan installed three land seismometers on the western portion of the island of Corsica to record our air gun shots. Marine mammal mitigation procedures were initiated prior to shooting. Shooting of profile P01 commenced at 15:15h with two G-gun arrays of 84 l total towed on the starboard and portside of RV MARIA S MERIAN. A 280 m long geo-eel streamer was deployed along the profile and recovered after we passed the last seafloor station. The vessel then turned on to a 45 nm long southward profile to shoot into the AlpArray broadband seismometer network. The turn was used for maintenance of both air gun arrays. Shooting was terminated on Feb 15 at 09:00h at 41°54,16'N/05°29,24'E.

This was followed by the recovery of five broadband OBS from the AlpArray network located in the southwestern part of the study area (A421A, A414A, A413A, A404A, A405A; all recovered between 10:45h and 22:20h on Feb 15, 2018). Recovery was continued the next day (A401A, A402A, A406A, A415, A423A, A430, A424A). During recovery, it was noticed that the radio beacon and flash light as well as the flag on the DEPAS and GEOMAR stations did not protrude from the water as the instrument ascended horizontally and due to insufficient weight did not turn into the vertical. Consequently, the radio beacon and flash light could not function and did not send any signals. We thus had to rely on a visual location of the instruments, at night aided by the ice flood lights of RV MARIA S MERIAN. As the weather conditions were optimal and the sea very still during recovery, we could also locate the instruments on the ship's ice radar. Despite our efforts, one station could not be recovered (A406A) as it could not be located on the surface.

French military operations made it necessary to schedule the recovery of stations A416A, A408A, A409A and A417A for Feb 17, as the maritime area where these stations are installed was to be closed to ship traffic afterwards. We thus continued recovery operations in this area. However, station A408A did not respond to the release or range signal and could not be recovered. We next headed towards OBS A418A, which was safely recovered before heading south to start recovery along the refraction profile at 21:30h, Feb 17. Due to scheduling issues we recovered stations along the western part of the profile first, starting with OBS 113 towards OBH 135. OBH 134 responded to our release signal, but due to technical failure could not turn the hook to release the anchor. Recovery along profile P01 was terminated at 17:00h on Feb 18, before we had to leave the area by Feb 19, 07:00h due to military operations. As we could also not access the broadband stations located to the south of profile P01 due to closure of the maritime region, we subsequently headed north and on Feb 19 at 05:00h arrived at station OBS A419A, which was safely recovered. Subsequent stations A411A, A434A and A420A were all located in Italian waters and safely recovered before we headed for station A427A, which was situated in French territory. All stations were safely recovered during daylight hours of Feb 19, 2018. We then continued to deploy a total of 15 sea floor stations (12 OBS and 3 OBH) along the second refraction profile P02, which starts at 43°05.07'N / 08°11.82'E and trends in a NE-SW direction covering

the central part of the Ligurian Basin to the crossing point with profile P01 at  $42^{\circ}21.00'N$  /  $07^{\circ}15.00'E$ . Mammal and turtle mitigation procedures proceeded the deployment of the air gun arrays and the streamer, before shooting commenced at 07:30h on Feb 20, 2018 and lasted until 01:45h on Feb 21, 2018. Prior to recovery of the stations on profile P02 we collected station A425A and A426A located east of profile P02 during the morning of Feb 21, 2018. A second XSV probe was launched at  $42^{\circ}52.80'N/08^{\circ}37.29'E$ . Instrument recovery on P02 was finished at 01:15h on Feb 22, 2018 and we continued with the recovery of the remaining stations on the eastern portion of P01 (OBS112-OBS101), which was achieved by 12h on Feb 22, 2018. The final four stations of the AlpArray network (A429A, A422A, A428A, A313A) were recovered on Feb 22 starting at 16:00h until Feb 23 at 07:15h.

On Feb 23, 2018 at 14:30h RV MARIA S MERIAN commenced the passage through the Strait of Bonifacio to begin our transit towards the port of Heraklion/Crete. During transit, we passed the Strait of Messina on Feb. 24, 2018 and stopped at a seafloor geodesy array (GeoSEA) offshore Catania, Sicily, located at  $37^{\circ}32,39'N/15^{\circ}15,53'E$  to test the newly installed SONARDYNE Ranger system on RV MARIA S MERIAN, as the GeoSEA array uses SONARDYNE acoustic transponders for telemetry measurements on the flank of Mt Etna. During the short stop of RV MARIA S MERIAN we could verify that all stations are up and running, before we commenced our final transit to Heraklion at 05:00h on Feb. 25, 2018.

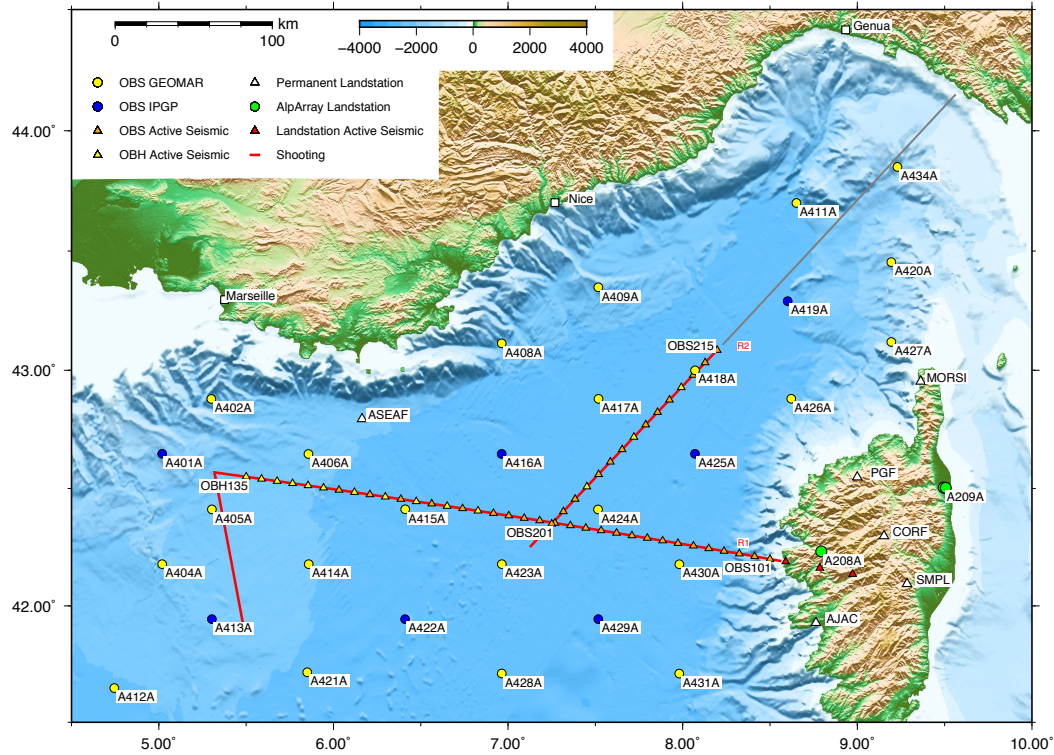


Figure 4.1: Station and profile distribution in the Ligurian Sea. Two refraction/reflection profiles were acquired with 35 and 15 stations, respectively. In addition, shooting along profile P01 was extended to the SE in order for the long-term AlpArray OBS to record the shots. Grey line shows profile by Makris et al. (1999).

RV MARIA S MERIAN safely reached the pilot station at Heraklion harbor on Feb 27 at 08:00h and berthed at 08:30h, terminating cruise MSM 71 (Fig. 4.2). Weather conditions were very variable during the cruise, with stormy phases (11 Bft) and intermittent calm seas.

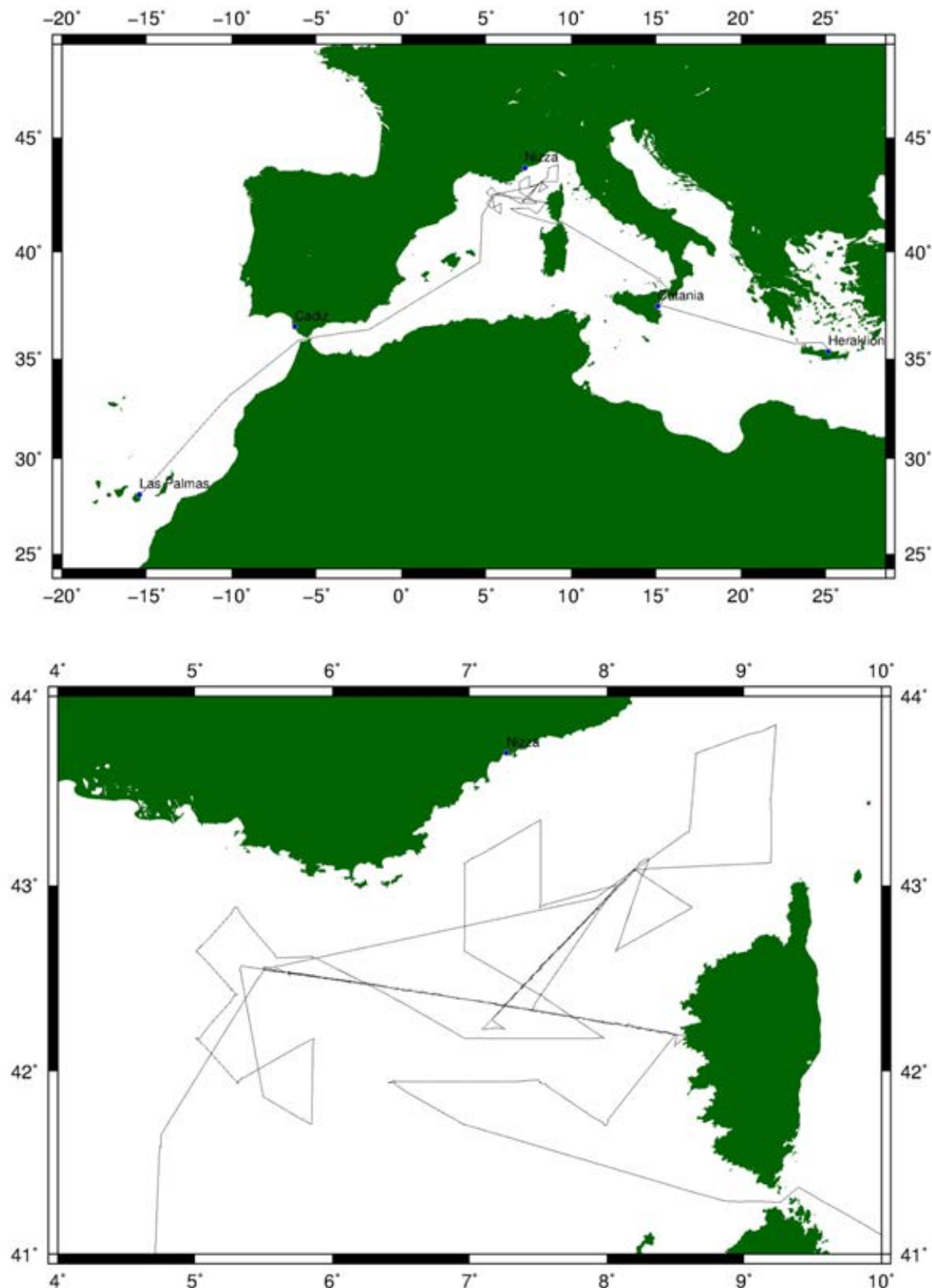


Figure 4.2: Ship track of RV Maria S. Merian cruise MSM 71. Upper panel shows track along route of MSM 71, lower panel shows track in working area in the Ligurian Sea.

## 5. Preliminary Results

(H. Kopp and all Cruise Participants)

### 5.1 Instrumentation

#### 5.1.1 Seismology

##### IPGP BBOBS

The first 3 BBOBS (Broad Band Ocean Bottom Seismometer) were acquired in 2006 from the Scripps Institution of Oceanography for the INSU (Institut National des Sciences de l'Univers - Institute for Earth Sciences and Astronomy), a division of the CNRS (Centre National de la Recherche Scientifique - French National Center for Scientific Research) and 4 more were acquired over the years for a total of 7 instruments.

The BBOBS carry two sensors:

- a DPG (differential pressure gauge) designed by the marine EM Laboratory of the Scripps Institution of Oceanography with a pass band of 500 seconds to 2 Hz
- a Nanometrics Trillium 240 Broadband sensor (T240) with a flat response to velocity from 240 seconds to 35 Hz, on the back of the BBOBS.

The T240 are enclosed in a titanium sphere, with its own leveling system (the T240 requires to be leveled with a precision of 5°) and electronics controlling the human-machine interface, the dropping of the sensor on the seafloor, the leveling sequences (checks if the T240 is leveled at different times) and finally the re-centering of mass within the T240. This sensor sphere rests on a titanium tripod for seafloor coupling. It is attached to the front arm of the BBOBS, and is dropped when ordered (by its deployment sequence) with the help of a burn wire. The sensor sphere is also attached to the bottom of the main frame by a strap for the recovery. The energy is provided to the sensor by the data logger via a cable also sending the data flow (x,y,z) to the data logger.

The units itself (see Fig. 5.1) consists of :

- the buoyancy, made of 8 glass balls from McLane Research Lab enclosed in two yellow plastic frames, attached on top of the BBOBS by a stainless structure
- the main frame in blue
- two anodized aluminum pressure tubes, one containing the data logger and lithium batteries, the second one full of lithium batteries.
- the release system, which is an edgetech acoustic release system in an anodized aluminum pressure tube, and linked to a dropping clamp attached to the weight by two burn wires
- the weight, specifically designed for the IPGP BBOBS consisting of galvanized steel grid
- a flash and radio beacon manufactured by Novatech for recovery.

The data logger and sensor ball are powered by the same pack of lithium batteries, but work independently from each other (the data logger simply records the dataflow coming from the sensor). The edgetech acoustic is powered by an independent alkaline battery, and has two codes for two releases, so providing two chances of dropping the weight (with the two burn wires) and can also be pinged.

The data loggers were programmed with a sampling frequency of 62.5 Hz. The BBOBS were deployed in free-falling mode and relocated once on the bottom using the edgetech acoustic transponder.

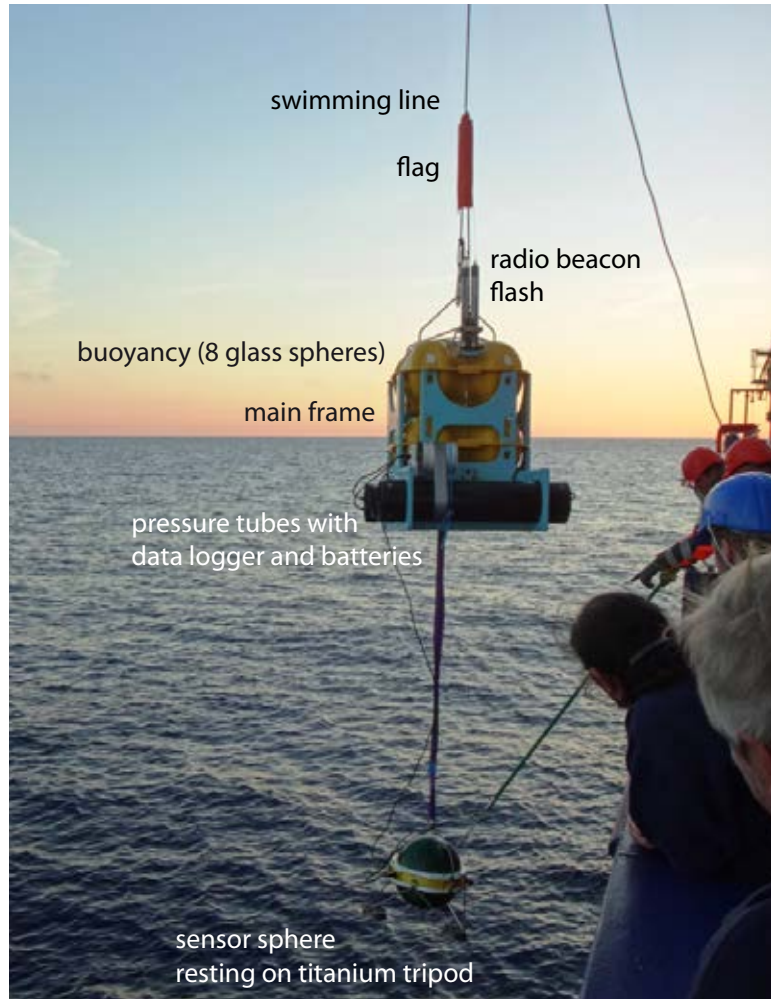


Figure 5.1: IPGP BBOBS upon recovery. The sphere containing the sensors is attached to the main body of the unit and sits on a tripod frame.

### **LOBSTER Broadband OBS**

The Ocean Bottom Seismometer LOBSTER (Long-term Ocean Bottom Seismometer for Tsunami and Earthquake Research) is a design by K.U.M Umwelt- und Meerestechnik Kiel GmbH and is used by the DEPAS (Deutscher Geräte-Pool für amphibische Seismologie / German instrument pool for amphibious seismology) (Alfred-Wegener-Institut Helmholtz-Zentrum für Polar- und Meeresforschung et al., 2017) pool as well as by GEOMAR. The system is constructed to carry a hydrophone and seismometer, but the modular design of the front end allows adaptation to different seismometers and hydrophones or pressure sensors. The sensors are HTI-01-PCA hydrophones from High Tech Inc. and Trillium compact OBS from Nanometrics and K.U.M. The sensitive three-component seismometer is housed in a titanium tube and is located between the anchor and the OBS frame (Fig. 5.2), which allows for optimal coupling with the sea floor. Four OBSs are equipped with CMG-40T seismometer from Guralp.

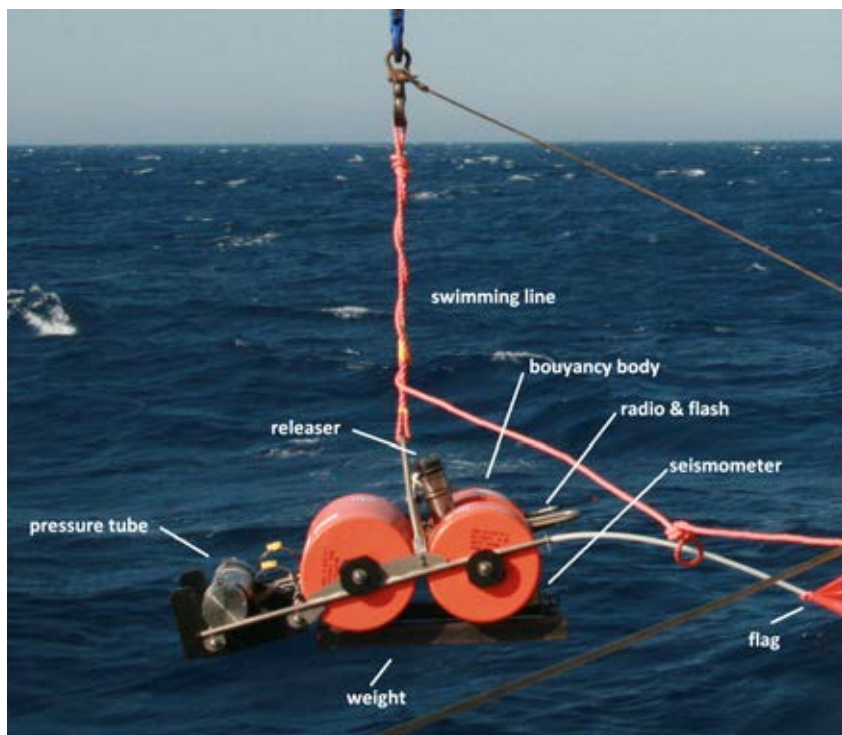


Figure 5.2: Setup of the DEPAS OBS with Trillium seismometer.

The recording device is either a 6D6 recorder of K.U.M or a MCS/MLS recorder of SEND GmbH, which is contained in its own pressure tube and mounted next to the buoyancy. Sampling of the seismic signal is 50 Hz for the MTS/MLS and 250 Hz for the 6D6. As energy source Lithium batteries were used. The release transponder is holding the anchor and drops the weight when an acoustic release command is send. The anchor consists of 60 KG untreated steel. All OBS stations were deployed in the free fall mode. For recovery the OBS is equipped with a flashlight, VHF radio beacon, flag and a swimming line.

### 5.1.2 Refraction and Reflection Seismics

A total of 35 short-period OBS and OBH instruments provided by the GEOMAR pool were available for deployment during cruise MSM71 and are described below.

#### The GEOMAR OBS-2002

The GEOMAR Ocean Bottom Seismometer 2002 (OBS-2002) is a design based on experience gained with the GEOMAR Ocean Bottom Hydrophone (OBH; Flueh and Bialas 1996) and the GEOMAR Ocean Bottom Seismometer (OBS, Bialas and Flueh, 1999). The basic system is constructed to carry a hydrophone and a small seismometer for higher frequency active-seismic profiling. However, due to the modular design of the front end it can be adapted to different seismometers and hydrophones or pressure sensors. The sensors are OAS and *HTI-01-PCA* hydrophones from High Tech Inc. The sensitive seismometer is deployed between the anchor and the OBS frame (Fig. 5.3), which allows for optimal coupling with the sea floor. The three-component seismometer (K.U.M), usually used for active seismic profiling, is housed in a titanium tube, modified from a package built by Tim Owen (Cambridge) earlier. Geophones of 4.5 Hz natural frequency were used during MSM71. The recording devices were GEOLOG loggers

developed at GEOMAR or 6D6 recorders of K.U.M., sampling at 250 Hz. GEOLOG recorders require a reduced power consumption with increased bandwidth for the hydrophone component and an autonomous time signal based on an atomic clock. The unit's floatation is made of syntactic foam and is rated, as are all other components of the system, for a water depth of 6000 m.

While deployed to the seafloor the entire system rests horizontally on the anchor frame. The instrument is attached to the anchor with a release transponder. The release transponder is the *K/MT562* made by K.U.M GmbH. Communication with the instrument for release and range is possible through a transducer hydrophone, which is lowered ~20 m into the water. Over ranges of 4 to 5 miles release and range commands are successful. After releasing its anchor weight of approximately 60 kg the instrument turns 90° into the vertical and ascends to the surface with the floatation on top. This ensures a maximally reduced system height and water current sensibility at the ground (during measurement). On the other hand the sensors are well protected against damage during recovery and the transponder is kept under water, allowing permanent ranging, while the instrument floats to the surface.

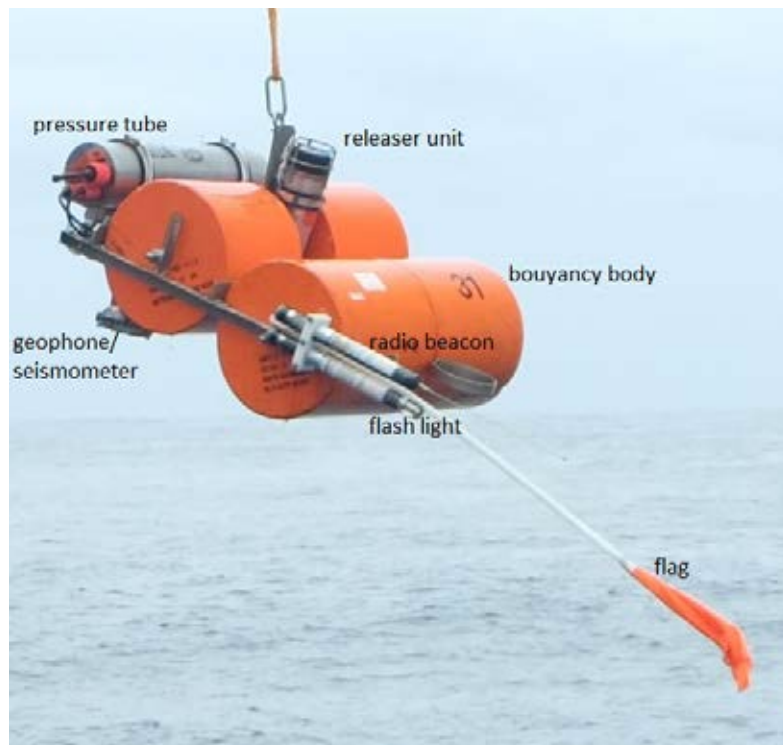


Figure 5.3: GEOMAR OBS (Design 2002).

### The GEOMAR OBH

The first GEOMAR Ocean Bottom Hydrophone was built in 1991 and tested at sea in January 1992. This type of instrument has proved to have a high reliability; there have been more than 6500 successful deployments since 1991.

The principle design and a photograph of the instrument during deployment are shown in Figure 5.4. The design is described in detail by Flueh and Bialas (1996).

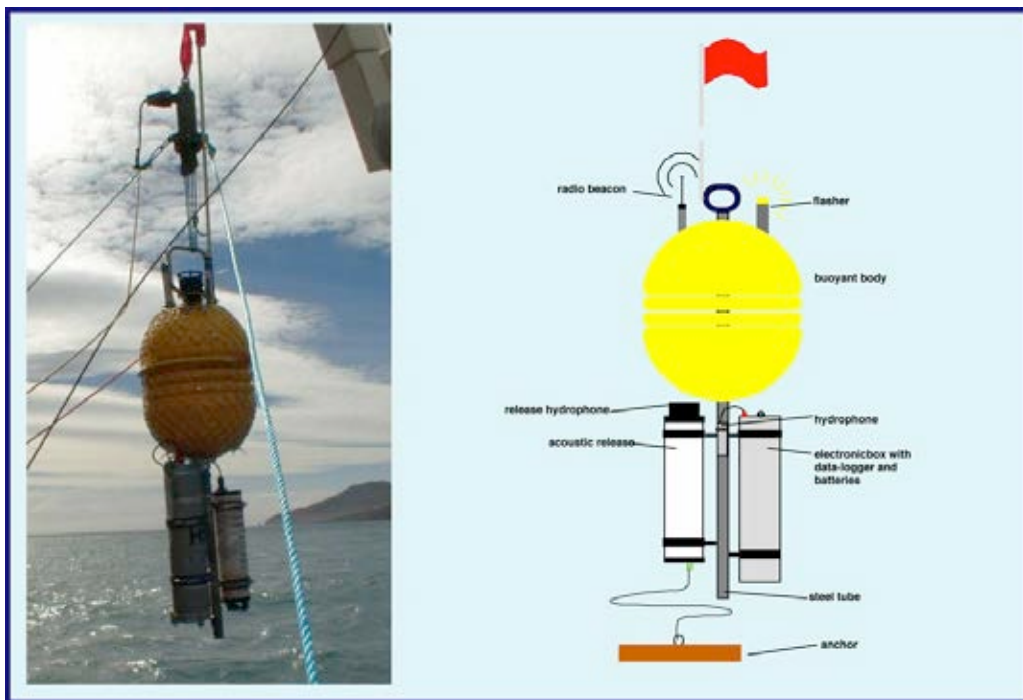


Figure 5.4: Principle design of the GEOMAR OBH (right panel, after Flueh and Bialas, 1996) and the instrument upon deployment (left panel).

The system components are mounted on a steel tube, which holds the buoyancy body on its top. The buoyancy body is made of syntactic foam and is rated, as are all other components of the system, for a water depth of 6000 m. Attached to the buoyant body are a radio beacon, a flash light, a flag and a swimming line for retrieving from aboard the vessel. The hydrophone for the acoustic release is also mounted here. The release transponder is a K/MT562 made by K.U.M GmbH. Communication with the instrument is possible through the ship's transducer system, and ranges of 4 to 5 miles release and range commands are successful. For anchors, we use pieces of railway tracks weighing about 40 kg each. The anchors are suspended 1 to 2 m below the instrument. The sensor is a HTI-01-PCA hydrophone from High Tech Inc, and the recording device is GEOLOG recorder, which is contained in its own pressure tube and mounted below the buoyant body opposite the release transponder (see Fig. 5.4).

### Seismic Streamer

Multichannel seismic data were acquired using a digital streamer of 144 channels with 1.5 m group offset (220 m active length) (Fig. 5.5). The streamer consists of 12.5 m long sections (Geometrics *GeoEel* streamer segments). The 14 sections closest to the vessel are oil-filled, while the remaining four sections are manufactured as solid-state sections. The streamer configuration included a tow cable and a vibro stretch section of 25 m length behind the tow cable to which the active sections are attached behind the stretch zone. The tow cable has a length of 20 m behind the vessel's stern.

Each active section contains 8 channels with a hydrophone group spacing of 1.56 m. One AD digitizer module belongs to each active section. These AD digitizer modules are small Linux computers. Communication between the AD digitizer modules and the recording system in the lab was transmitted via *TCP/IP*. A repeater was located between the deck cable and the tow cable

(Lead-In). The SPSU managed the power supply and communication between the recording system and the AD digitizer modules. Two birds controlled and monitored the desired streamer depth of 5 m. One was attached to the first streamer section and the second bird at the last *GeoEel* streamer segment. On the last solid-state segment a small buoy was attached to the tail swivel of the 2D streamer.

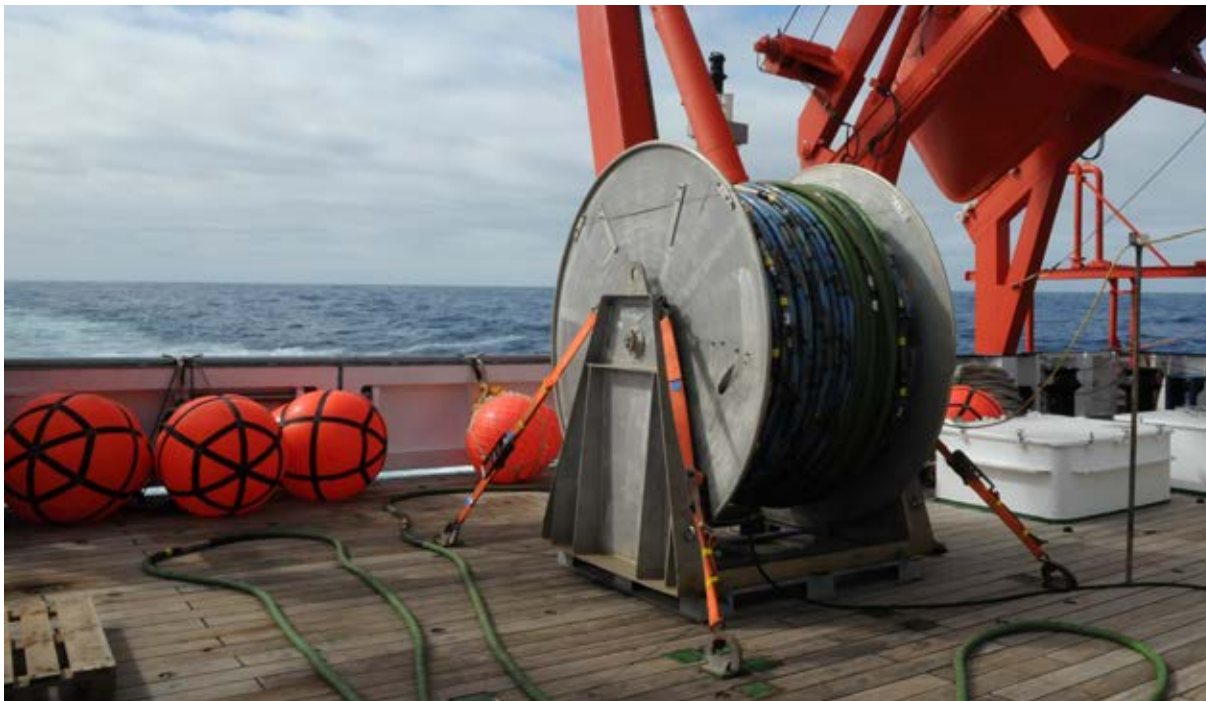


Figure 5.5: Streamer on winch on aft deck of RV Maria S Merian.

### Bird Controller

Two Oyo Geospace Bird Remote Units (RUs) were deployed on the streamer. The RUs have adjustable wings to keep the streamer at the desired depth. A bird controller in the seismic lab controlled the RUs. Controller and RUs communicate via communication coils nested within the streamer. A twisted pair wire within the deck cable connects controller and coils. Designated streamer depth was 5 m in accordance with good weather conditions and low swell noise. The RUs thus forced the streamer to the chosen depth by adjusting the wing angles accordingly. The birds were deployed at the beginning of a survey and worked very reliably and kept the streamer at the designated depth.

### MCS Data Acquisition System

MCS data were recorded with acquisition software provided by Geometrics. The analogue signal was digitized with 2 kHz. The seismic data were recorded as multiplexed SEG-D. Recording length was 8 seconds. One file with all channels within the streamer configuration was generated per shot. The corresponding logged shot file reports shot number and time information contained in the RMC string. The acquisition PC allowed online quality control by displaying shot gathers, a noise window, and the frequency spectrum of each shot. The cycle time of the shots were displayed as well. The vessel's GPS was simultaneously logged in the RMC string along with logged time and position information.

## Seismic Sources

During cruise MSM71 reflection seismic data were acquired simultaneously to wide-angle refraction data acquisition. The source was a 84-liter G-Gun array. Figure 5.6 provides an overview of the system setup during cruise MSM 71.

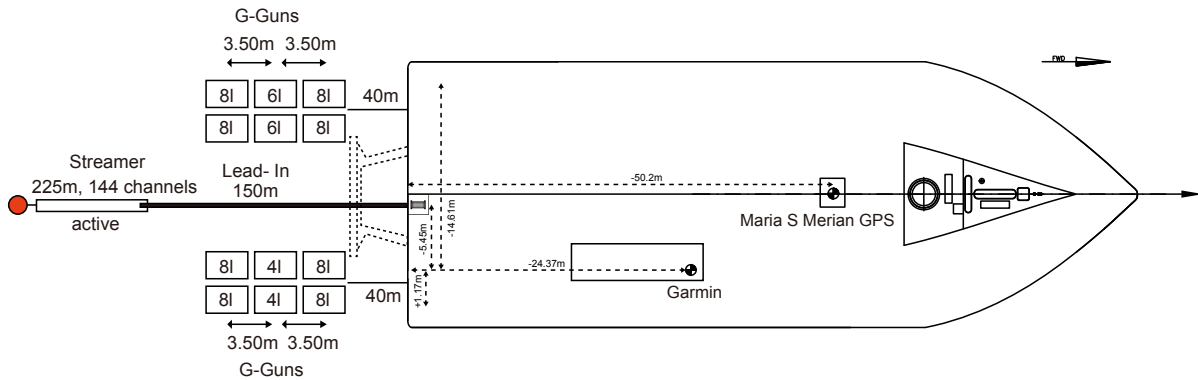


Figure 5.6: Deck with seismic gun and streamer setting and GPS offset during Cruise MSM 71.

## G-Gun Array

The source used during surveying was a G-Gun array manufactured by Sercel Marine Sources Division (former SODERA) and Seismograph Services Inc. and consisted of 2 sub-arrays (Fig. 5.6). Six guns were set up in 3 clusters. Each cluster comprises G-Guns of 4x8 liters and in the middle either 2x6 liters or 2x4 liters (Fig. 5.6). The cluster arrangement provides a good primary-to-bubble signal ratio. Operating all twelve guns simultaneously provides a total volume of 84 liters (5440 cu.in.). Airgun-deployment rails mounted on RV Maria s Merian were used to deploy G-Gun sub-arrays on aft port and starboard sides of the ship. The arrays were towed 40 meters behind the ship's stern and 8 meters below the sea-surface. All guns were shot at ~190 bar. The guns worked very reliably during the entire cruise.

## Trigger Unit

To trigger the G-guns a time-signal was generated, and fed into the Longshot trigger box used as gun controller. In addition, the trigger pulses are stored on a GEOLOG recorder. The Clock Time Break (CTB) of the Longshot device is a TTL pulse that is 5 ms wide and represents the aim-point or the time when the guns are fired. This aim-point was set to 60 ms after the trigger pulse. All guns were operated in auto mode; thus, guns are automatically tuned to aiming point. Exact position calculation for each shot was calculated using the streamer navigation along the seismic profile. For pure shot profiling, positioning is achieved through post-processing using shot times (stored in UTC time on the GEOLOG recorder) and GPS coordinates from the ship's database.

## 5.2 The AlpArray Broadband Station Network

### 5.2.1. Recovery Operations

29 broadband instruments were deployed as part of the AlpArray network in June 2017 using the RV POURQUOI PAS? as platform. The array is complemented by an additional station operated by GeoAzur in Nice, totaling a network of 30 OBS (Fig. 5.7). Recovery of the DEPAS/GEOMAR LOBSTER OBS proved challenging as neither the flashlight nor the radio beacon worked properly.

This was due to the fact that the instrument ascended in a horizontal position instead of turning into the vertical so that the flash and radio beacon, as well as the flag, did not protrude above the sea surface. Locating the instruments hence had to be achieved visually and, weather conditions permitting, with the assistance of the ice radar. At night, the search lights of RV MARIA S MERIAN were used in addition.

When approaching OBS A406A, we received an answer upon the release signal, however, the instrument was not observed on the surface. It remains unclear whether the release command worked properly and the unit was not spotted on the surface or whether the instrument did not ascend. OBS A408A did not respond to our release or ranging signals and could not be retrieved.



Figure 5.7: Location map of the seismological stations installed in the Ligurian basin and on its margins; color-coded for instrument type.

## 5.2.2 First Results of OBS Deployment June 2017 – February 2018

Of the 27 recovered broadband OBS stations, 25 instruments recorded throughout the entire deployment period between June 2017 – February 2018. First inspection of the data quality aboard RV MARIA S MERIAN showed an overall very good data quality. The long-period and seismometer channels are of excellent quality, while the hydrophone channel shows a significantly weaker signal, in particular for local events of higher frequency. In the following we present data examples for regional events, a teleseismic event and recordings of the air gun shots. Furthermore, we observe events of durations of less than  $\sim 2$  s, for which we use the term “short duration” events.

### Data Example 1: Mw 4.6 Parma earthquake of Nov. 19, 2017

Figure 5.8 shows the vertical component records of selected OBS and onshore stations of the Parma region event on Nov 19, 2017 with a magnitude of Mw 4.6.

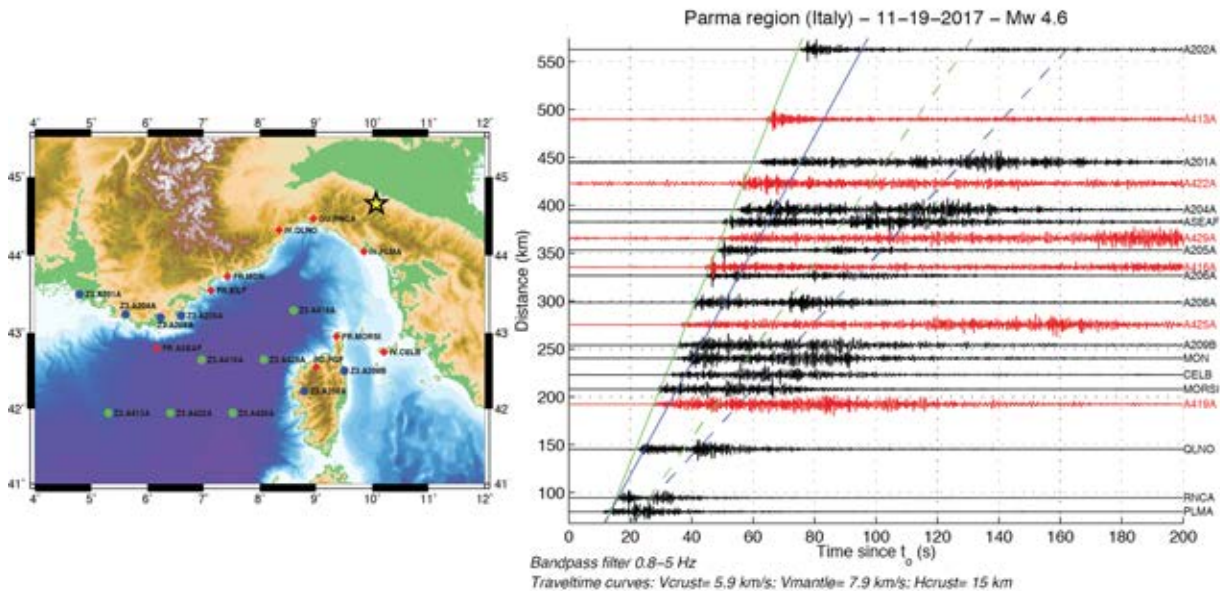


Figure 5.8: Location map of OBS and onshore stations (left) selected to generate a record section of vertical components shown in the right panel. OBS records are shown in red, land stations are shown in black.

### Data Example 2: Regional Event

Local and regional events are observed to large distances of up to 400 km. Figure 5.9 presents an Ml 2.9 event at regional distance of ~400 km. The body waves (P-, S-phase) are separated by ~30 s and are followed by a T-phase. Generally, the P-Phase is not clearly identified on the hydrophone channel (upper time series in Fig. 5.9), suggesting poor recording quality of the hydrophone for high frequencies. The corresponding record sections are shown in Figure 5.10.

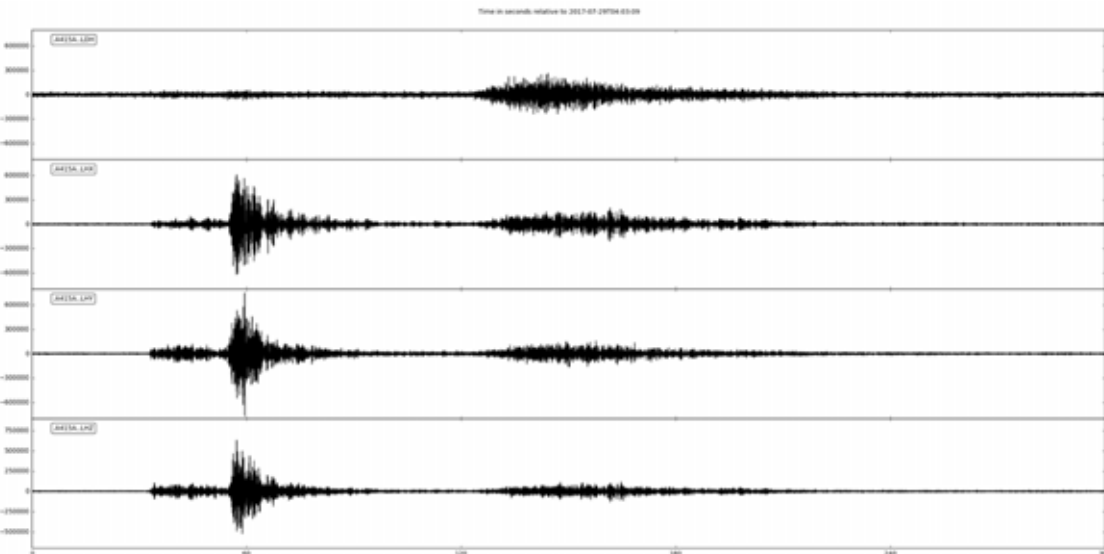


Figure 5.9: Data example from an Ml 2.9 event (29 July 2017, 04:03:09 at 42.31°/9.03°, ISC catalogue) at ~260 km epicentral distance on OBS A415A. The hypocenter is located at 17 km depth beneath Corsica. The data is filtered between 3 Hz and 20 Hz.

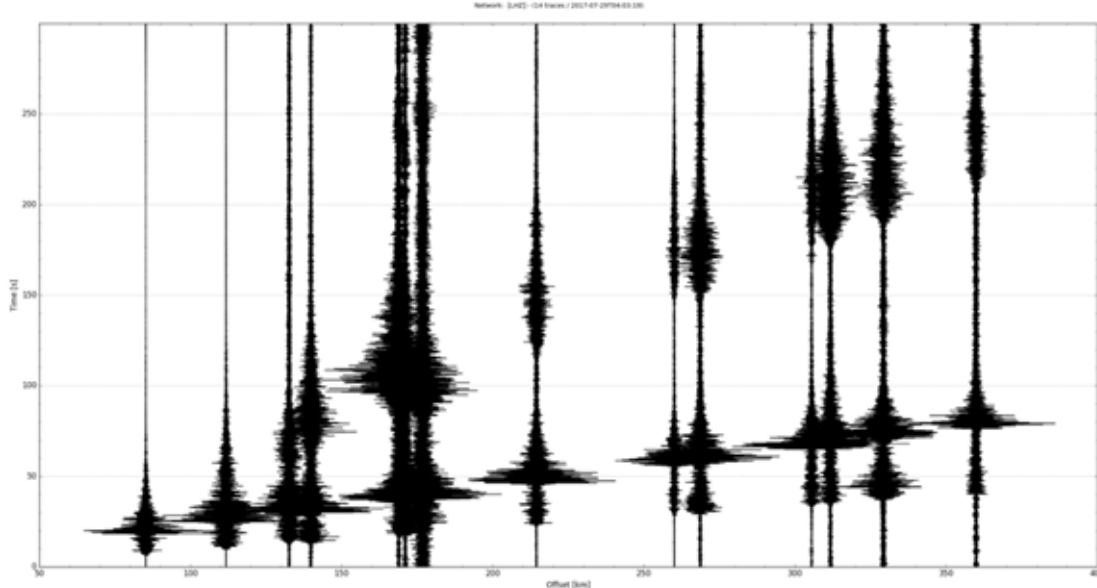


Figure 5.10: Record section of vertical component for regional event presented in Figure 5.9.

### Data Example 3: Teleseismic Event

We inspected 76 events from the NEIC global catalogue between July 01, 2017 and Feb 01, 2018 with magnitudes larger than Mw 6. 22 events are well observed with clear surface wave trains. 21 additional events are visible mainly on the vertical component and are less clear on the other channels, while the remainder is not visible. This corresponds to a good quality. Figure 5.11 shows the surface wave arrivals from the Sep. 08, 2017 Mw 8.2 earthquake offshore Mexico. The wave trains are clearly visible on all components indicating a very good data quality. For these higher frequencies the hydrophone clearly resolves the different wave trains (Fig. 5.11, upper panel), however, the hydrophone is less sensitive for lower frequencies. The corresponding record sections are shown in Figure 5.12.

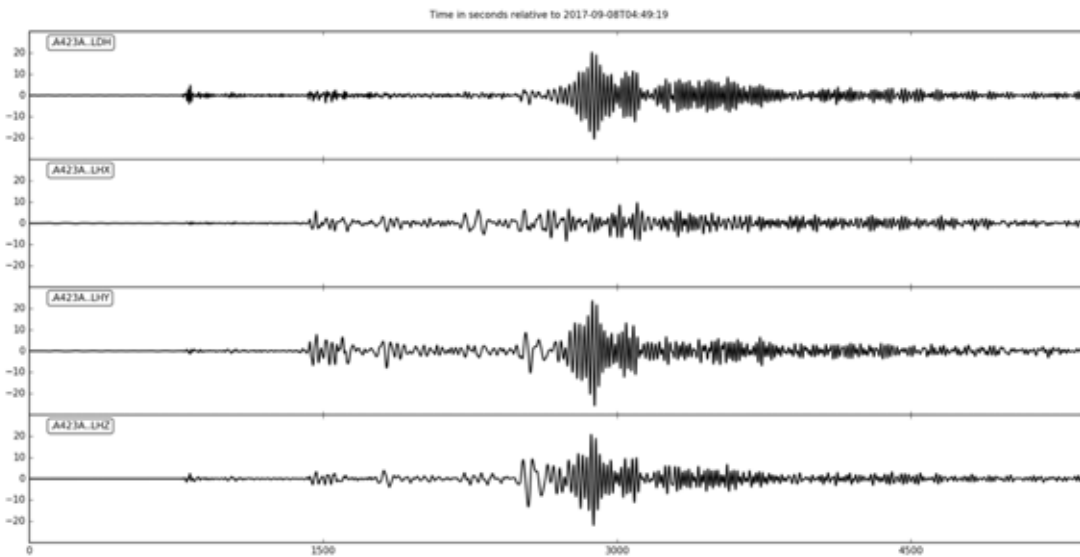


Figure 5.11: Data example showing the teleseismic arrivals from the Mw 8.2 subduction zone earthquake offshore Mexico from 08 September 2017 (15.022°N/93.899°W, 47.4 km depth, 04:49:19 UTC). The data is filtered between 0.01 Hz and 0.07 Hz and window length is 90 minutes.

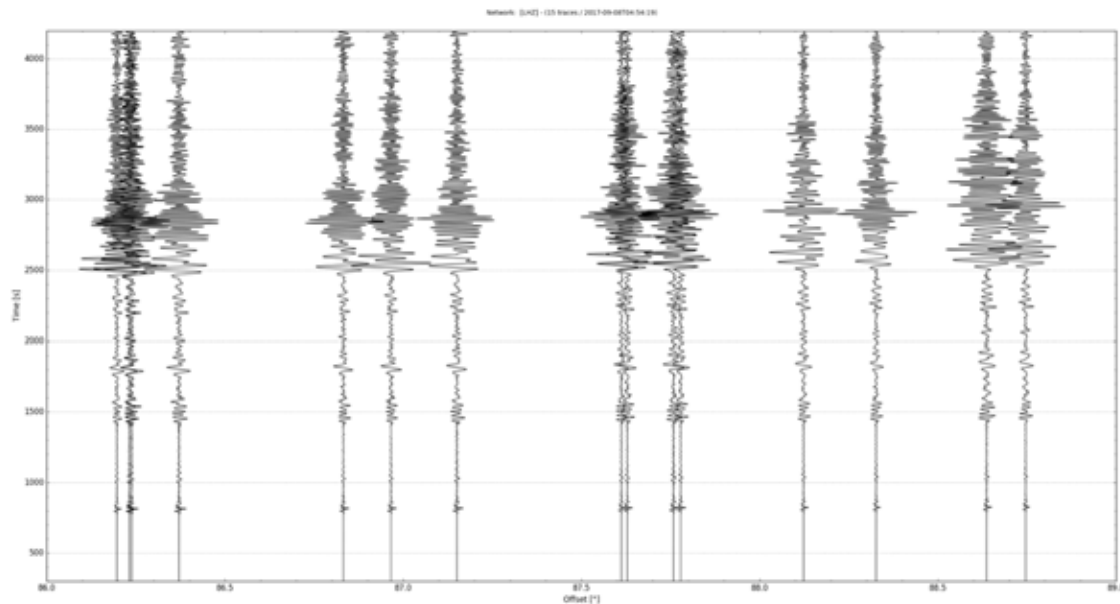


Figure 5.12 Record sections for Chiapas earthquake of Sept. 8, 2017 presented in Figure 5.11

#### Data Example 4: Airgun Shots

Air gun shots along profile P1 are clearly visible up to offsets of at least 290 km. Figure 5.13 shows the airgun registrations shot on the eastern part of profile P1 registered on the long-term AlpArray stations located in the western part of the working area and hence at offsets of between 250 and 290 km. In contrast to the local events, the signal on the hydrophone channel is of similar quality as the vertical component .

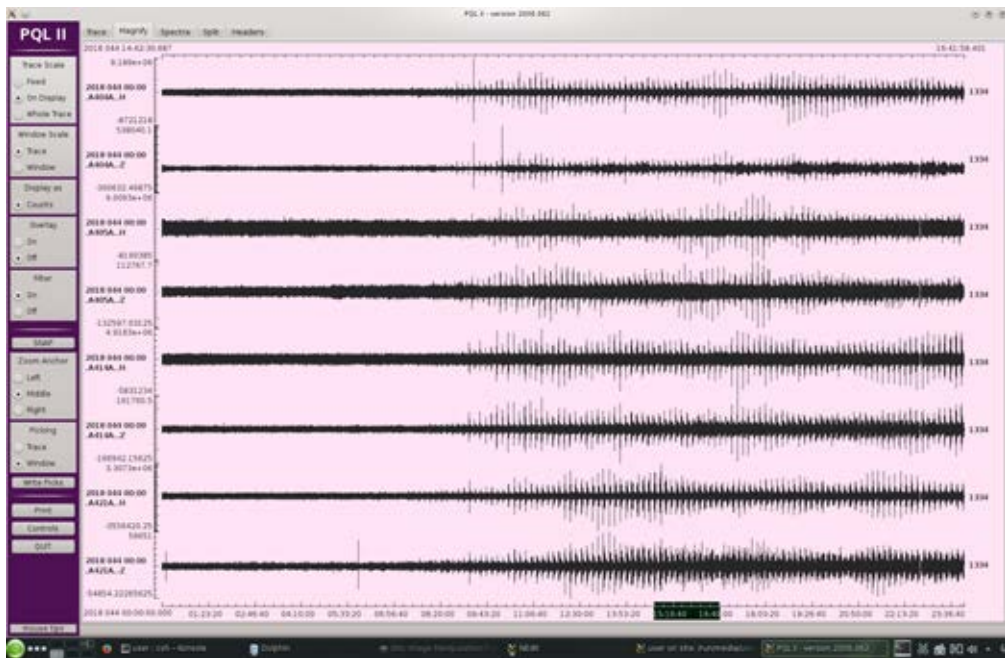


Figure 5.13: Hydrophone and vertical components of four long-term OBS Stations located on the western side of profile P1 showing the airgun shots at ~250 km epicentral distance from the eastern termination of profile P1 (e.g. close to Corsica). The amplitudes increase around 08:20 UTC because RV Maria S. Merian rapidly gained deeper water while travelling across the steeply inclined slope of Corsica. The data are filtered between 3 Hz and 8 Hz. Window length is 2 hours.

### Data Example 5: Short Duration Event

We find repeated short duration events with strong amplitudes and durations less than 2 to 3 s (Fig. 5.14). These events are clearly identified in the daily registrations since they are characterized by amplitudes significantly above the background noise level. The events are characterized by their impulsive waveform followed by a mono-frequent coda. Some events have two distinct phases with time differences between 0.1 and 0.5 s. So far, we were not able to track these across the network indicating that these events are of a very local origin.

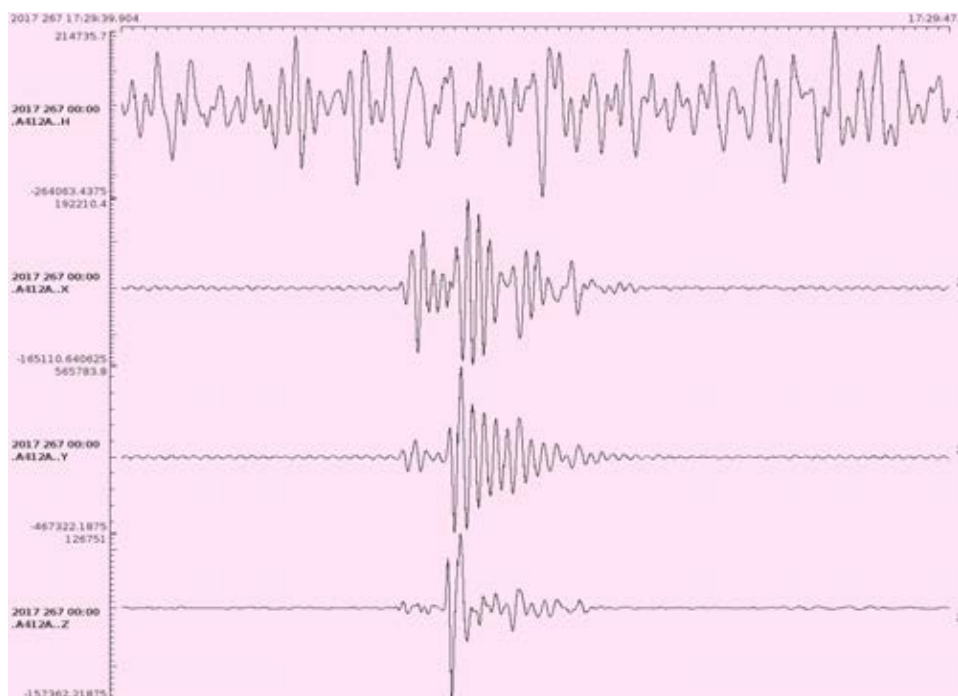


Figure 5.14: Data example of 7.2 s long time window of enigmatic short period events observed on OBS A412A.

First inspection of the short duration events suggest that they can be observed on individual stations and cannot be tracked across the OBS network. The difference between the pronounced wave trains is typically between 0.3 and 0.5 s. The data is filtered between 3 Hz and 8 Hz.

### 5.3 Seismic Refraction and Reflection Lines

Seismic data along the two profiles acquired during MSM 71 simultaneously recorded on the OBS/OBH as well as on the streamer. Both lines target the upper and deep structure of the crust and upper mantle as well as the sedimentary layers in the Ligurian Basin. The streamer data will provide important *a priori* information for the modeling and inversion of the refraction seismic data, as shallow sedimentary structures are commonly not resolved by sea floor stations spaced more than a few cables or hundred meters apart. The main research targets regard the architecture of the crust and lithosphere, as basic parameters such as crustal thickness or structural changes across or along-strike of the basin axis are not well resolved from previous existing data.

The seismic profiles were acquired using the G-gun array introduced above. Prior to shooting, we conducted mammal and turtle mitigation procedures in order to protect marine wildlife during the seismic survey, including ramp-up and visual monitoring. Ramp-up means the gradual increase in emitted sound levels by systematically turning on the full complement of the array's air guns over a period of time. Visual monitoring of an exclusion zone and adjacent waters is intended to establish and maintain a zone around the sound source that is clear of affected species thereby

reducing or eliminating the potential for interference. Exclusion zone means the area of the sea surface within a radius of 500 m surrounding the center of the air gun array. The intent of ramp-up is to allow sufficient time for animals to leave the immediate vicinity. Animals sensitive to the activities are expected to move out of the area. Measures to conduct ramp-up procedures, including air gun testing are as follows:

- Visual monitoring of the exclusion zone and adjacent waters for the absence of sensitive wildlife for at least 30 minutes before initiating ramp-up procedures. Ramp-up is only initiated when visual monitoring of the exclusion zone is possible (i.e. at least 500 m visibility).
- Ramp-up is initiated by firing the smallest air gun in terms of energy output (dB) and volume ( $\text{in}^3$ ). Initial shot interval is 4 minutes. Additional air guns are gradually activated over a period of at least 20 minutes but no longer than 40 minutes until the desired operating level of the air gun array is obtained. The shot interval was then gradually adjusted to 50 s (200 s – 150 s – 100 s – 50 s) for profile P01 and 60 s (240 s – 180 s – 120 s – 60 s) for profile P02.
- All air guns would immediately be shut down, thus ceasing seismic operations, at any time a whale is detected entering or within the exclusion zone. Seismic operations would only be recommenced after the exclusion zone has been visually inspected for at least 30 minutes.
- The observers looked for whales and other marine mammals using the naked eye and hand-held binoculars, standing watch in a suitable location that will not interfere with navigation or operation of the vessel and that affords the observers an optimal view of the sea surface; they will adjust their positions appropriately to ensure adequate coverage for the entire area. If a marine mammal is observed, the observer will note and monitor the position (incl. Lat./Long. of the vessel and estimated distance) until the animal dives or moves out of visual range. At any time a whale is observed within the exclusion zone, the observer will call for immediate shut-down of the seismic operation.

No mammals or turtles were detected during the mitigation procedures or during shooting. At other times, the officers on the bridge observed a school of dolphins during the transit to our working area (near the Balearic islands), but never within our operating region.

### 5.3.1 Refraction / Reflection Profile P01

A total of 35 stations, comprised of 24 OBS and 11 OBH, were deployed along the 147 nm long refraction line P01, which trends W-NW from central Corsica towards the Gulf of Lions (Fig. 5.15). In addition, three land stations located at 42.2°N/8.6°E, at 42.2°/8.8°E and at 42.1°N/8.9°E were installed on Corsica to record the air gun signals (Figs. 5.16 and 5.17). Furthermore, a permanent land station located on our extended profile track at 42.1°N/9.3°E also recorded the shot signals. The profile was shot from east to west with a shot interval of 50 seconds at 4.5 kn speed, resulting in a shot point spacing of 115 m. A total of 2418 shots were fired along the line. Water depths along the profile ranged from 623 m near the Corsican coast, rapidly dropping to below 2500 m and reaching values greater than 2750 m in the central Ligurian Basin, before decreasing to 2302 m near the northwestern termination of the line. During recovery, OBH 134 did not release the anchor and could not be retrieved. Four stations unfortunately did not record useful data (OBS111, OBH120, OBH122, OBH126).

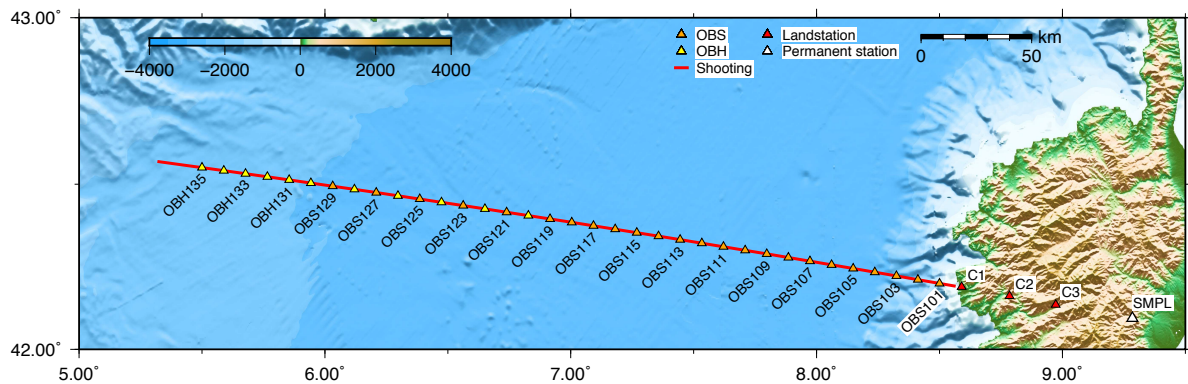


Figure 5.15: Location map with station numbers of seismic refraction profile P01.



Figure 5.16: Eastern termination of profile P01 showing the air gun bubbles offshore Corsica. Orange arrow indicates position of one of the temporary land stations installed close to the shore by INRC.

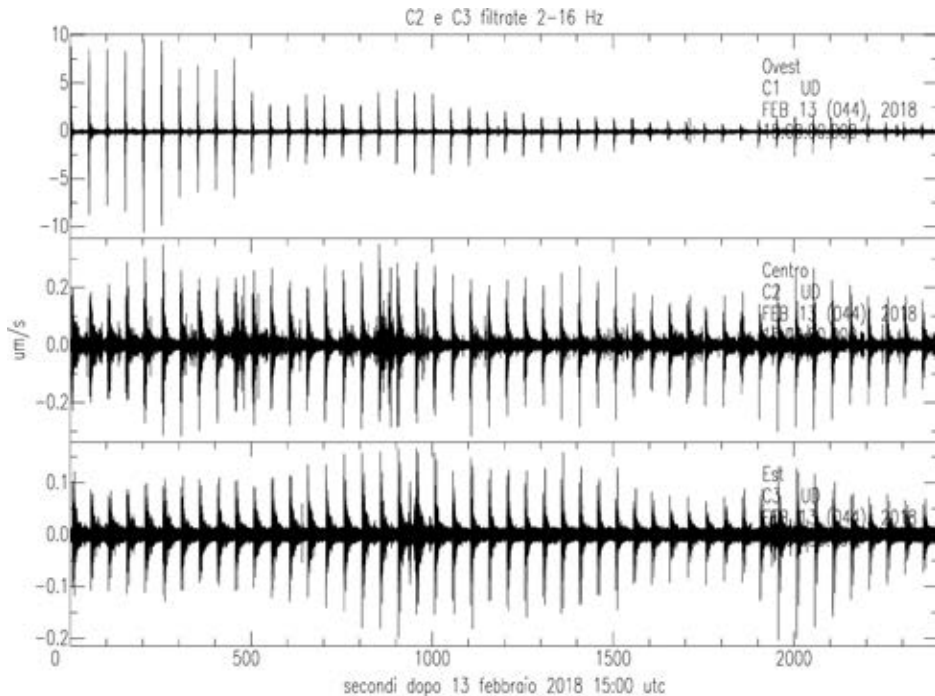
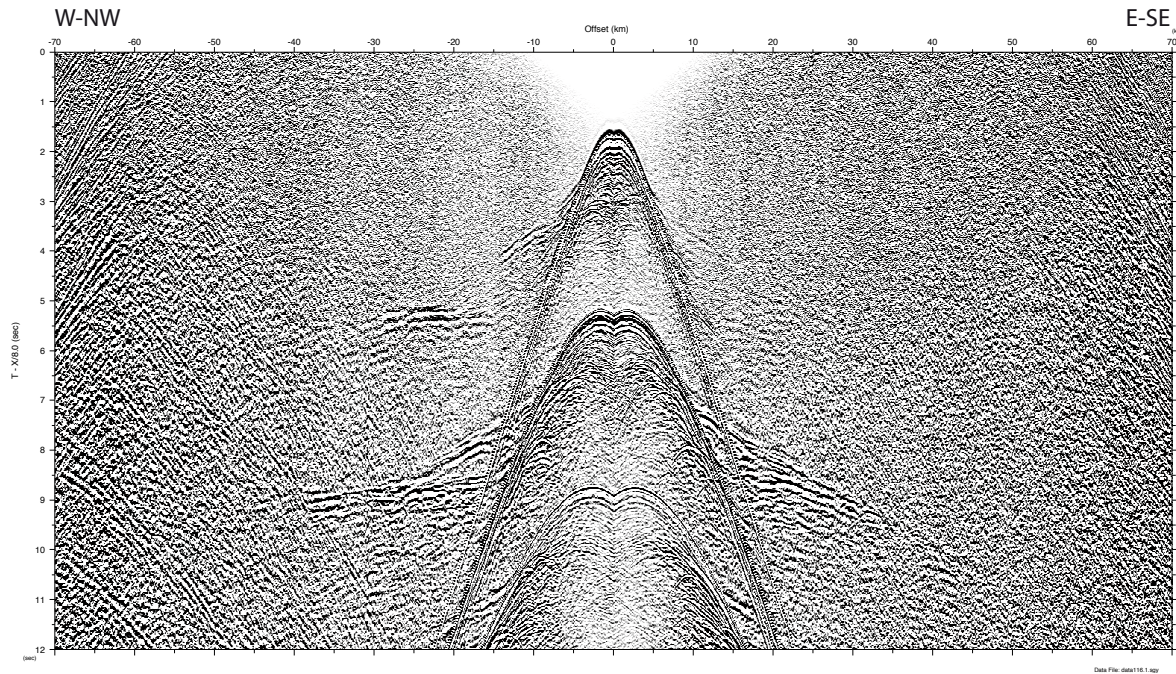


Figure 5.17: Air gun shots recorded by land station cor1 on Corsica on Feb. 13, 2018.

Profile P01 extends from the Central Corsican margin across the Ligurian Basin to the Ligurian-Provencal margin. The line covers the transitional domains to both margins as well as the oceanic

crust in the extensional central basin. The exact nature of the crust is enigmatic and it has been termed ‘atypical oceanic crust’ by Rollet et al. (2002). The refraction seismic data along profile P01 recorded clear PmP and Pn phases on a number of stations (Figs. 5.18 and 5.19), especially along the NW portion of the line. Mantle phases are observed at negative and positive offsets and a first preliminary analysis of the data indicates thinned crust with seismic velocities typical of oceanic crust. The overlying sediment cover has a mean thickness of 0.5 km in the center of the basin.



MSM 71 Profile P01 Record Section OBS117

Figure 5.18: Hydrophone record section of OBS 117, located in the center of the Ligurian Basin.

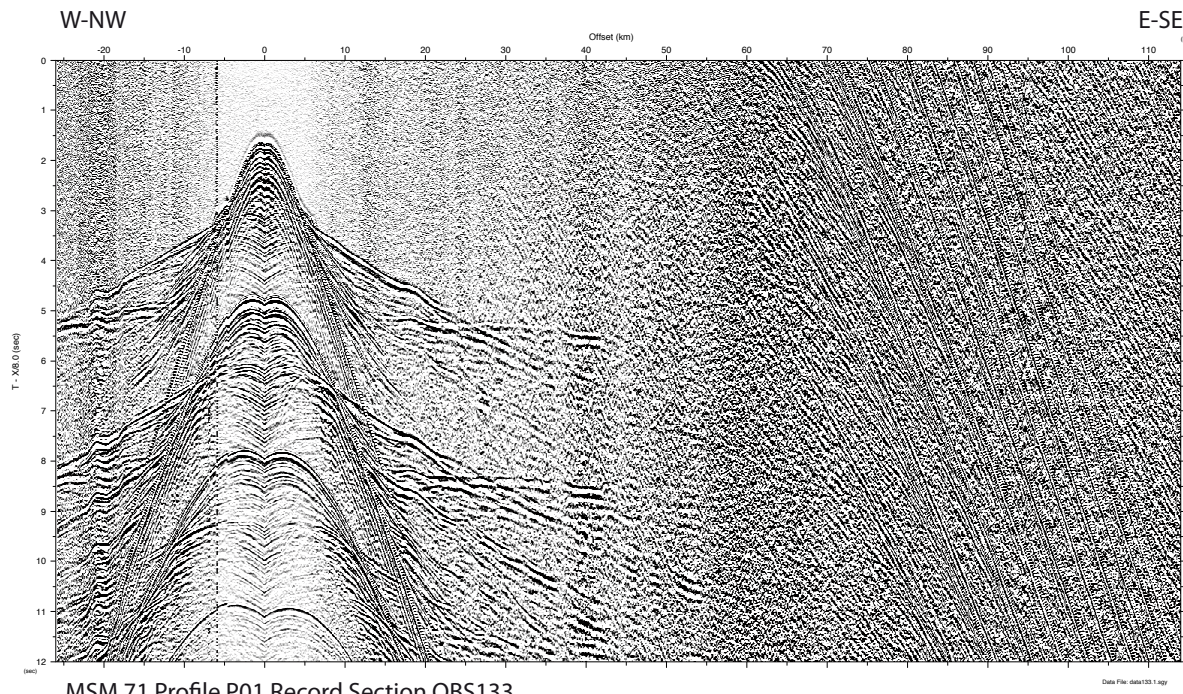


Figure 5.19: Hydrophone record section of OBS 133, located on the foot of the Ligurian margin.

### 5.3.2 Refraction / Reflection Profile P02

Seismic refraction line P02 lies in the prolongation of an existing refractin profile in the northern Ligurian Basin (Makris et al, 1999; compare Fig. 3.7). It consists of a total of 15 stations (12 OBS and 3 OBH) deployed along a NE-SW trending transect that terminates at the crossing point with profile P01 at  $42^{\circ}21.00'N$  /  $07^{\circ}15.00'E$  (Fig. 5.20). Shot interval was 60 seconds at 4 kn speed, resulting in a shot point distance of 123 m. A total of 1033 shots were fired along the 73.5 nm long line; shooting direction was from the SW to the NE. Shooting had to terminate at the territorial boundary between France and Italy, located close to the last station on the profile. Water depth is fairly uniform, gradually deepening from 2593 m at OBS215 in the NE to 2734 m at OBS201 at the crossing point with profile P01 in the SW. The profile covers the central portion of the Ligurian basin. We used a mean water velocity of 1530 m/s for re-locating the stations along both profiles (compare XSV profile in Appendix A) (Fig. 5.21). All stations recorded data and the majority of instruments show clear Pn mantle phases and PmP Moho reflections (see example in Fig. 5.22). MCS streamer data were recorded along the entire profile with a recording length of 8 s TWT (Fig. 5.23). The MCS section shows app. 500-600 m of stratified sediment underneath the gently SW-NE inclined seafloor, underlain by an evaporate layer. Minor extensional faulting is observed around shot/trace number 150. There are numerous indications for small-scale magmatic intrusions (for example, but not exclusively, around shots 450, 520, 625, 700, 775). The largest of these breaches the sea floor around shot number 875 and is also observed in the corresponding PARASOUND data (Fig. 5.24). The PARASOUND section also shows indications of salt tectonics, however, this needs further verification from detailed data anaylsis. Magmatic intrusions were previously identified from reflection seismic and magnetic data in the region of our profile, verified by dredge samples from Monte Doria in the north of the Ligurian Basin (Rollet et al., 2002).

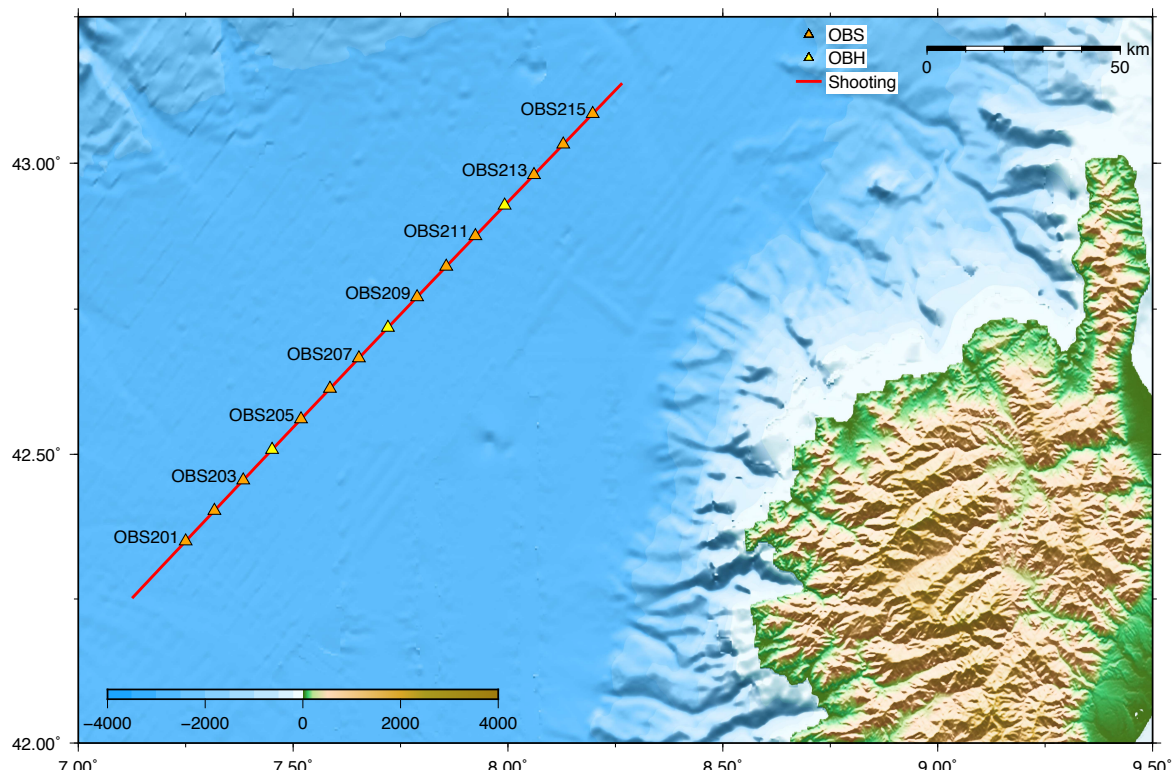


Figure 5.20: Location map with station numbers of seismic refraction profile P02.

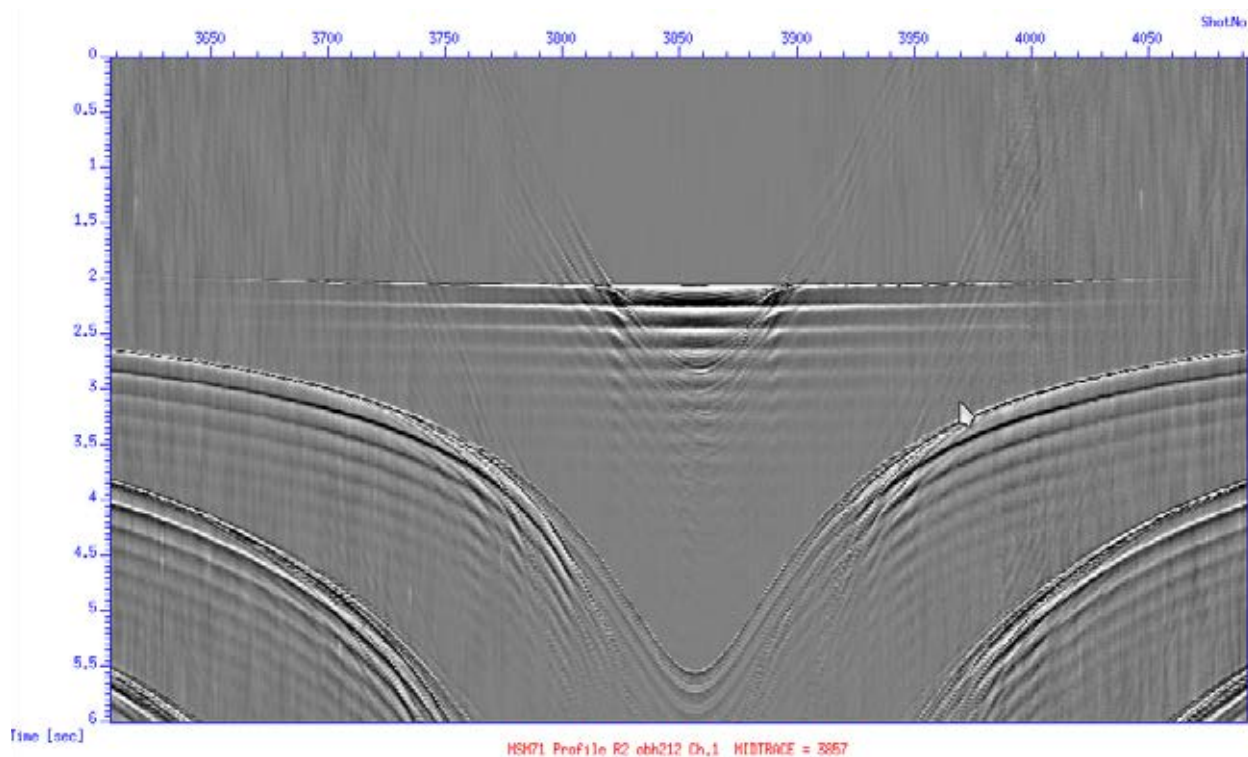


Figure 5.21: Re-located shot section of OBS212.

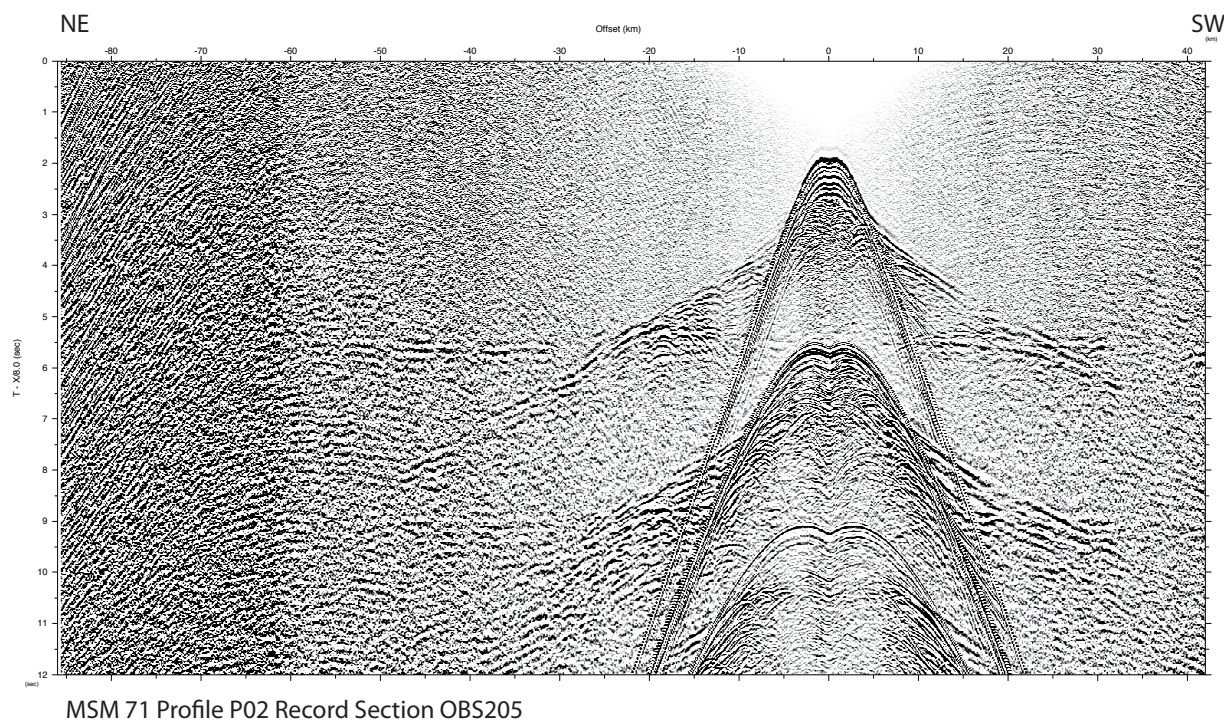


Figure 5.22: Record section of OBS205. Distinct Pn and PmP phases are observed in both offset directions.

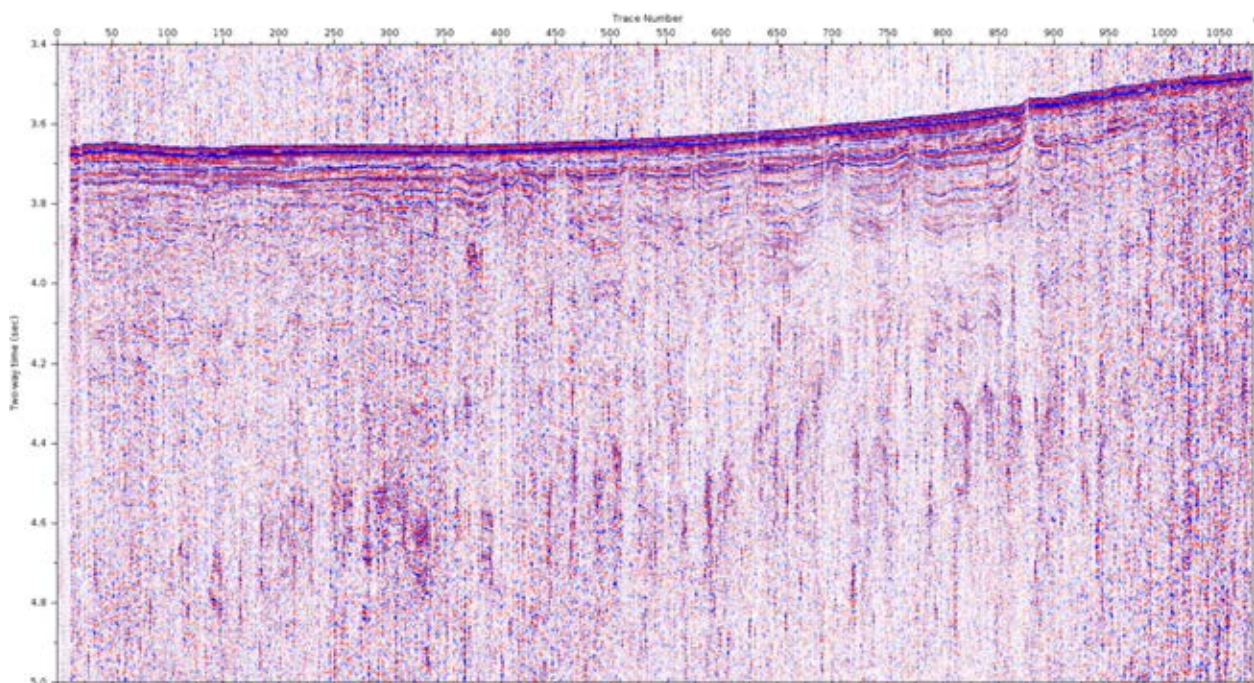


Figure 5.23: Raw stack of GeoEEL streamer data along P02. NE is to the right, SW to the left.

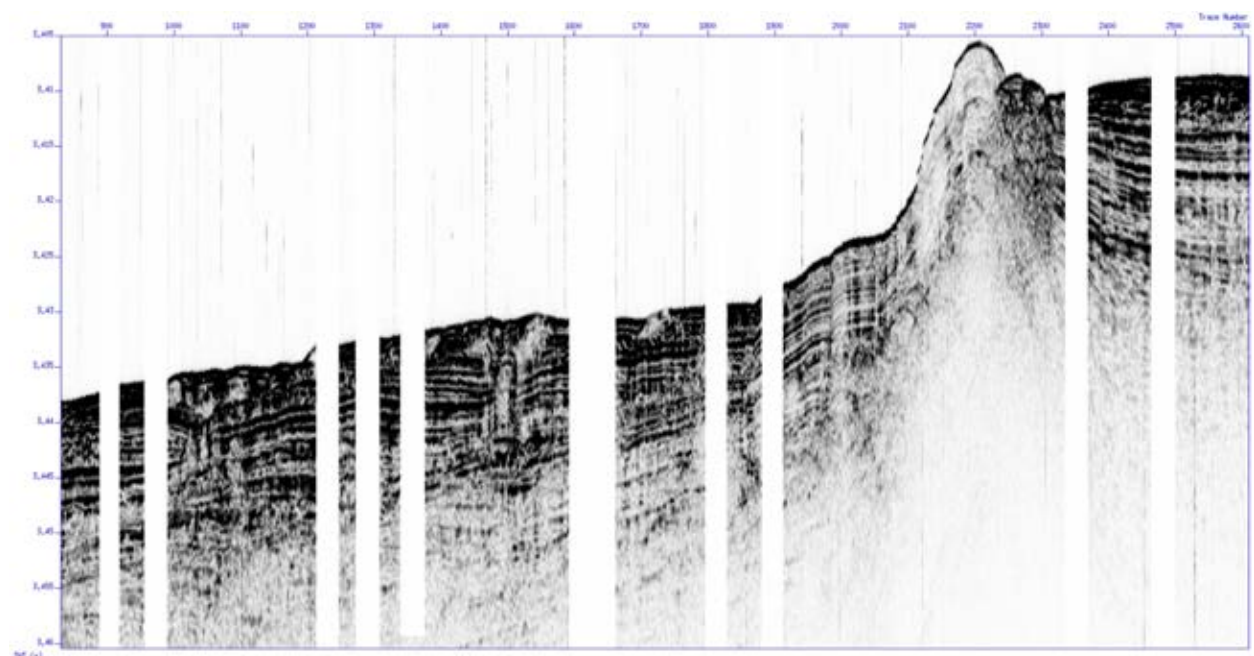


Figure 5.24: Parasound section across a prominent seafloor topography, likely resulting from a magmatic intrusion on profile P02.

Figure 5.25 shows a preliminary velocity-depth model based on a first arrivals tomography (Korenaga et al., 2000). A simple layered starting model was used as input (lower panel in Figure 5.25), generated from a preliminary forward model using Rayinvr (Zelt and Smith, 1992). Arrivals were picked using PasteUp (Fujie et al., 2008). Ray coverage of the lower crust and upper mantle slightly decreases along the northeastern portion of the profile to the southwestern end, as more mantle and deep crustal phases could be identified on the northern stations. The crustal thickness in the model is fairly uniform along the profile (resolution is better along the north-eastern part of the line) with a thickness of 5 km, however, these values need to be verified by including PmP

reflections from the Moho. Significant velocity inversions as would be expected from a massive salt or anhydrite layer are not observed in the data, though a 1-1.5 km thick evaporite layer is present within the sediments.

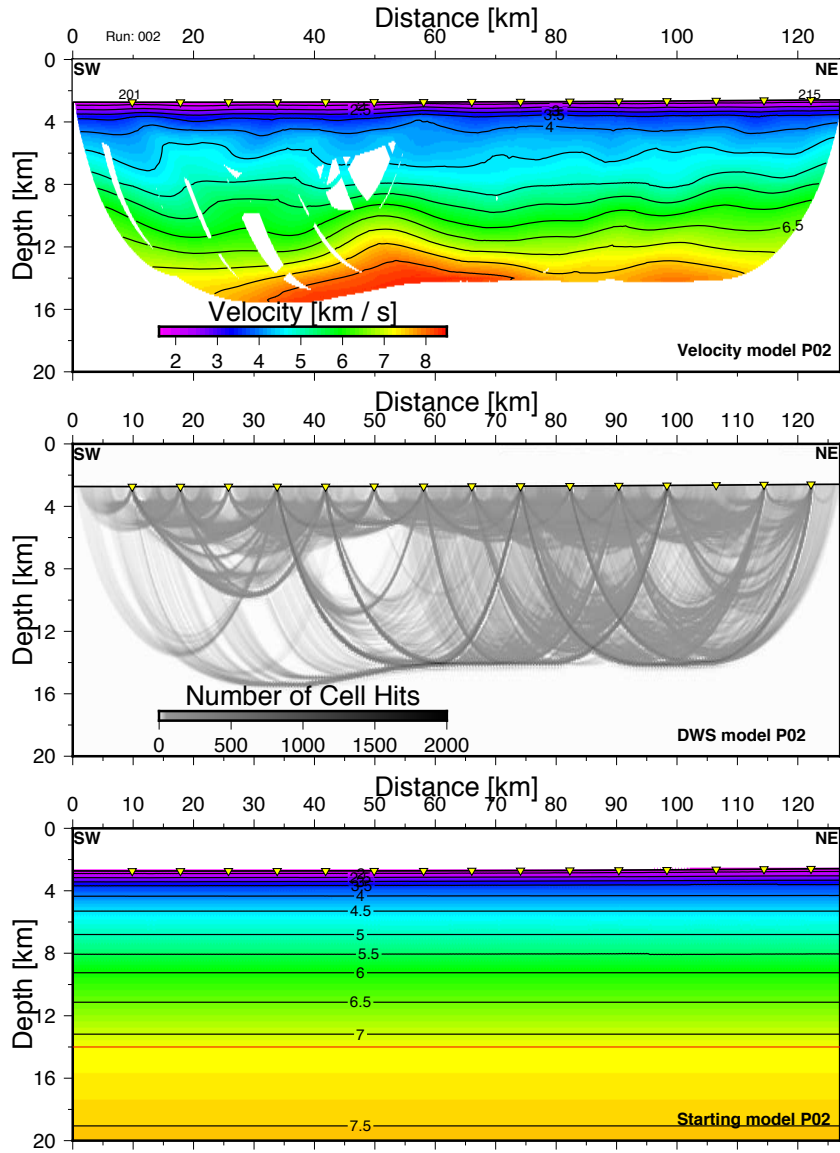


Figure 5.25: Preliminary first arrivals tomography of profile p02. A simple layered starting model (lower panel) was used as input. Middle panel shows the ray coverage along the profile (first arrivals only) and upper panel displays the tomographic inversion from these arrivals.

## 5.4 Multibeam Bathymetry

### 5.4.1 The Kongsberg EM122 and EM710 systems

RV MARIA S MERIAN is equipped with two Kongsberg Maritime multibeam echosounders: The EM122 system operates at 12 kHz and covers water depths from 20 meters below the transducers up to full ocean depth, while the EM712 system offers three different frequency ranges (40-100 kHz, 50-100 kHz, 70-100 kHz) of signals for water depths ranging from 3 m below transducers to roughly 3500 m. Two different transmit pulses can be selected: a CW (Continuous Wave) or FM (Frequency Modulated) chirp. In case of the EM712, the latter is part of the full performance version that is installed on RV MARIA S MERIAN. The sounding mode can be either equidistant or

equiangle, depending on operation preferences and requirements. Both systems can be operated in single-ping or dual-ping mode, where one beam is slightly tilted forward and the second ping slightly tilted towards the aft of the vessel. The whole beam can also be inclined towards the front of the back and the pitch of the vessel can be compensated dynamically. The EM122 system produces 432 beams covering a swath angle of up to 150° while the EM712 system produces 512 beams for a maximum swath angle of 140°. The latter offers a high-density beam-processing mode with up to 800 soundings per swath. The swath angle, however, can be reduced, if required.

The transducers of both multibeam echosounder systems of RV MARIA S MERIAN are mounted in a so-called Mills cross array, where the transmit array is mounted along the length of the ship and the receive array is mounted across the ship. The system on RV MARIA S MERIAN is of a 1° x 1° design. The EM712 system installed on RV MARIA S MERIAN is of a 0.5° x 0.5° design, but transducers are much smaller.

The echo signals detected from the seafloor go through a transceiver unit (Kongsberg Seapath) into the data acquisition computer or operator station (Fig. 5.26). In turn, the software that handles the entire data acquisition procedure is called Seafloor Information System (SIS). In order to correctly determine the point on the seafloor, where the acoustic echo is coming from, information about the ship's position, movement and heading, as well as the sound velocity profile in the water column are required. Positioning is implemented onboard RV MARIA S MERIAN with conventional GPS/GLONASS plus differential GPS (DGPS) by using either DGPS satellites or DGPS land stations resulting in quasi-permanent DGPS positioning of the vessel. These signals also go through the transceiver unit (Seapath) to the operator station. Ship's motion and heading are compensated within the Seapath and SIS by using a Kongsberg MRU 5+ motion sensor. Beamforming also requires sound speed data at the transducer head, which is available from a Valeport MODUS SVS sound velocity probe. This signal goes directly into the SIS operator station.

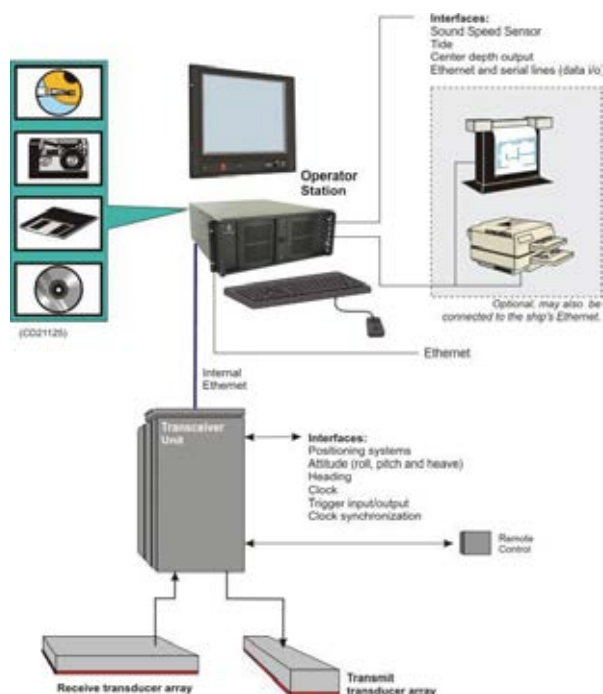


Figure 5.26: Configuration drawing of the EM122 system units and interfaces.

Finally, a sound velocity profile for the entire water column can be obtained from either a sound velocity probe or from a CTD (conductivity, temperature and density) probe. During cruise MSM 71 two expendable sound velocimeter probes (XSV) were launched for profiling the water column on Feb. 12, 2018 at 42°32,45'N / 05°35,33'E to a depth of 1959 m and again on Feb. 21, 2018 at 42°52,80'N/08°37,29'E to a depth of 1986 m. The XSV-02 probes used during MSM 71 are an expendable profiling system manufactured by Lockheed Martin and rated for a ship's speed of up to 8 kn, for which it returns a vertical resolution of 32 cm. After launching the probe, a wire de-reels from it as the probe descends vertically through the water column. Sound velocity data are telemetered to the ship-board data processor during descent and are presented in Appendix A.

#### 5.4.2 Multibeam Bathymetry Data

The Kongsberg EM122 system was used for mapping the seafloor while the vessel operated in the study region, but was not running during transit from Las Palmas and to Heraklion, respectively. We surveyed an irregular track throughout the Ligurian Basin (Fig. 5.27) during seismic operations. Figure 5.22 shows morphological features on the seafloor in the central part of the basin and on the Corsica margin. The left panel in Figure 5.28 shows randomly distributed highs on the seafloor, which likely originate from volcanic intrusions as these are ubiquitous throughout the basin (Rollet et al., 2002). The right panel presents a multibeam bathymetry sweep across the deeply incised steep Corsica margin, characterized by tilted blocks which have been modulated by numerous canyons.

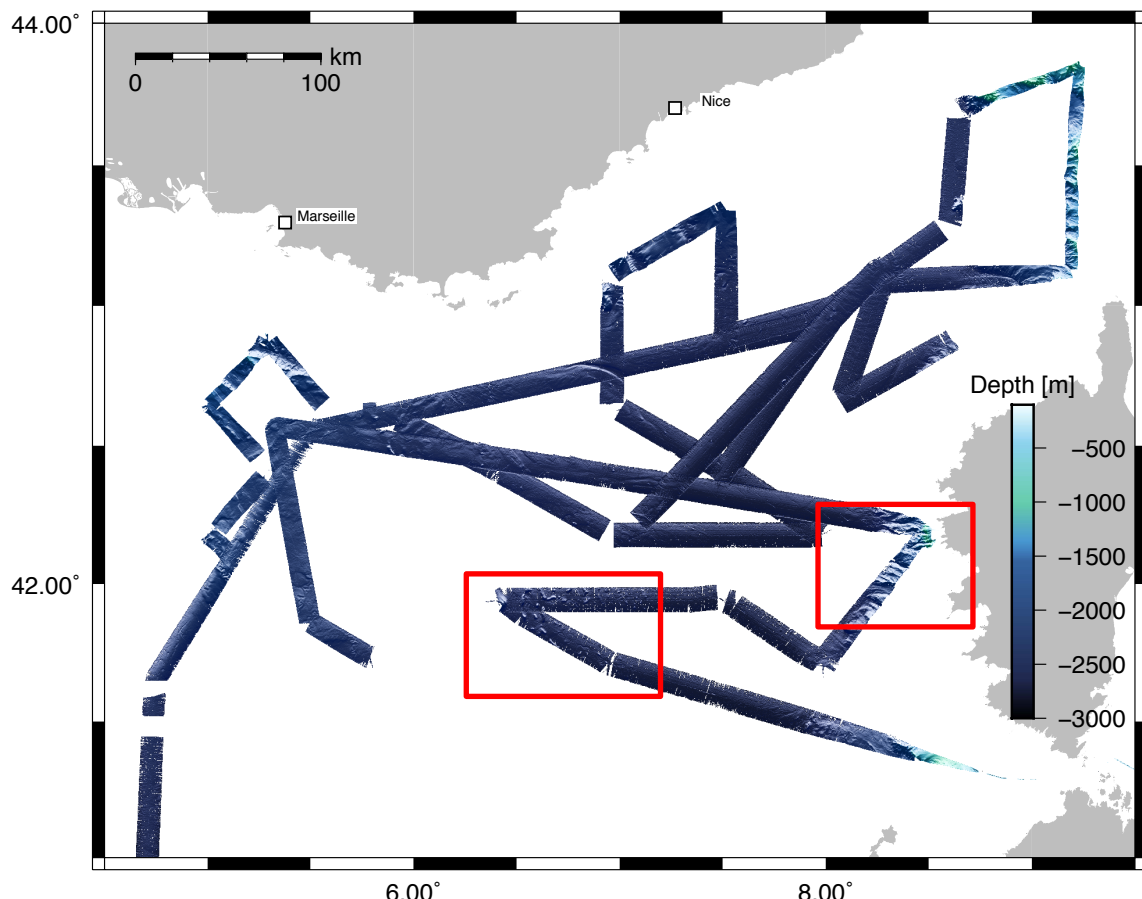


Figure 5.27: Bathymetric track recorded during MSM 71. Red squares indicate locations of blow-ups shown in Figure 5.28.

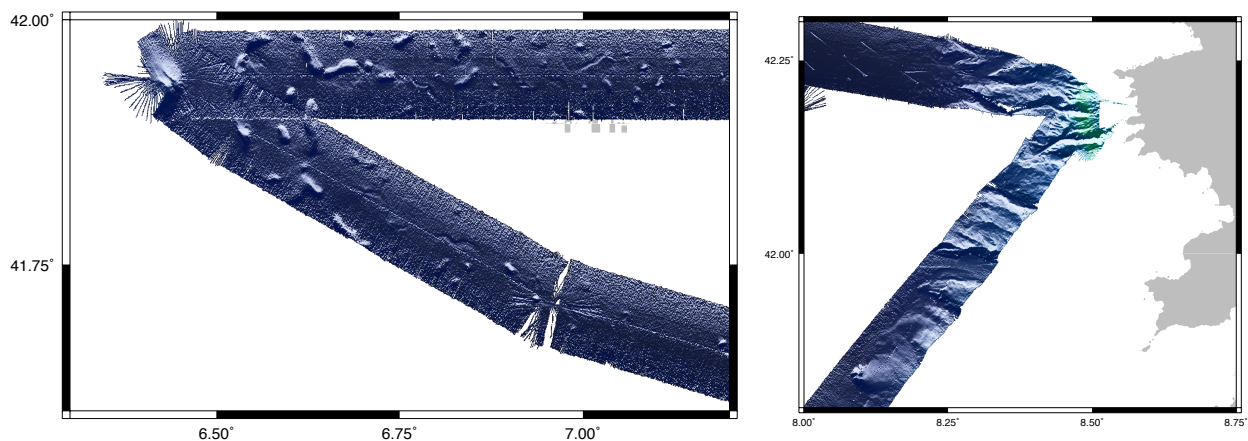


Figure 5.28: Details of bathymetric track. Locations shown in Fig. 5.27.

## 6. Ship's Meteorological Station

(H. Kopp and all Cruise Participants)

There was no meteorologist on board during cruise MSM 71.

## 7. Station List MSM 71

(H. Kopp and all Cruise Participants)

Please see Attachment B.

## 8. Data and Sample Storage and Availability

(D. Lange and H. Kopp)

The bathymetry data were transferred to the BSH immediately after the cruise.

All metadata of the onboard DSHIP-System is publicly available through the information and data archival system of the Kiel Data Management Team (KDMT). This Ocean Science Information System (OSIS-Kiel) provides information on the scientific program of the cruise and availability of data files. The KDMT serves as data curators to fulfill data publication in PANGAEA, a database of the Alfred-Wegner-Institute in Bremerhaven. PANGAEA provides long-term archival and access to the data within WDC-MARE. This connection with WDC-MARE will make the data globally searchable, and links to the data owners will provide points of contact to project-external scientists. The seismic, bathymetric and hydro-acoustic raw data as well as processed seismic data will be archived on a dedicated server at GEOMAR, which is daily backed up and which holds all data since the founding days of GEOMAR. OSIS provides contact information for these large data files.

Furthermore, the LOBSTER OBS data will be accessible at GEOFON (<http://geofon.gfz-potsdam.de/>) using the standardized software interfaces provided by the European Integrated Data Archive (EIDA, <https://www.orfeus-eu.org/data/eida/>). EIDA is a distributed data centre established to securely archive seismic waveform data and related metadata, gathered by European research infrastructures, and to provide transparent access to the archives by the geosciences research communities.

Availability of metadata in OSIS-Kiel( [portal.geomar.de/osis](http://portal.geomar.de/osis)): 2 weeks after the cruise.

Availability of data in OSIS-Kiel ( [portal.geomar.de/osis](http://portal.geomar.de/osis)): 6 months after the cruise.

Availability of data in a WDC/PANGAEA ([www.pangaea.de](http://www.pangaea.de)): The seismic, bathymetric and hydro-acoustic raw data as well as processed seismic data will be available 3 years after the cruise.

Availability of data using EIDA node at GFZ Potsdam: 3 years after the cruise.

Data and metadata of the INSU-IPGP OBS pool will be archived and distributed by the RESIF EIDA node (<http://seismology.resif.fr/>) within 2 months after the cruise.

## 9. Acknowledgements

### (H. Kopp and all Cruise Participants)

The cruise MSM71 was financed by the Deutsche Forschungsgemeinschaft DFG under grant MerMet 14- 94. Long-term deployment of DEPAS instruments was financed by the DFG under grant KO 2961/6-1 in the scope of the DFG priority program SPP MB 4D. The French component of AlpArray is funded by Agence Nationale de la Recherche (AlpArray-FR). We are grateful for the continuous support of marine sciences with an outstanding platform such as RV MARIA S MERIAN. The authors wish to express their gratitude to the various colleagues who have supported the work prior and during the cruise. Particular thanks are directed to our colleagues from the Italian National Research Council CNR/Istituto per la Dinamica dei Processi Ambientali di Milano. The Leitstelle Deutsche Forschungsschiffe in Hamburg, Germany and Briese Schifffahrts GmbH & Co. KG are acknowledged for their support and assistance. The experiment was only made possible by the crew's experience; without the excellent support of the ship's master, Captain Ralf Schmidt and the entire crew of RV MARIA S MERIAN throughout the cruise this project could not have been realized.

## 10. References

### (H. Kopp and all Cruise Participants)

- Alfred-Wegener-Institut Helmholtz-Zentrum für Polar- und Meeresforschung et al.. (2017). DEPAS (Deutscher Geräte-Pool für amphibische Seismologie): German Instrument Pool for Amphibian Seismology. Journal of largescale research facilities, 3, A122. <http://dx.doi.org/10.17815/jlsrf-3-165>
- Béthoux, N., Tric, E., Chery, J., Beslier, M-O., 2008. Why is the Ligurian Basin (Mediterranean Sea) seismogenic? Thermomechanical modeling of a reactivated passive margin. Tectonics, 27, doi:10.1029/2007TC002232.
- Bialas, J., and Flueh, E. R., Ocean Bottom Seismometers, Sea Technology, 40, 4, 41-46, 1999.
- Boschi, E., Ferrari, G., Gasperini, P., Guidoboni, E., Smriglio, G., Valensise, G., 1995. Catalogo dei forti terremoti in Italia dal 461 a. C. al 1980, report, 973 pp. Ist. Naz. Di Geofis., Bologna, Italy.
- Burrus, J., 1984. Contribution to a geodynamic synthesis of the Provencal basin (north western Mediterranean), Mar. Geol., 55, 247-269.
- Chamot-Rooke, N., Gaulier, J., Jestin, F., 1999. Constraints on Moho depth and crustal thickness in the Liguro-Provencal basin from 3D gravity inversion: Geodynamic implications, in The Mediterranean Basins: Tertiary Extension within the Alpine Orogen, edited by B. Durand et al., Geol. Soc. Spec. Publ., 156, 37-62.
- Contriucci, I., Nercessian, A., Mauffret, A., Béthoux, N., Pascal, G., 2001. A Ligurian (Western Mediterranean Sea) geophysical transect revisited, Geophys. J. Int., 146, 74-97, doi:10.1046/j.0956-540x.2001.01418.x.
- Courboulex, F., et al., 2007.. Seismic hazard on the French Riviera: Observations, interpretations and simulations, Geophys. J. Int., 170, 387-400, doi:10.1111/j.1365-246X-2007.03456.x.
- Crawford, W., Brisbourne, A., D'Anna, G., Flüh, E. R., Galve, A., Graindorge, D., Harmon, N., Henstock, T., Klingelhöfer, F., Mangano, G., Matias, L., Peirce, C., Sallares, V., Schmidt-Aursch, M., Tilman, F.

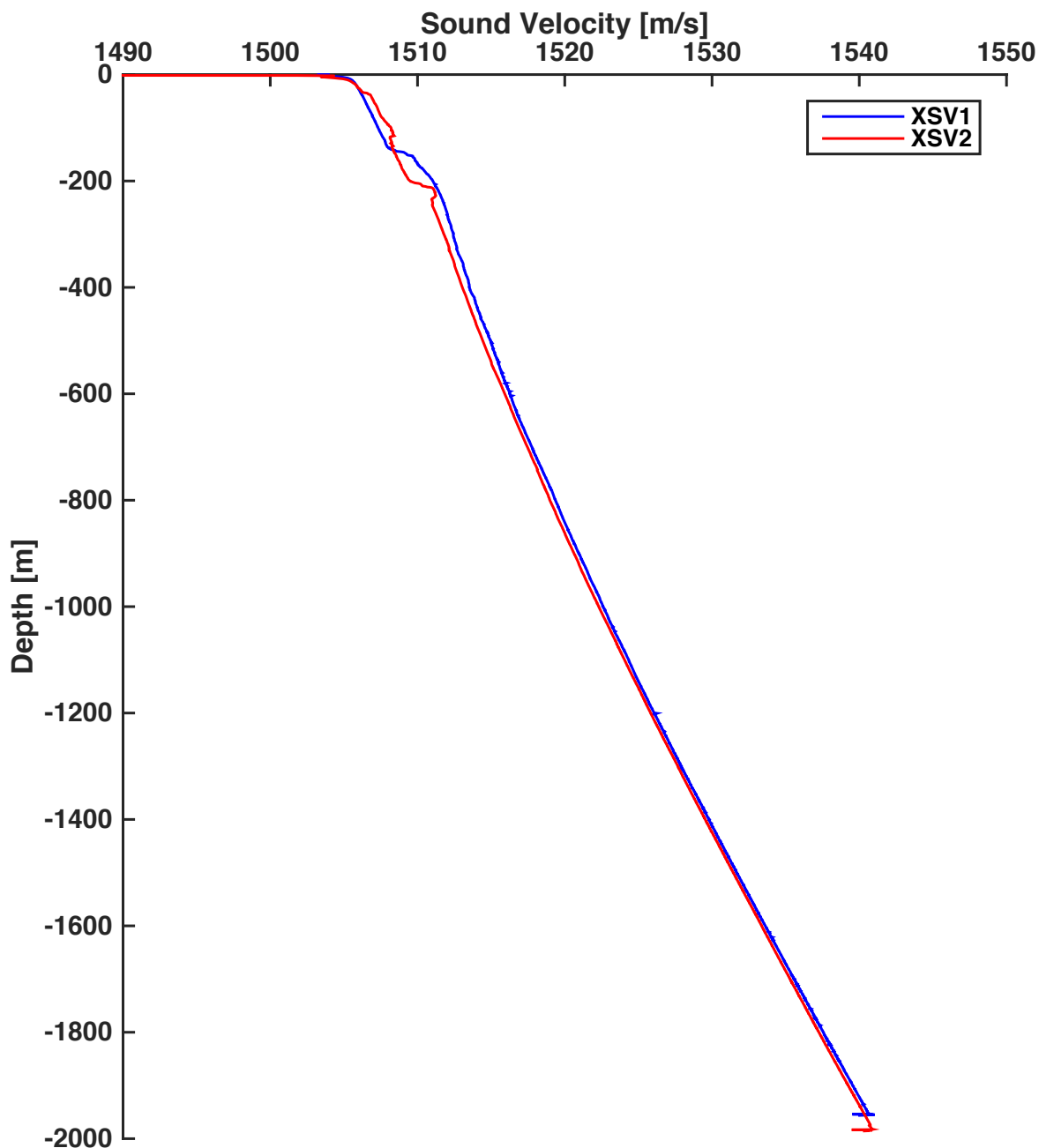
- und Voss, P. (2012) Coordinating OBS Parks in Europe. Geophysical Research Abstracts, Vol. 14, EGU2012-9536, EGU General Assembly.
- Dessa, J.-X., Simon, S., Lelievre, M., Beslier, M.-O., Deschamps, A., Béthoux, N., Solarino, S., Sage, F., Eva, E., Ferretti, G., Bellier, O., Eva, C., 2011. The GROSMarin experiment: three dimensional crustal structure of the North Ligurian margin from refraction tomography and preliminary analysis of microseismic measurements, Bull. Soc. Geol. France, 182, 305-321, 10.2113/gssgbull.182.4.305
- Doglioni, C., Gueguen, E., Sàbat, F., Fernandez, M., 1997. The Western Mediterranean extensional basins and the Alpine orogen, Terra Nova, 9, 109-112.
- Eva, E., Solarino, S., Spallarossa, D., 2001. Seismicity and crustal structure beneath the western Ligurian Sea derived from local earthquake tomography: Tectonophysics, 339, 495-510, doi:10.1016/S0040-1951(01)00106-8.
- Faccenna, C., Becker, T.W., Lucente, F.P., Jolivet, L., and Rossetti, F., 2001. History of subduction and back-arc extension in the Central Mediterranean, Geophys. J. Int., 145, 1-21.
- Ferrari, G., 1991. The 1887 Ligurian earthquake: A detailed study from contemporary scientific observations, Tectonophysics, 193, 131-139, doi:10.1016/0040-1951(91)90194-W.
- Flueh, E.R., and Bialas, J. 1996 A digital, high data capacity ocean bottom recorder for seismic investigations, Int. Underwater Systems Design, 18, 3, 18-20.
- Fujie, G., Kasahara, J., Murase, K., Mochizuki, K., Kaneda, Y., 2008. Interactive analysis tools for the wide-angle seismic data for crustal structure study (Technical Report), Geophysical Exploration (BUTSURI-TANSA), Vol. 61, No. 1, pp26-33.
- Gailler, A., Klingelhofer, F., Oliver, J.-L., Aslanian, D., Sardinia scientific party, technical OBS team, 2009. Crustal structure of a young margin pair: New results across the Liguro-provencal Basin from wide-angle seismic tomography, Earth Planet. Sci. Lett., 286, 333-345, doi:10.1016/j.epsl.2009.07.001.
- Ginzburg, A., Makris, J., Nicolich, R., 1986. European Geotraverse: A seismic refraction profile across the Ligurian Sea, Tectonophysics, 126, 85-97.
- Handy, M.R., Schmid, S.M., Bousquet, R., Kissling, E., Bernoulli, D., 2010. Reconciling plate-tectonic reconstructions with the geological-geophysical record of spreading and subduction in the Alps. Earth Science Reviews, 102, 121-158.
- Hetényi, G. and 39 others, 2018. The AlpArray Seismic Network – a large-scale European experiment to image the Alpine orogen, Surveys in Geophysics, in review.
- Jolivet, L., Faccenna, C., 2000. Mediterranean extension and the African-Eurasia collision, tectonics, 19(6), 1095-1107, doi:10.1029/2000TC900018.
- Korenaga, J., W. S. Holbrook, and T. Dahl-Jensen (2000). Crustal structure of the southeast Greenland margin from joint refraction and reflection seismic tomography. J. Geophys. Res., 105, 21 591-21 614, doi: 10.1029/2000JB900188.
- Larroque, C., Béthoux, N., Calais, E., Courboulex, F., Deschamps, A., Déverchère, J., Stéphan, J.-F., Ritz, J.-F., Gilli, E., 2001. Active and recent deformation at the Southern Alps-Ligurian basin junction, Netherlands Journal of Geosciences, 80, 255-272.
- Larroque, C., Delous, B., Godel, B., Nocquet, J.-M., 2009. Active deformation at the southwestern Alps-Ligurian basin junction (France-Italy boundary): Evidence for recent change from compression to extension in the Argentera massif. Tectonophysics, 467, 22-34-, doi:10.1016/j.tecto.2008.12.013.
- Laubscher, H., Biella, G., Cassinis, R., Gelati, R., Lozej, A., Scarascia, S., Tabacco, I., 1992. The collisional knot in Liguria, Geologische Rundschau, 81/2, 275-289.
- Loubrieu, B., Mascle, J., et al. (19 authors), “Medimap Group” 2007. Morpho-bathymetry of the Mediterranean Sea. Ifremer and CIESM, scale 1/3 000 000, ISBN 92-990003-2-1.
- Makris, J., Egloff, F., Nicolich, R., Rihm, R., 1999. Crustal structure from the Ligurian Sea to the Northern Apennines – a wide angle seismic transect, Tectonophysics, 301, 305-319.
- Morelli, C., Nicolich, R., 1990. A cross section of the lithosphere along the European Geotraverse Southern Segment (from the Alps to Tunisia), Tectonophysics, 176, 229-243.

- Nocquet, J.-M., 2012. Present-day kinematics of the Mediterranean: A comprehensive overview of GPS results. *Tectonophysics*, 579, 220-242, doi:10.1016/j.tecto.2012.03.037.
- Rehault, J.P., Boillot, G., Mauffret, A., 1984. The western Mediterranean basin: Geological evolution, *Mar. Geol.*, 55, 447-477, doi:10.1016/0025-3227(84)90081-1.
- Rollet, N., Déverchère, J., Beslier, M.-O., Guennoc, P., Réhault, J.-P., Sosson, M., Truffert, C., 2002. Back arc extension, tectonic inheritance, and volcanism in the Ligurian Sea, Western Mediterranean. *Tectonics*, 21, 10.1029/2001TC900027.
- Sage, F., Beslier, M.-O., Thinon, I., Larroque, C., Dessa, J.-X., Migeon, S., Angelier, J., Guennoc, P., Schreiber, D., Michaud, F., Stephan, J.-F., Sonnette, L., 2011. Structure and evolution of a passive margin in a compressive environment: Example of the south-western Alps-Ligurian basin junction during the Cenozoic, *Mar. Petr. Geol.*, 28, 1262-1282, doi:10.1016/j.marpgeo.2011.03.012.
- Solarino, S., Spalarossa, D., Parolia, S., Cattaneo, M., Eva, C., 1996. Litho-asthenospheric structures of northern Italy as inferred from teleseismic P wave tomography: *Tectonophysics*, 260, 271-289, doi:10.1016/0040-1951(95)00201-4.
- Thouvenot, F., Paul, A., Fréchet, J., Béthoux, N., Jenatton, L., Guiguet, R., 2007. Are there really superposed Mohos in the south-western Alps? New seismic data from fan-profiling reflections, *Geophys. J. Int.*, 170, 1180-1194, doi:10.1111/J.1365-246X.2007.03463.x.
- Vignaroli, G., Faccenna, C., Jolivet, L., Piromallo, C., Rossetti, F., 2008. Subduction polarity reversal at the junction between the Western Alps and the Northern Apennines, Italy, *Tectonophysics*, 450, 34-50, doi:10.1016/j.tecto.2007.12.012.
- Waldhauser, F., Kissling, E., Ansorge, J., Mueller, S., 1998. Three-dimensional interface modelling with two-dimensional seismic data: the Alpine crust-mantle boundary, *Geophys. J. Int.* 135, 264-278, doi:10.1046/j.1365-246X.1998.00647.x.
- Zelt, C., and R. Smith, 1992. Seismic travelttime inversion for 2-D crustal velocity structure, *Geophys. J. Int.*, 108, 16-34.

## Appendices

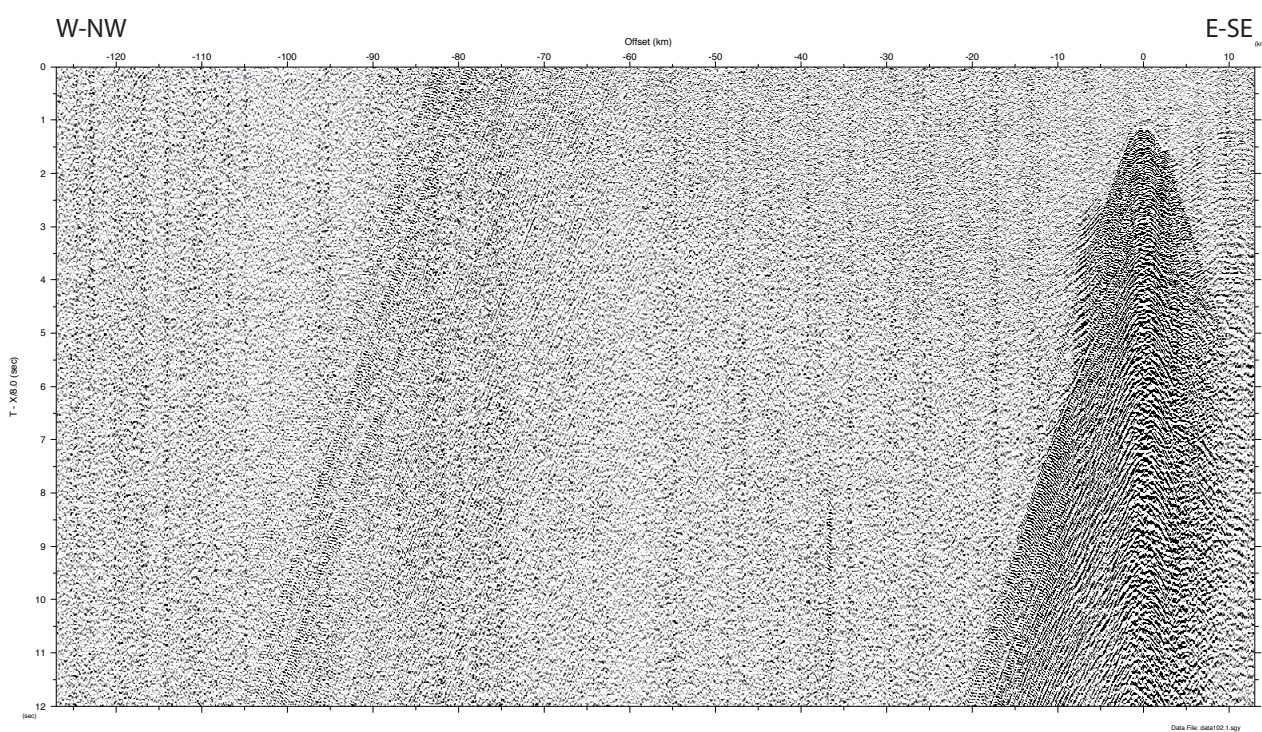
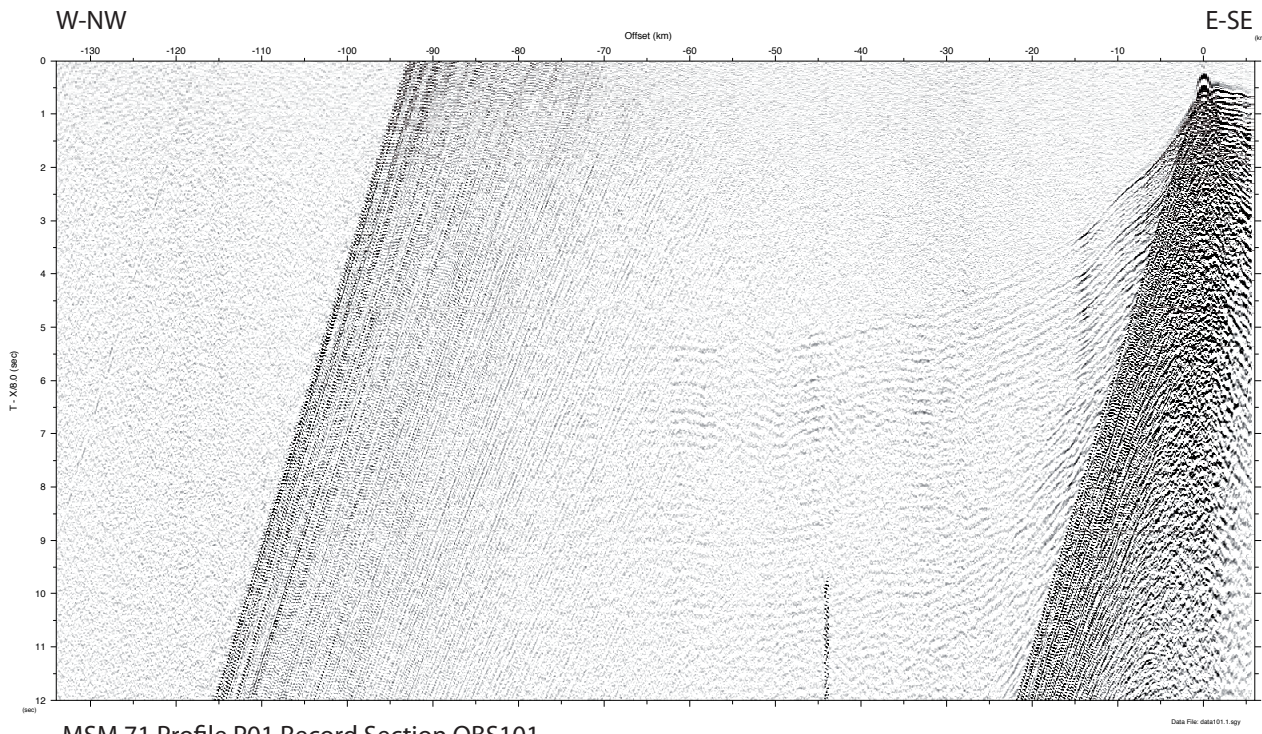
(H. Kopp and all Cruise Participants)

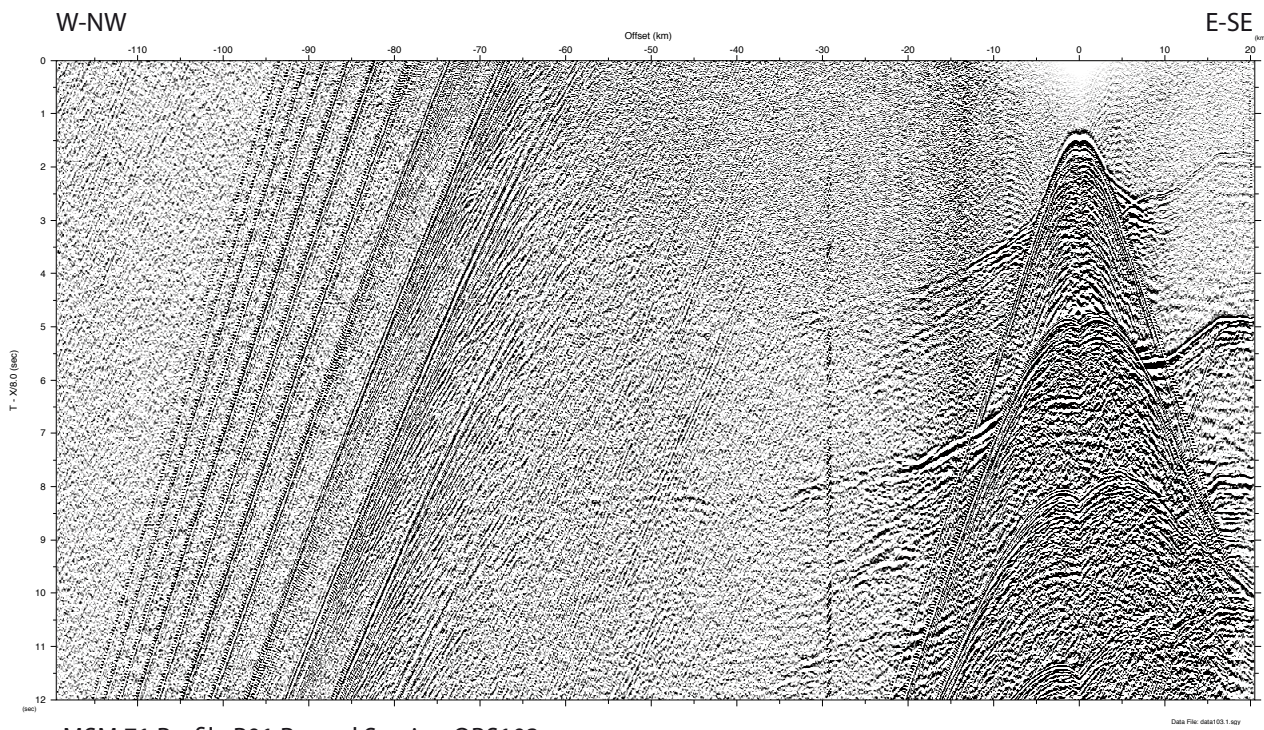
### Appendix A: XSV Sound velocity profiles



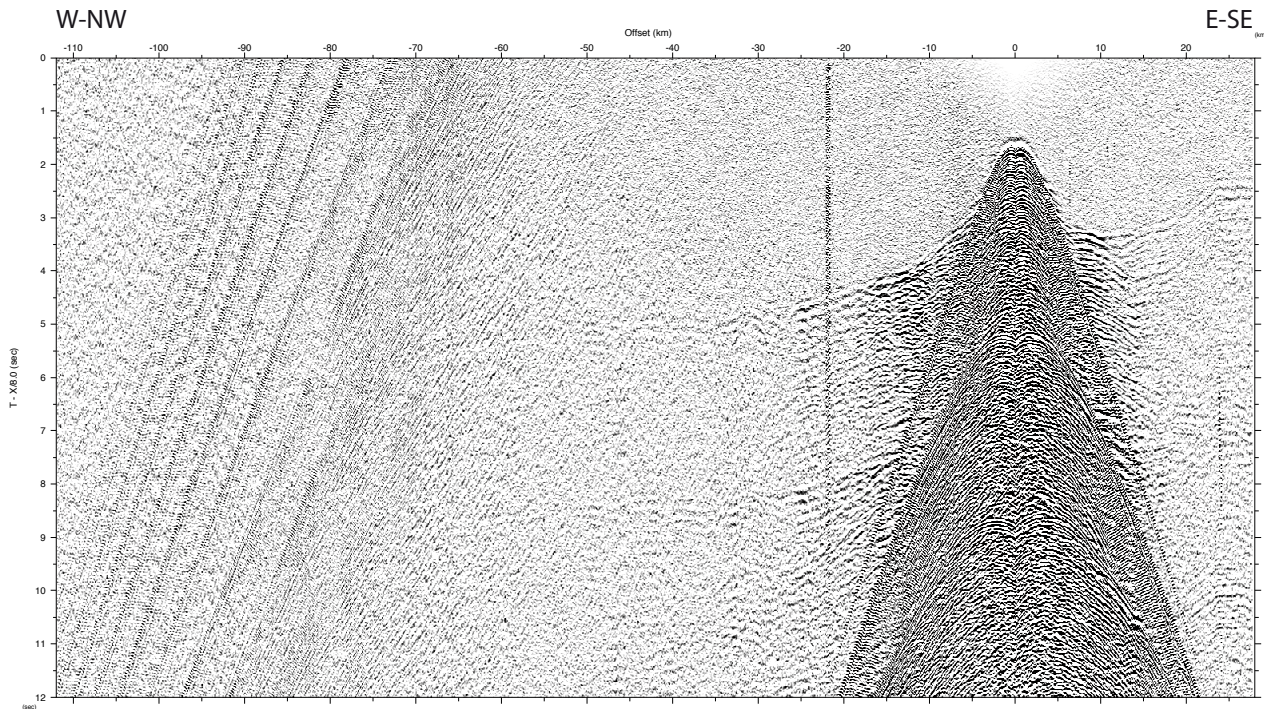
XSV1 was launched at  $42^{\circ}32,45'N / 05^{\circ}35,33'E$ , reaching a final depth of 1956 m, XSV2 was launched at  $42^{\circ}52.80'N/08^{\circ}37,29'E$ , reaching a depth of 1986 m.

## Appendix B: OBS Record Sections (Profiles P01, P02)

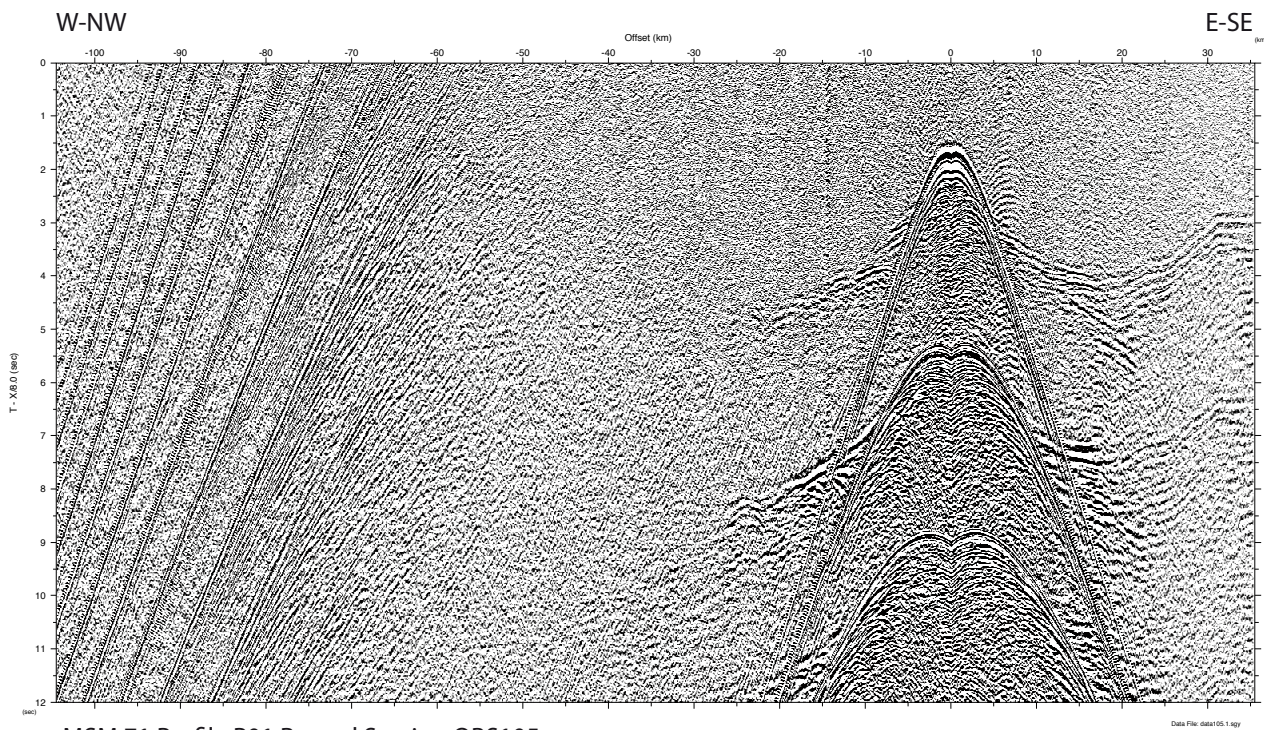




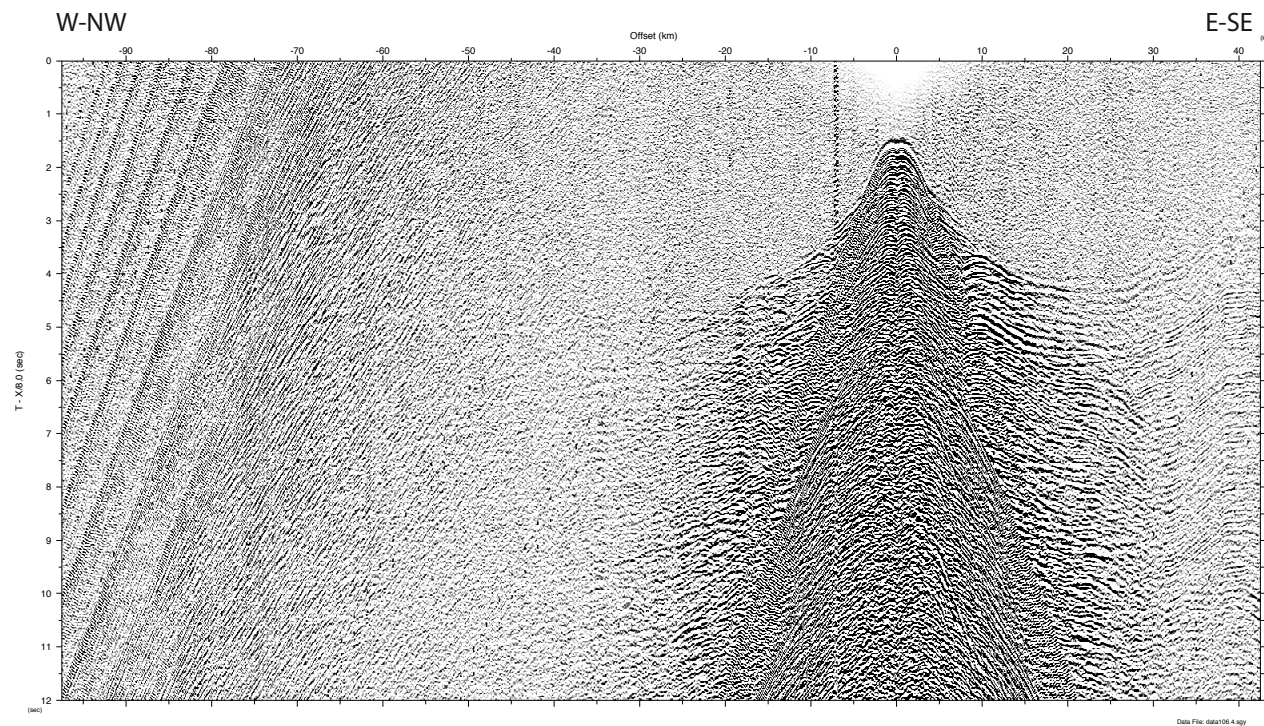
MSM 71 Profile P01 Record Section OBS103



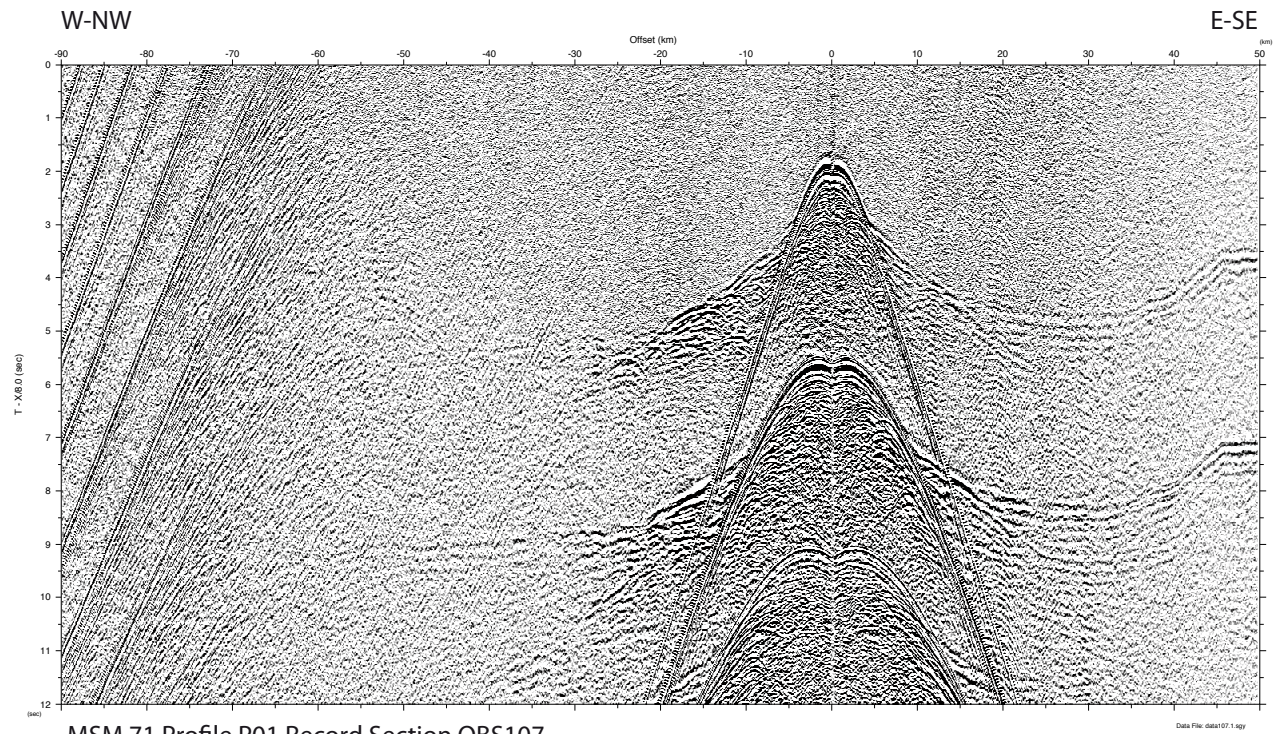
MSM 71 Profile P01 Record Section OBS104 - vertical component



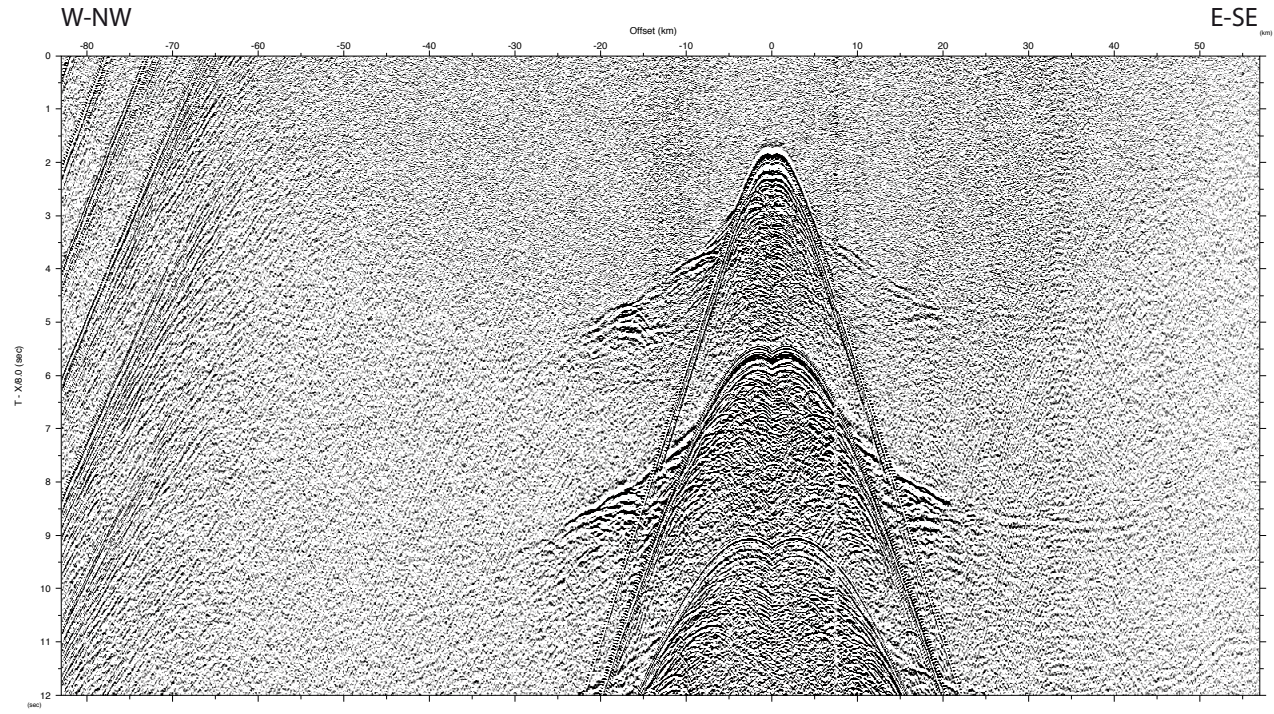
MSM 71 Profile P01 Record Section OBS105



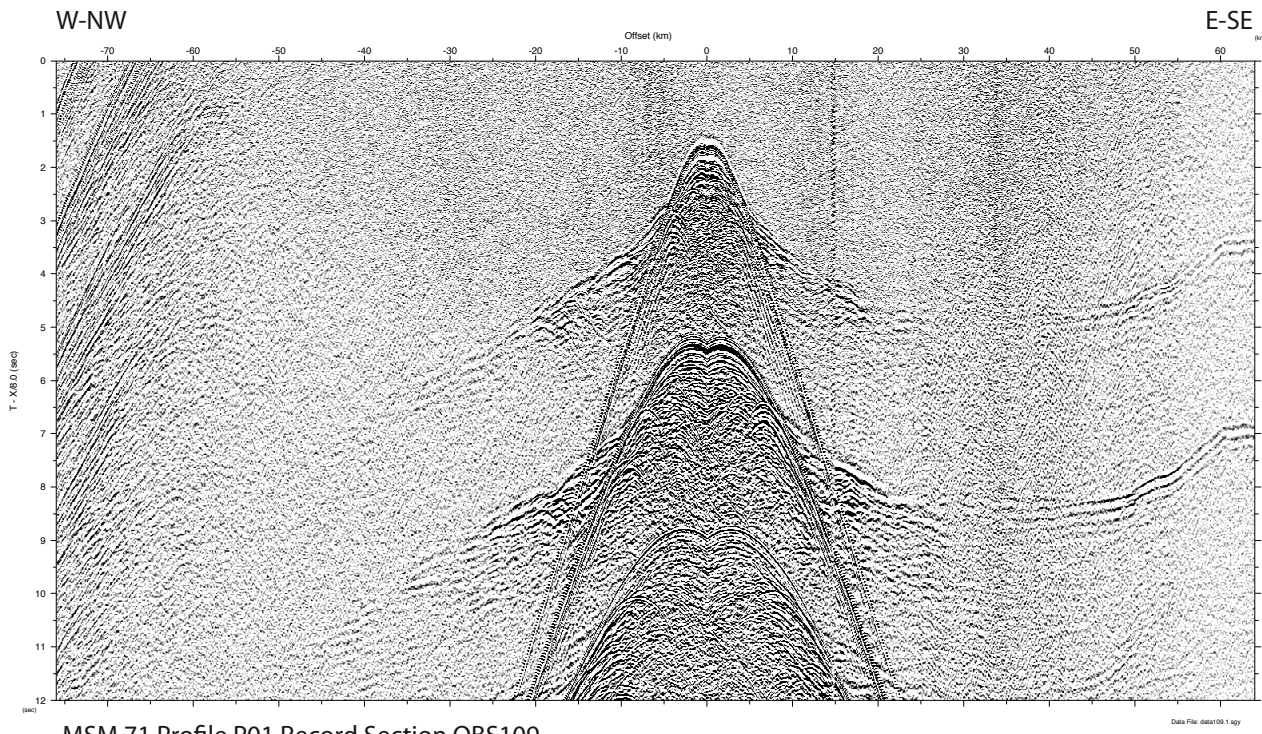
MSM 71 Profile P01 Record Section OBS106 - vertical component



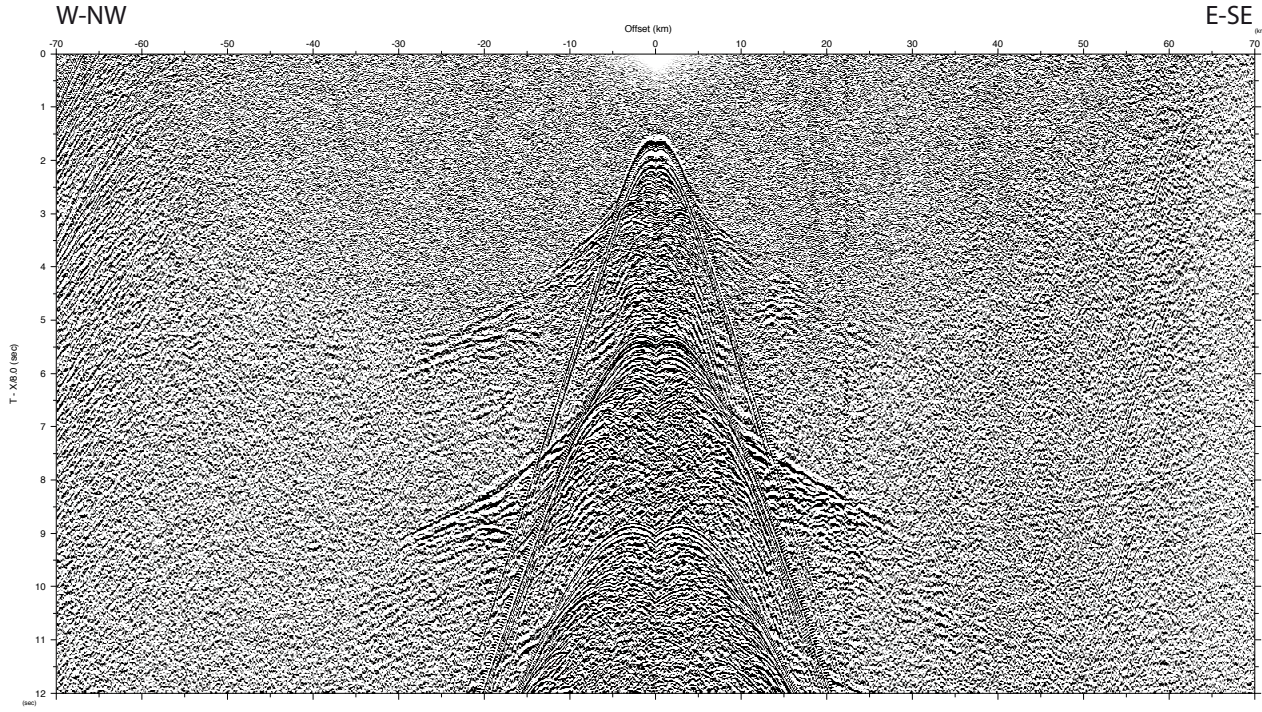
MSM 71 Profile P01 Record Section OBS107



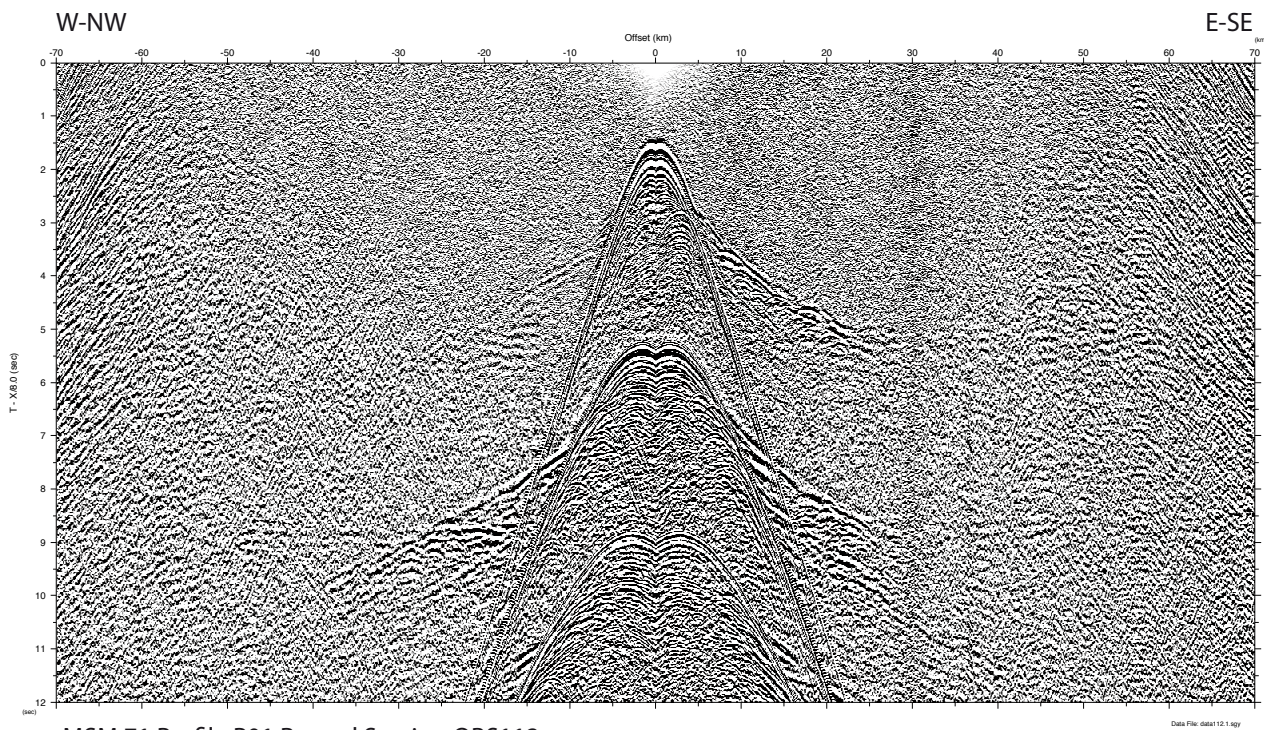
MSM 71 Profile P01 Record Section OBS108



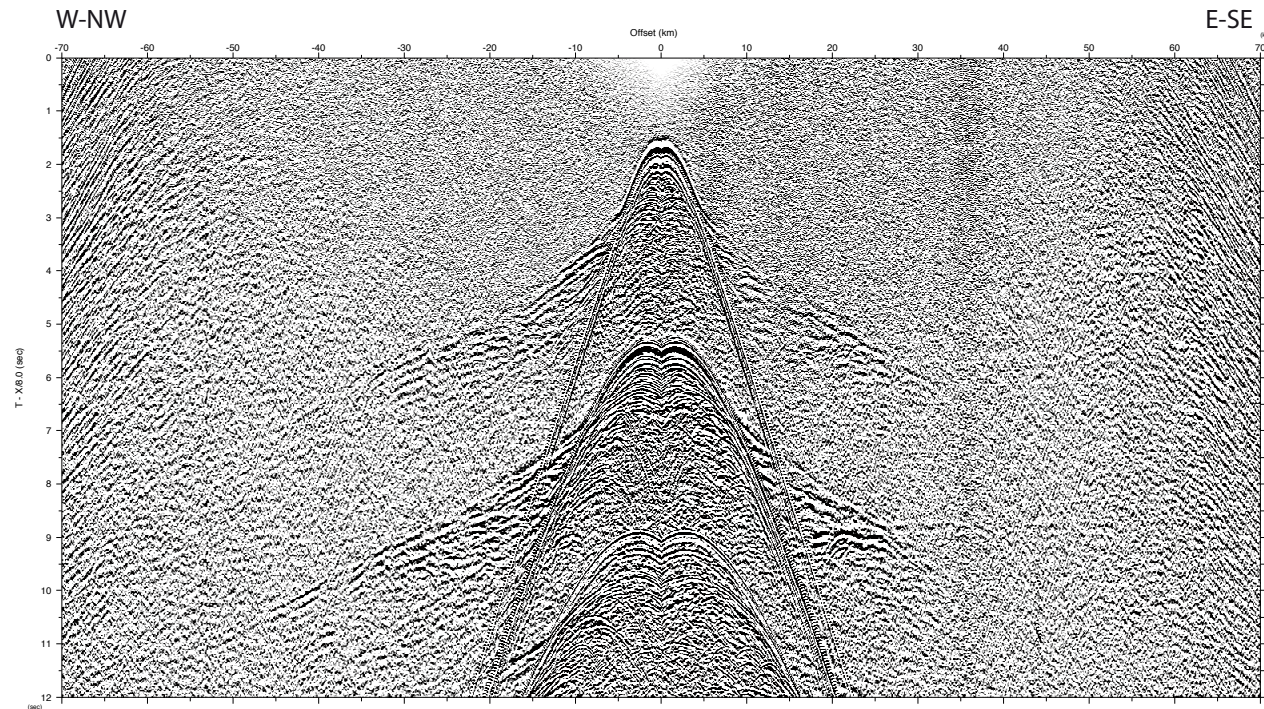
MSM 71 Profile P01 Record Section OBS109



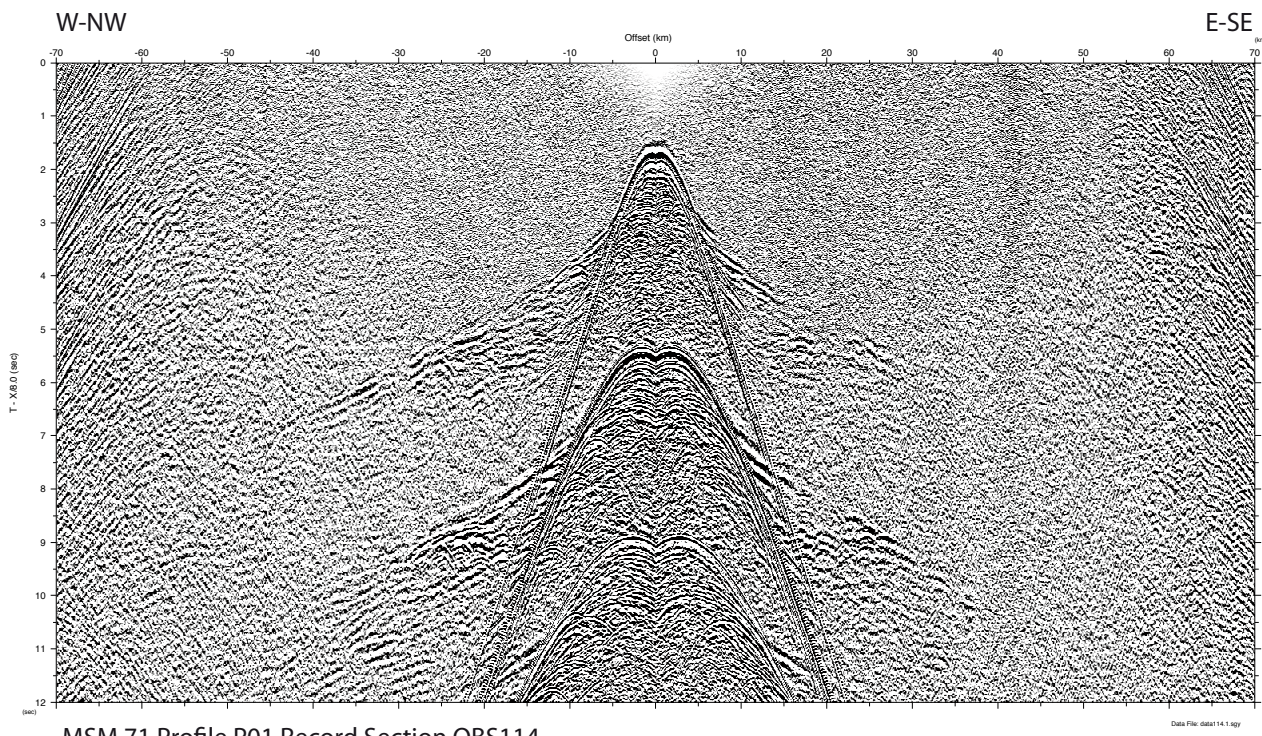
MSM 71 Profile P01 Record Section OBS110



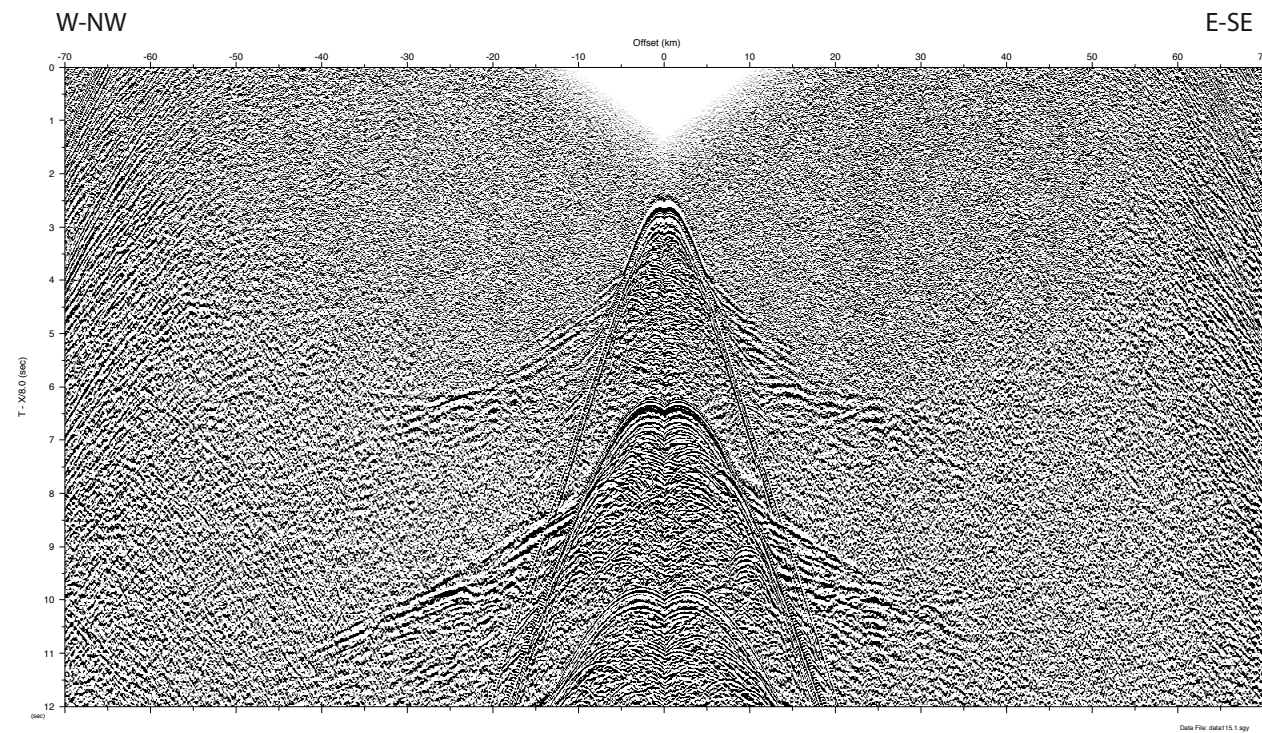
MSM 71 Profile P01 Record Section OBS112



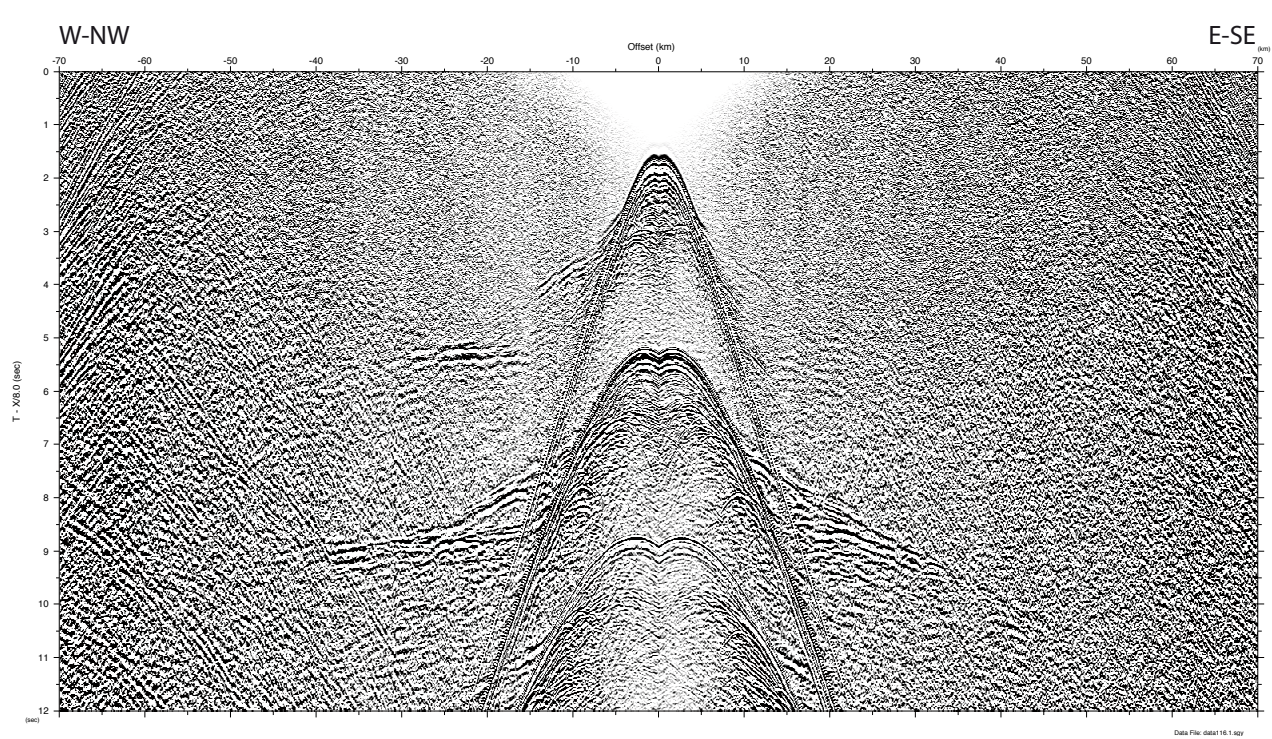
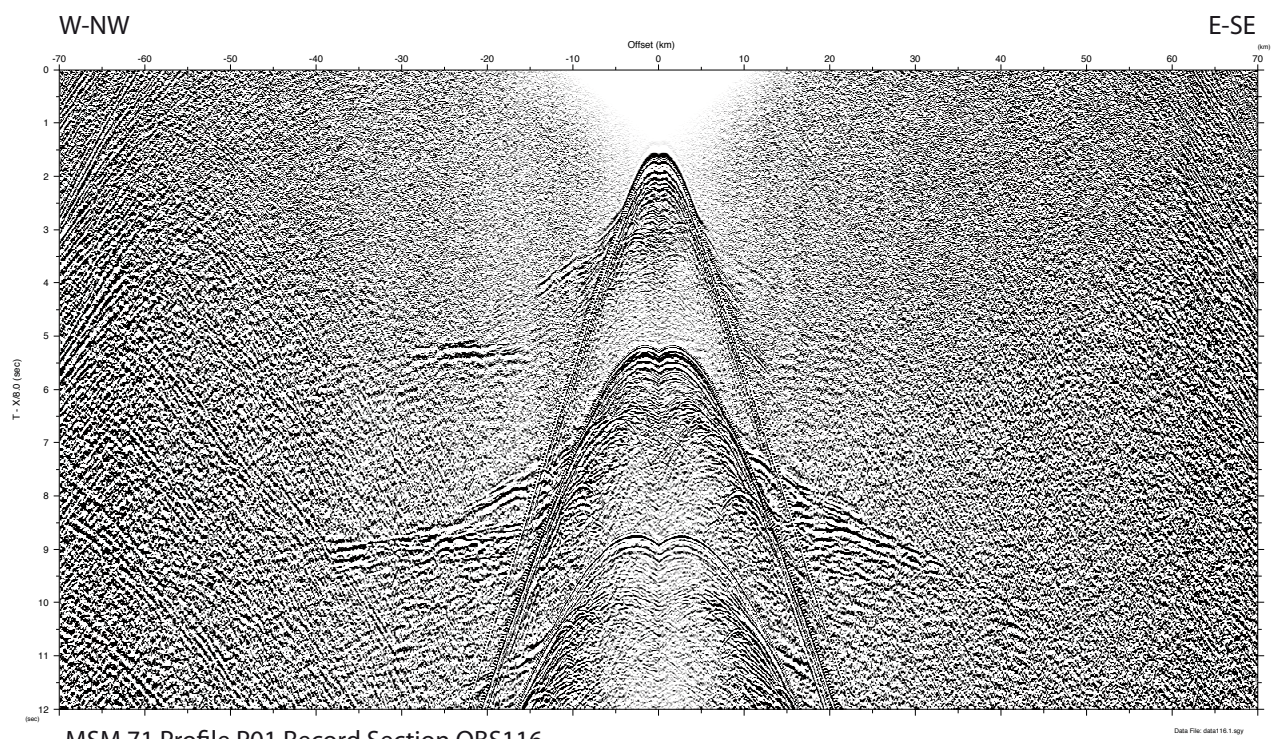
MSM 71 Profile P01 Record Section OBS113

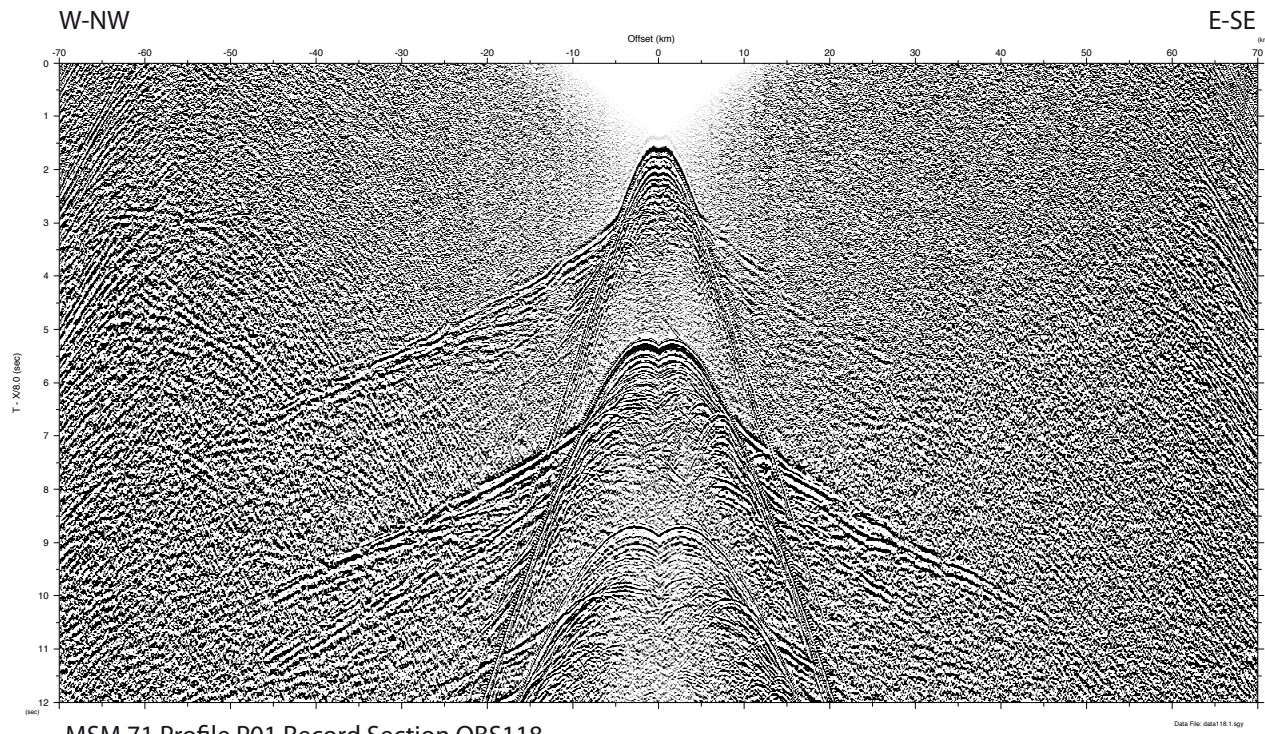


MSM 71 Profile P01 Record Section OBS114

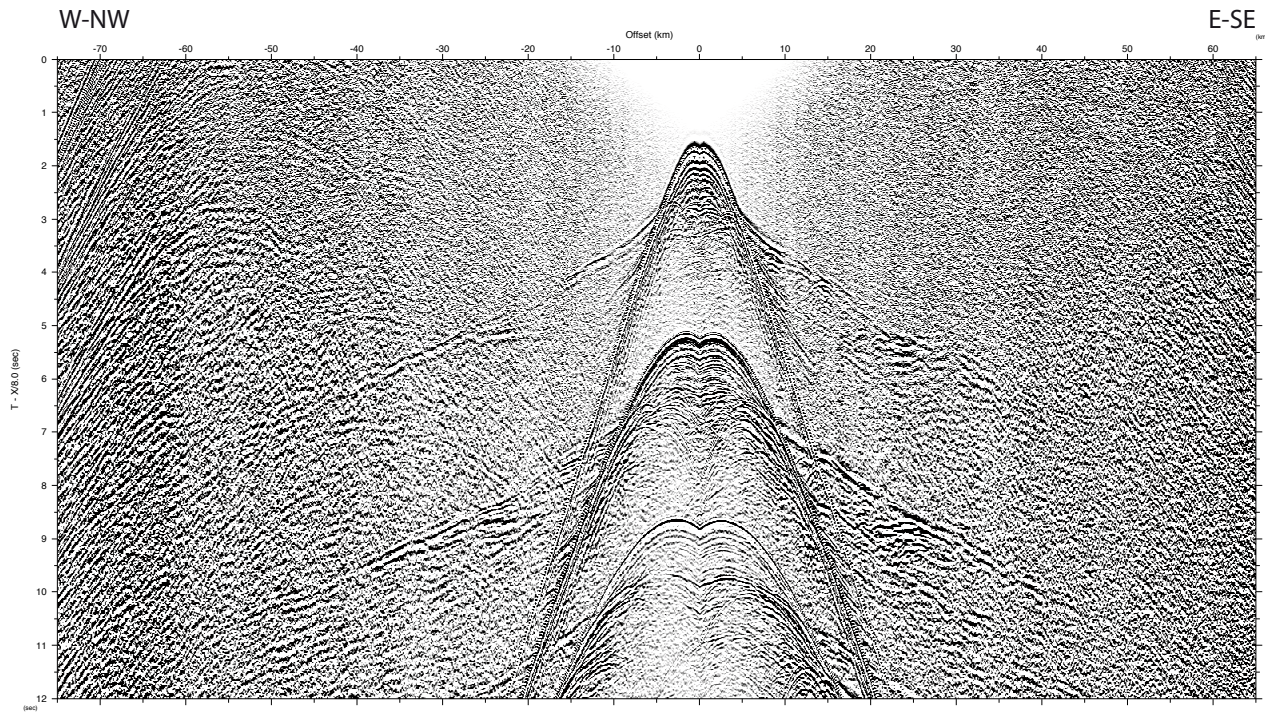


MSM 71 Profile P01 Record Section OBS115

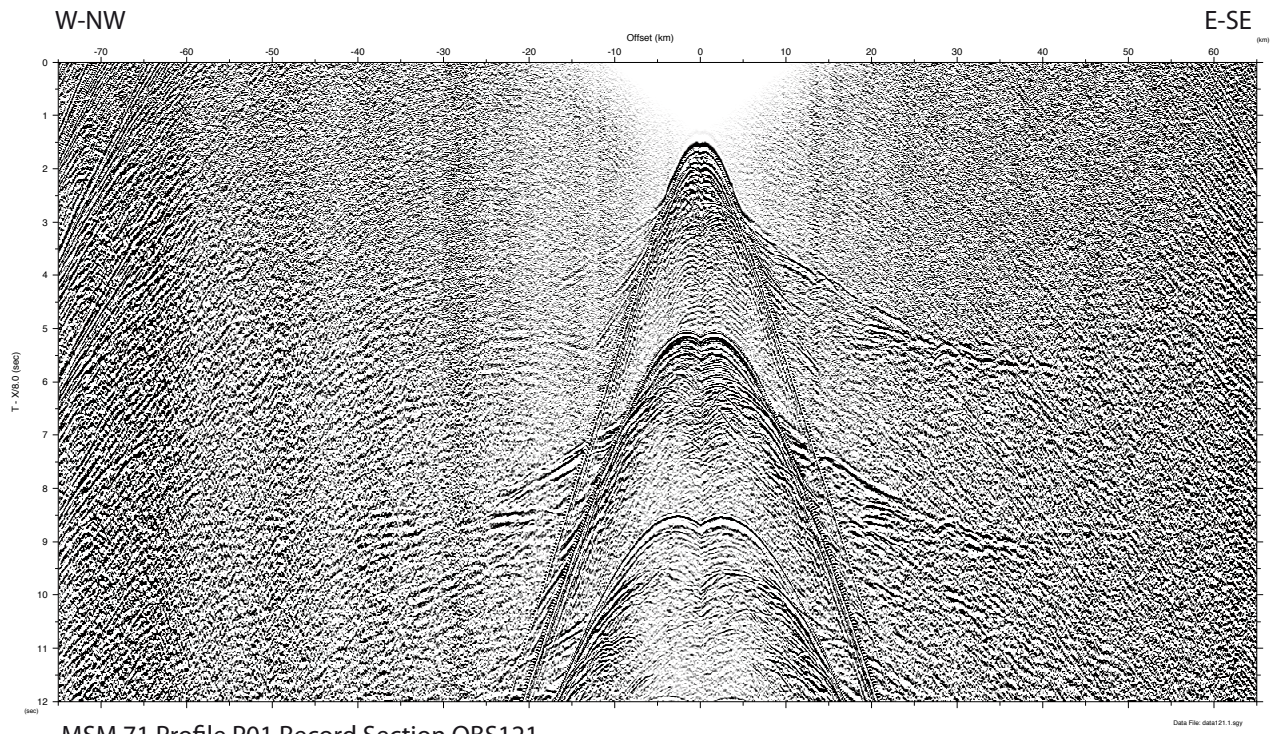




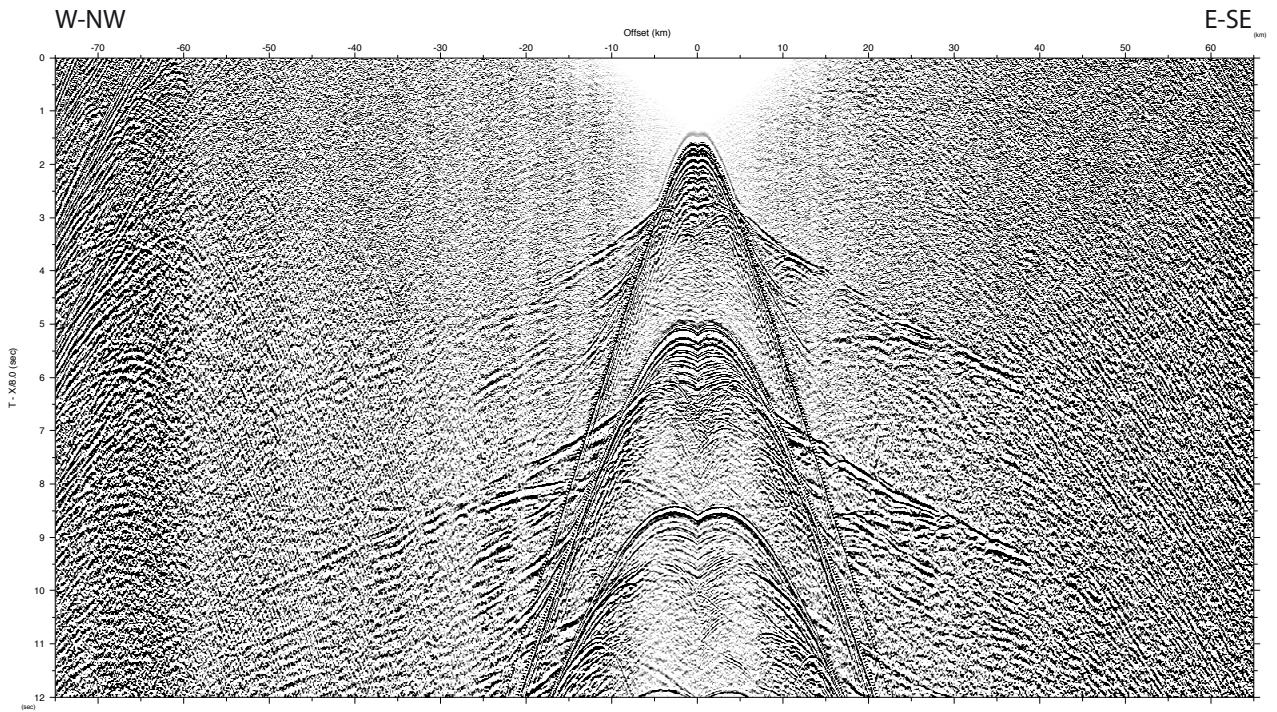
MSM 71 Profile P01 Record Section OBS118



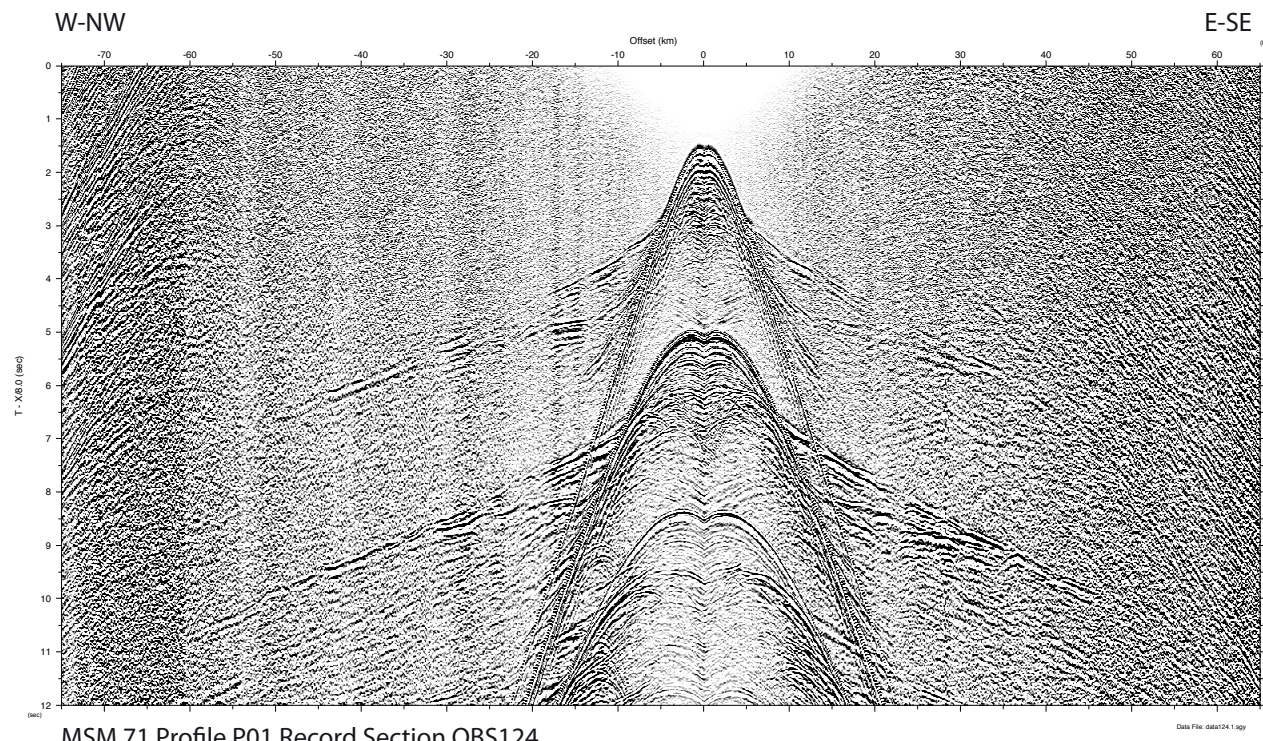
MSM 71 Profile P01 Record Section OBS119



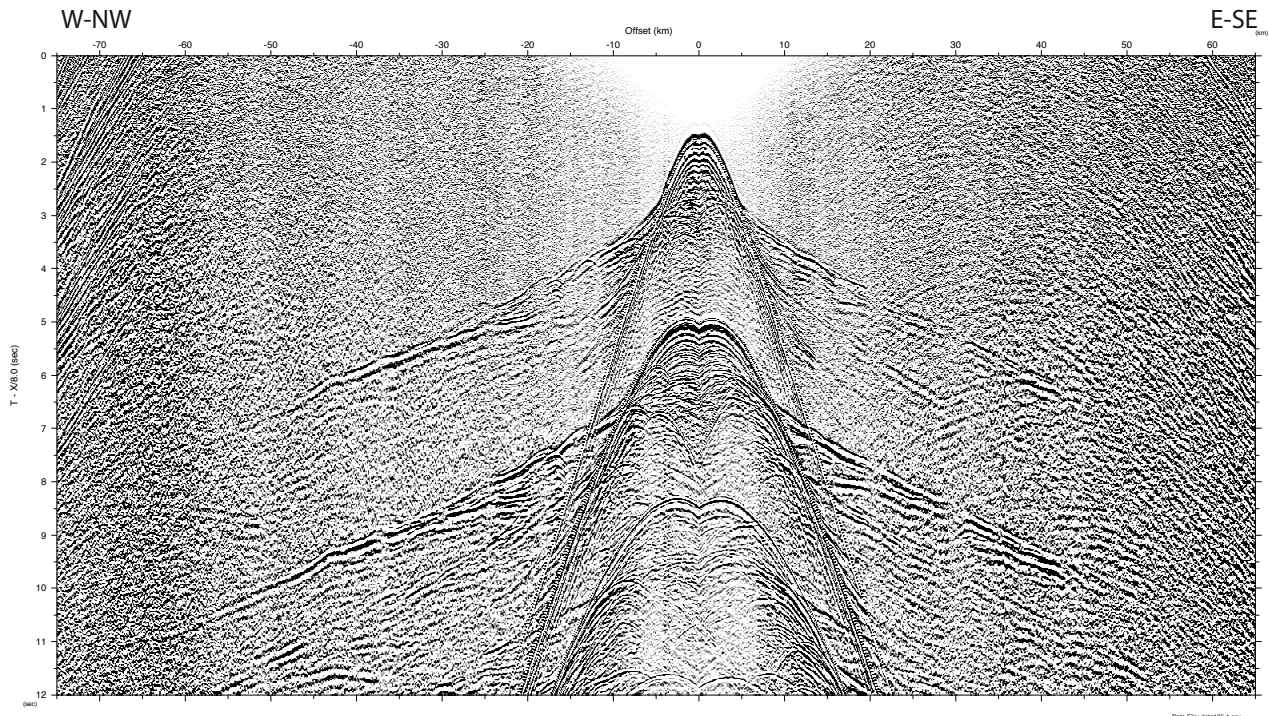
MSM 71 Profile P01 Record Section OBS121



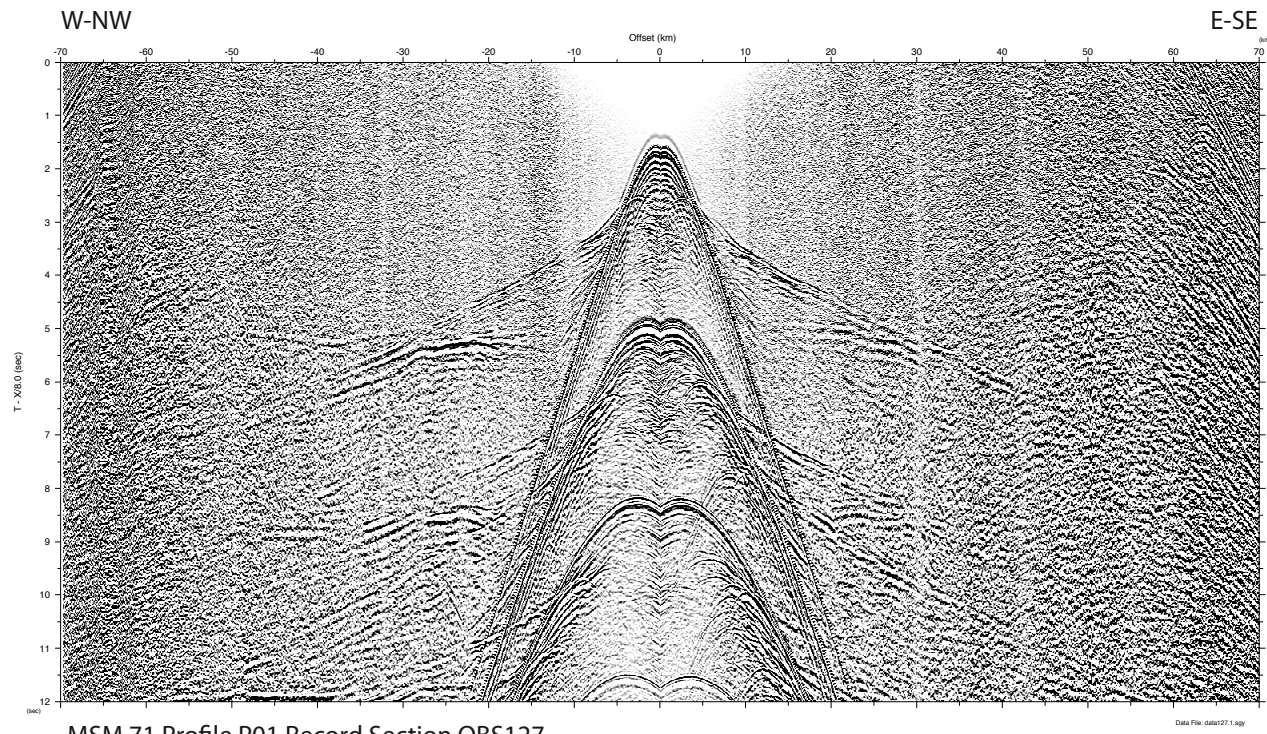
MSM 71 Profile P01 Record Section OBS123



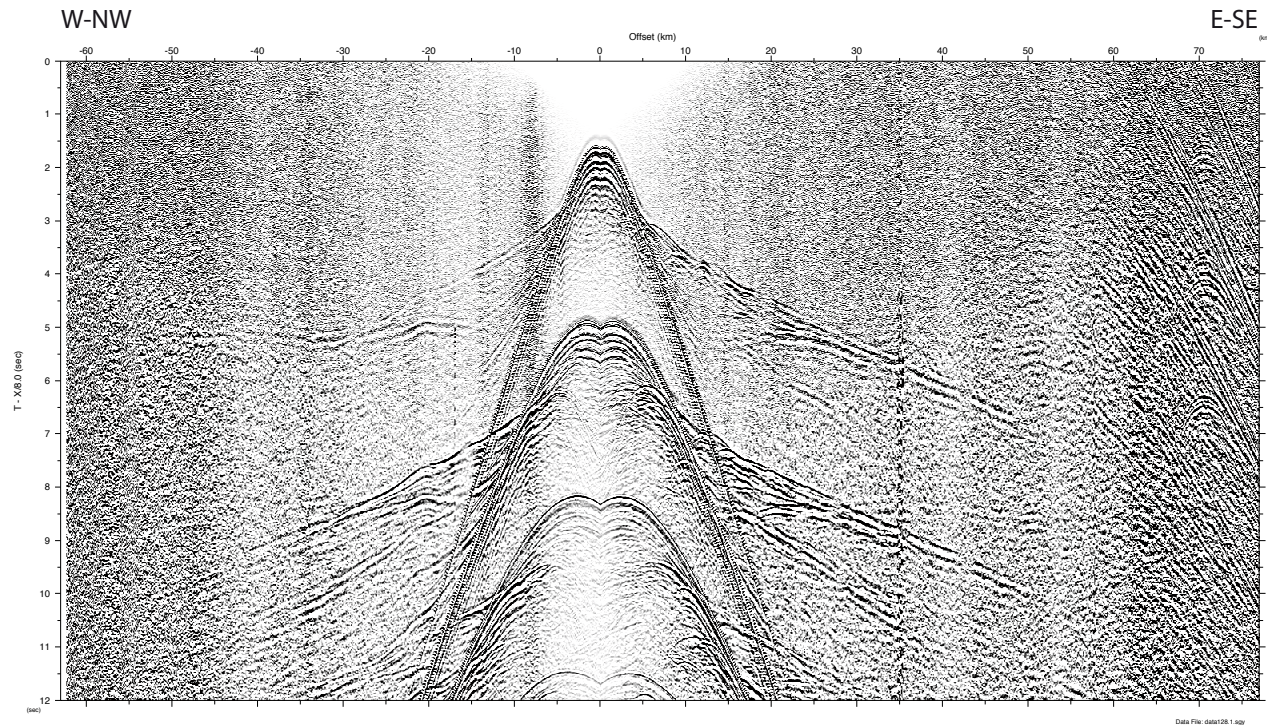
MSM 71 Profile P01 Record Section OBS124



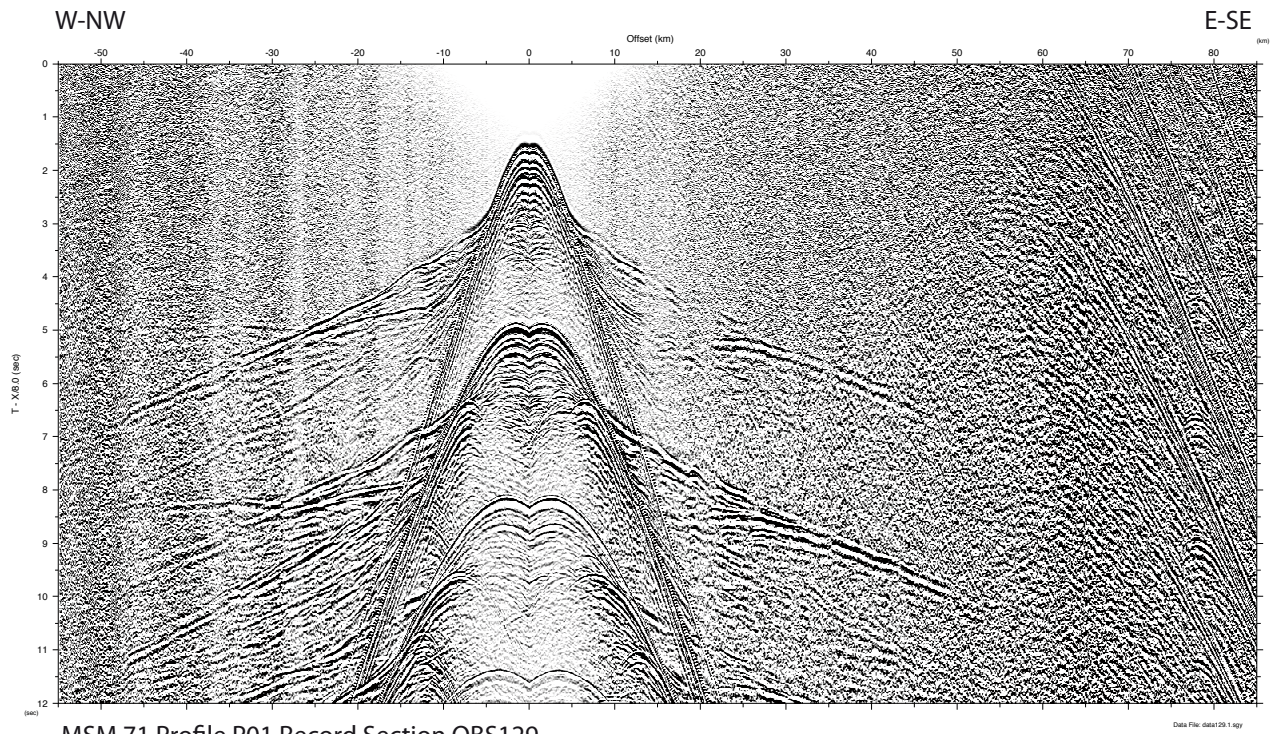
MSM 71 Profile P01 Record Section OBS125



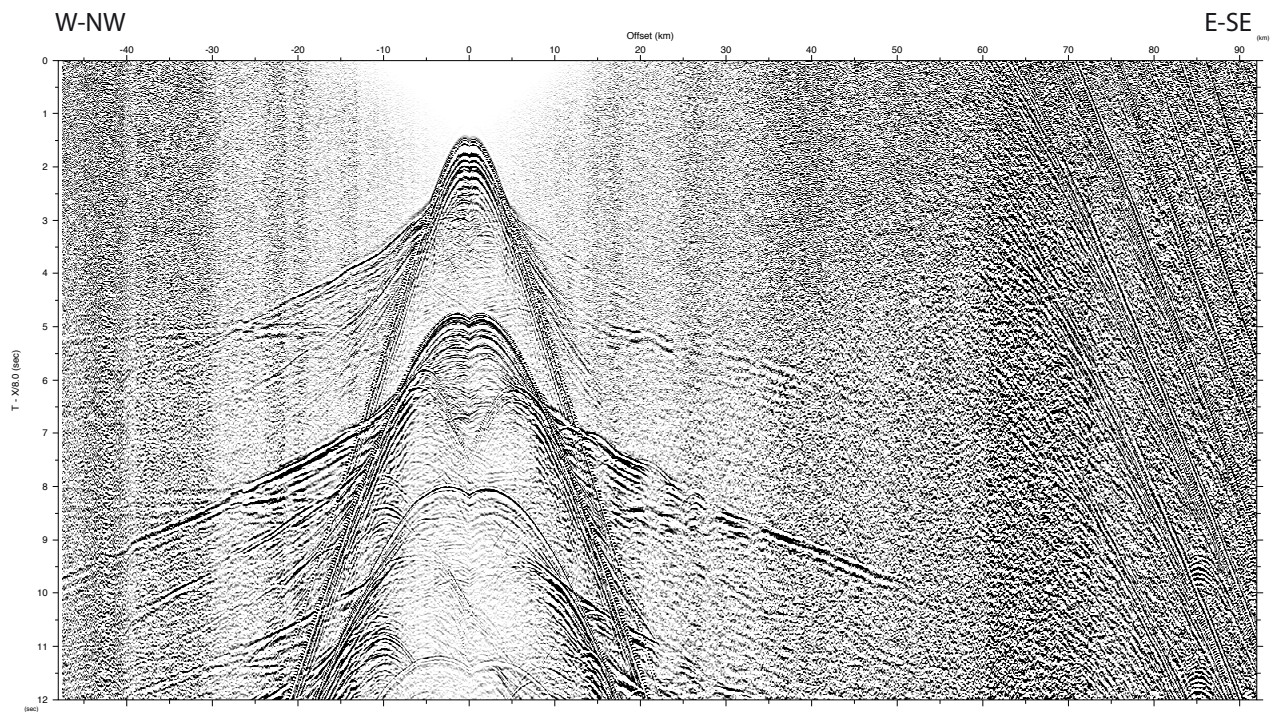
MSM 71 Profile P01 Record Section OBS127



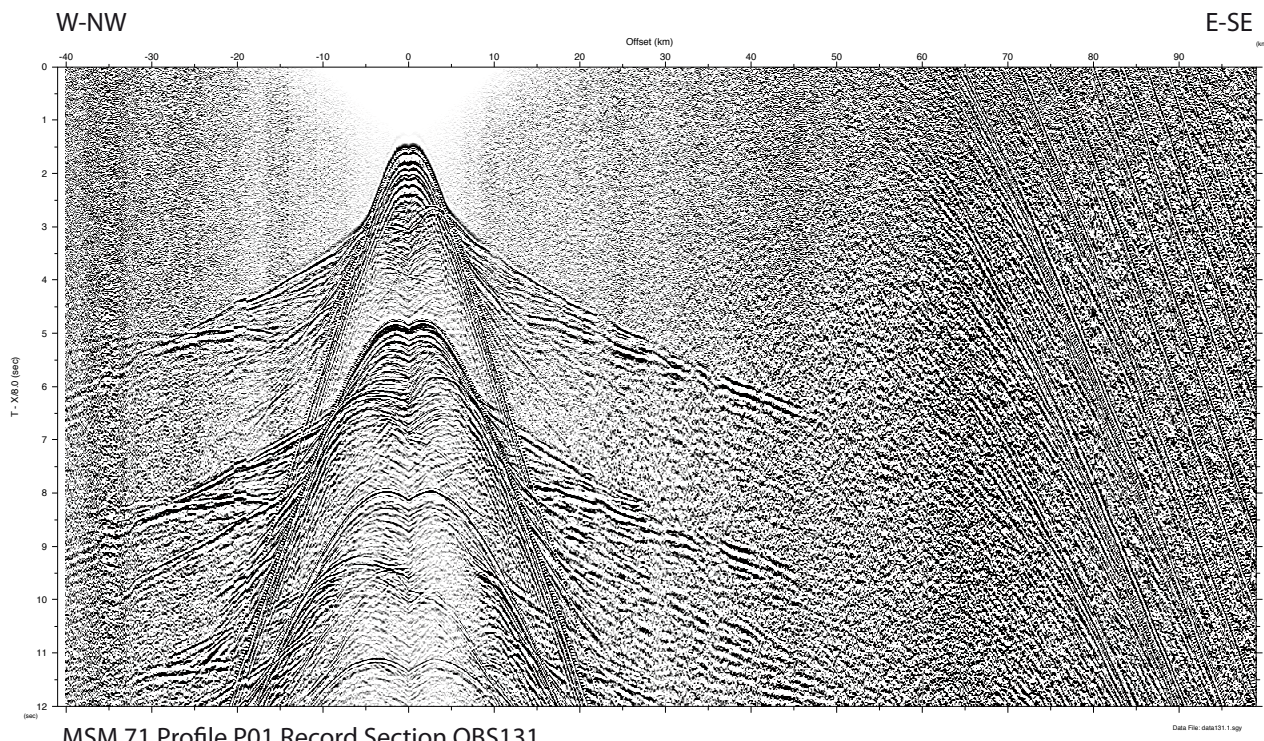
MSM 71 Profile P01 Record Section OBS128



MSM 71 Profile P01 Record Section OBS129

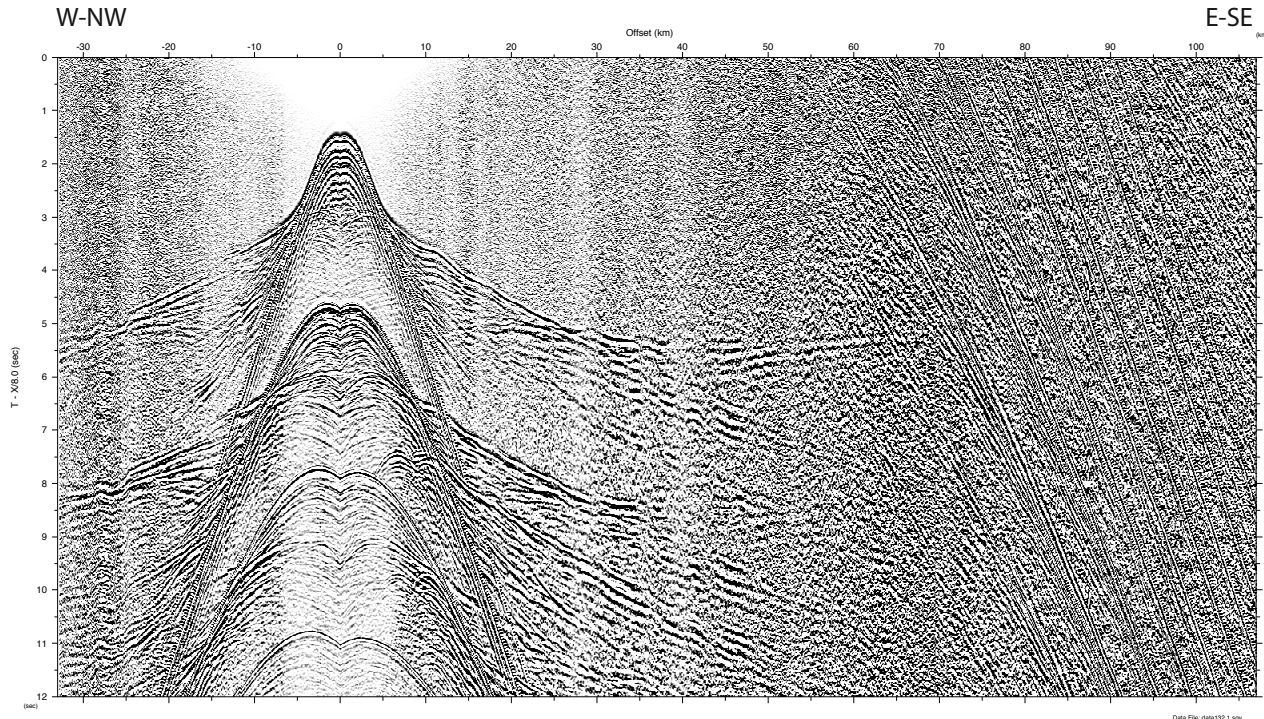


MSM 71 Profile P01 Record Section OBS130



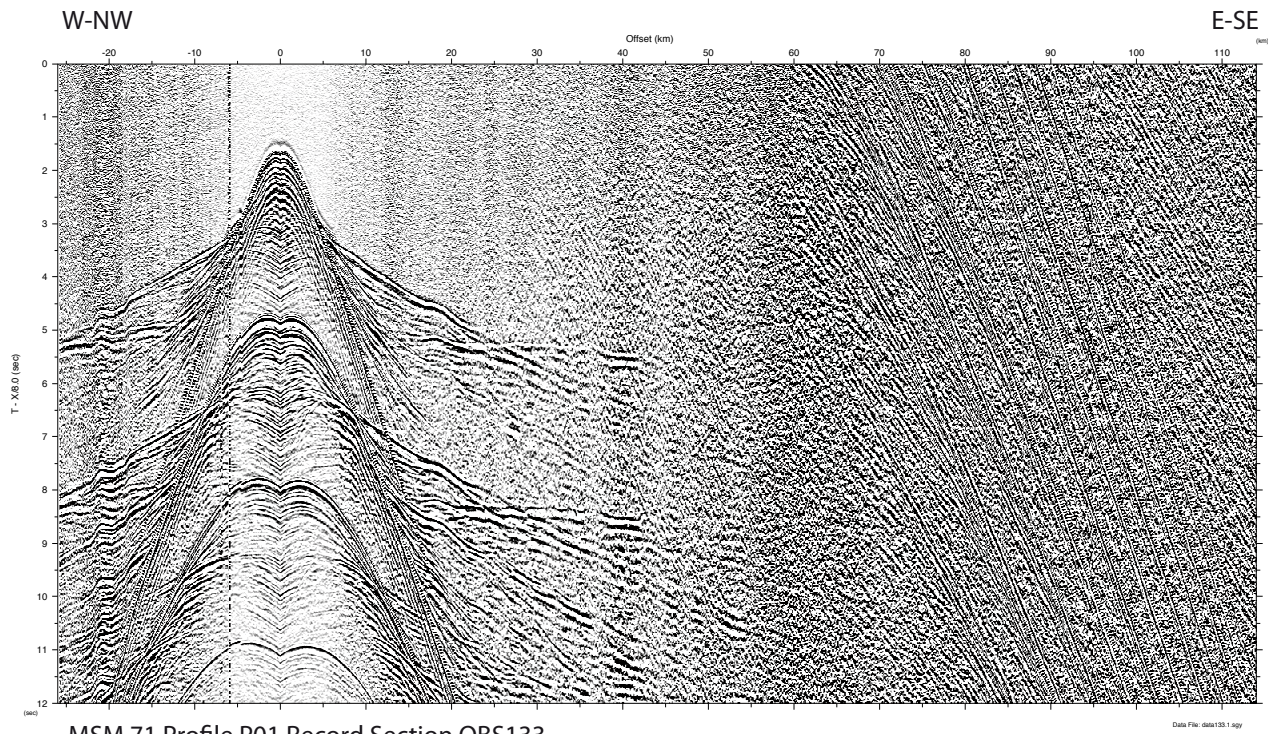
MSM 71 Profile P01 Record Section OBS131

Data File: data131.1.sgy

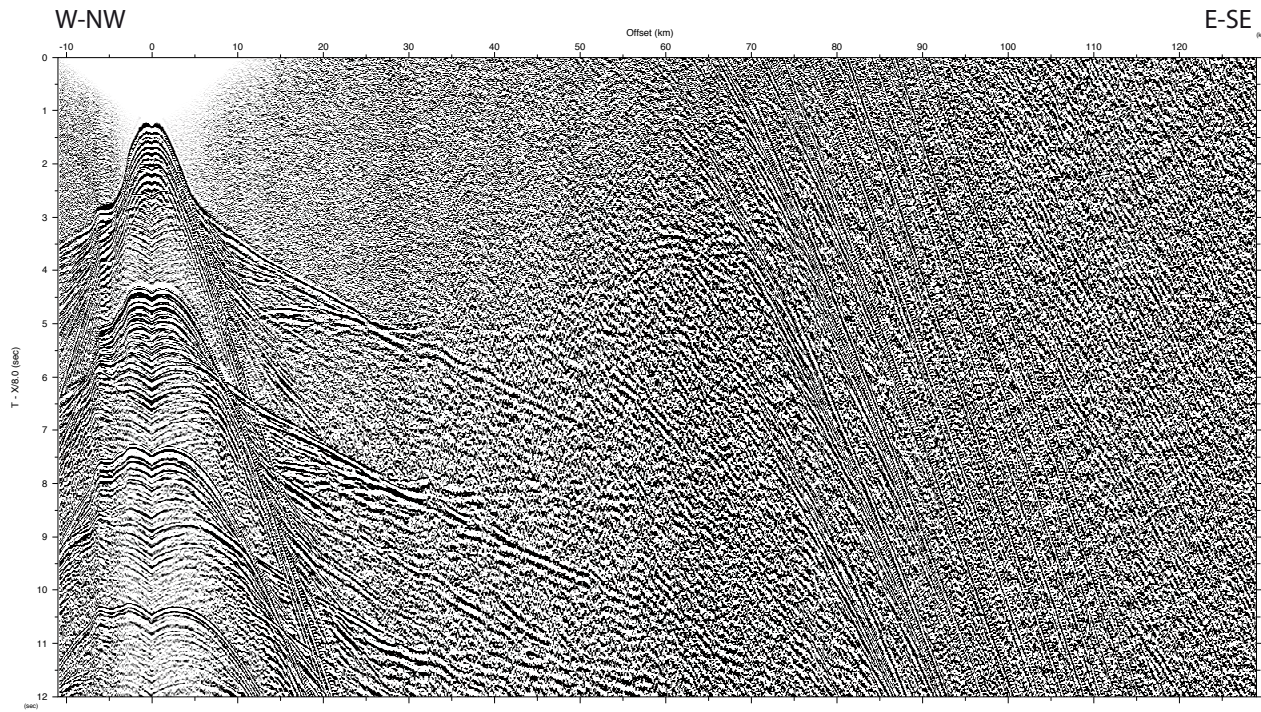


MSM 71 Profile P01 Record Section OBS132

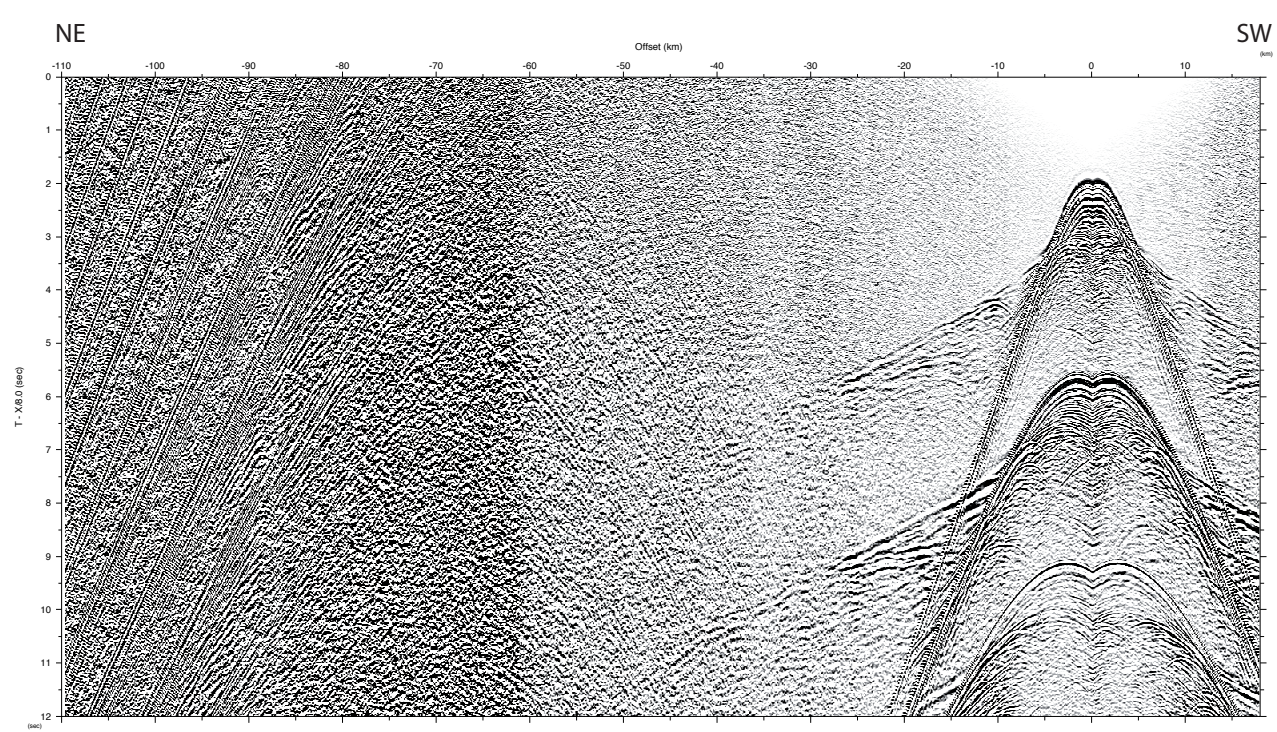
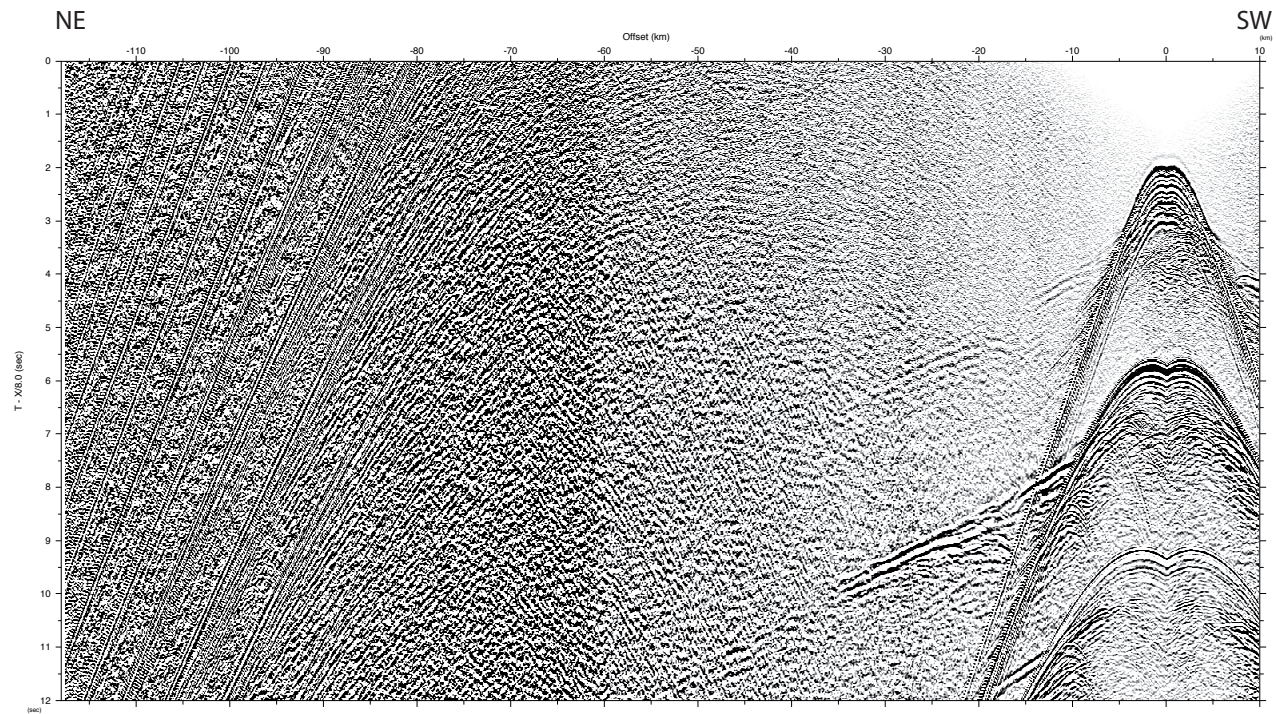
Data File: data132.1.sgy

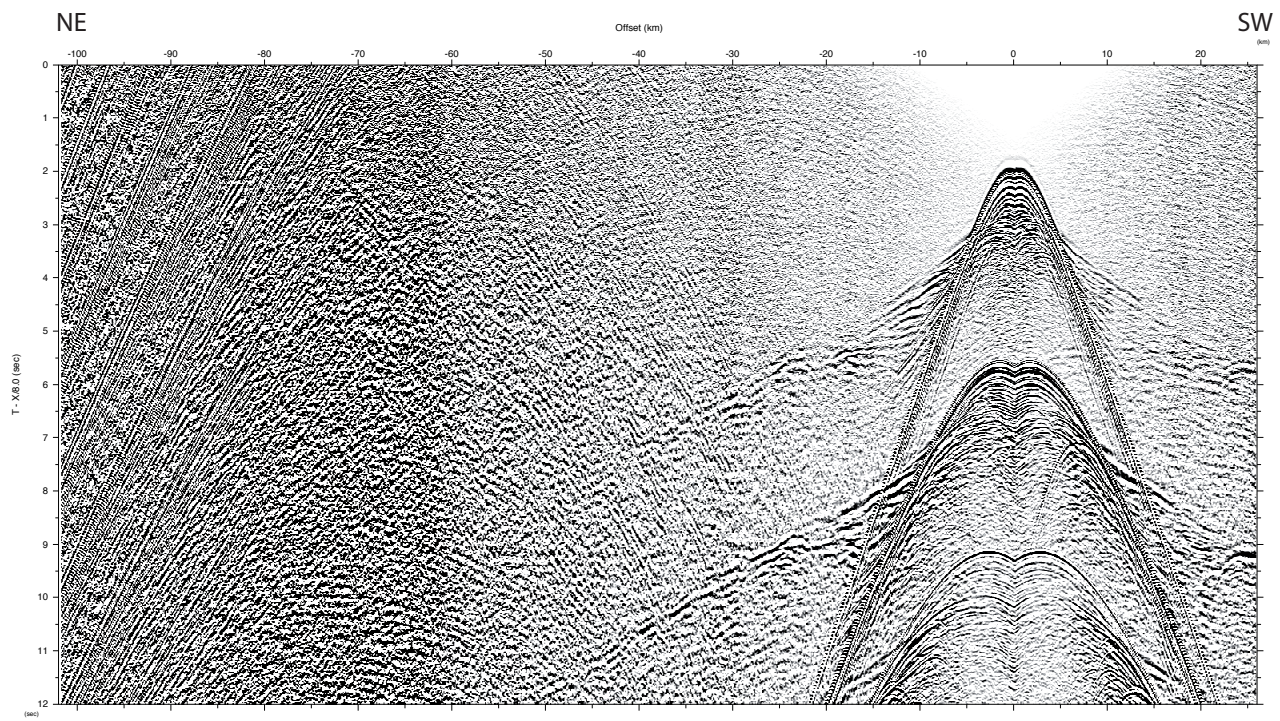


MSM 71 Profile P01 Record Section OBS133

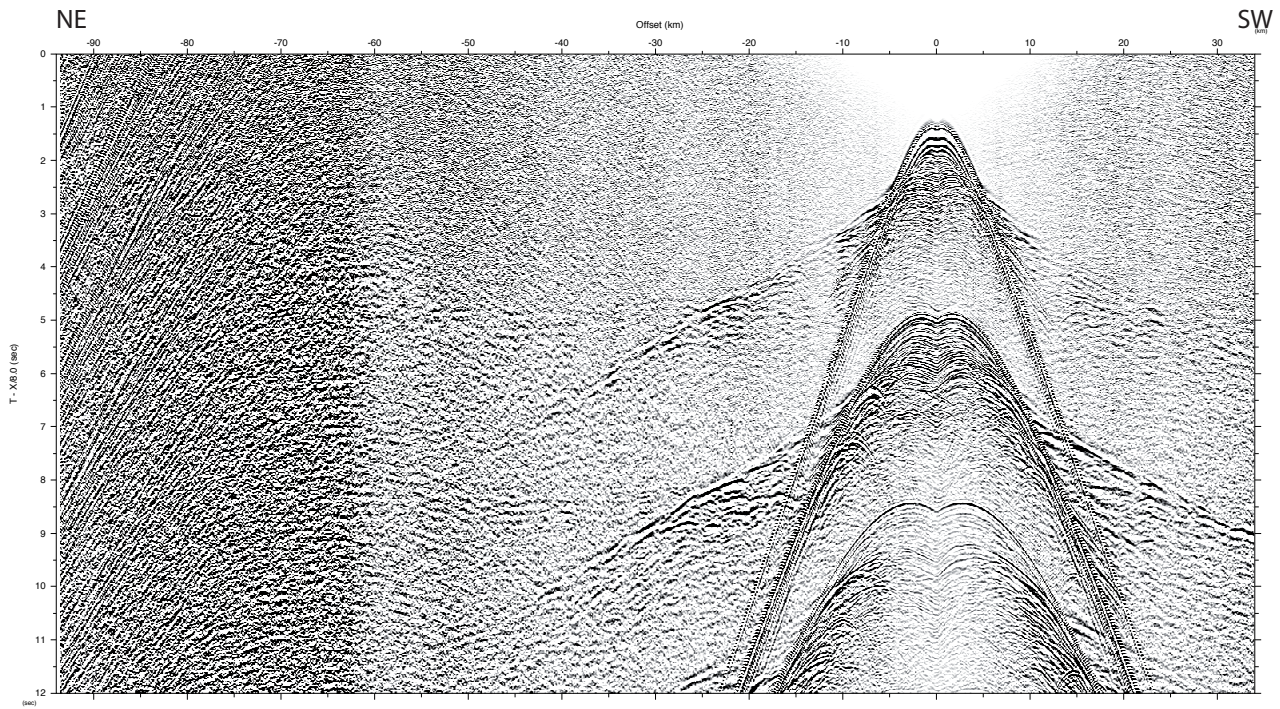


MSM 71 Profile P01 Record Section OBS135

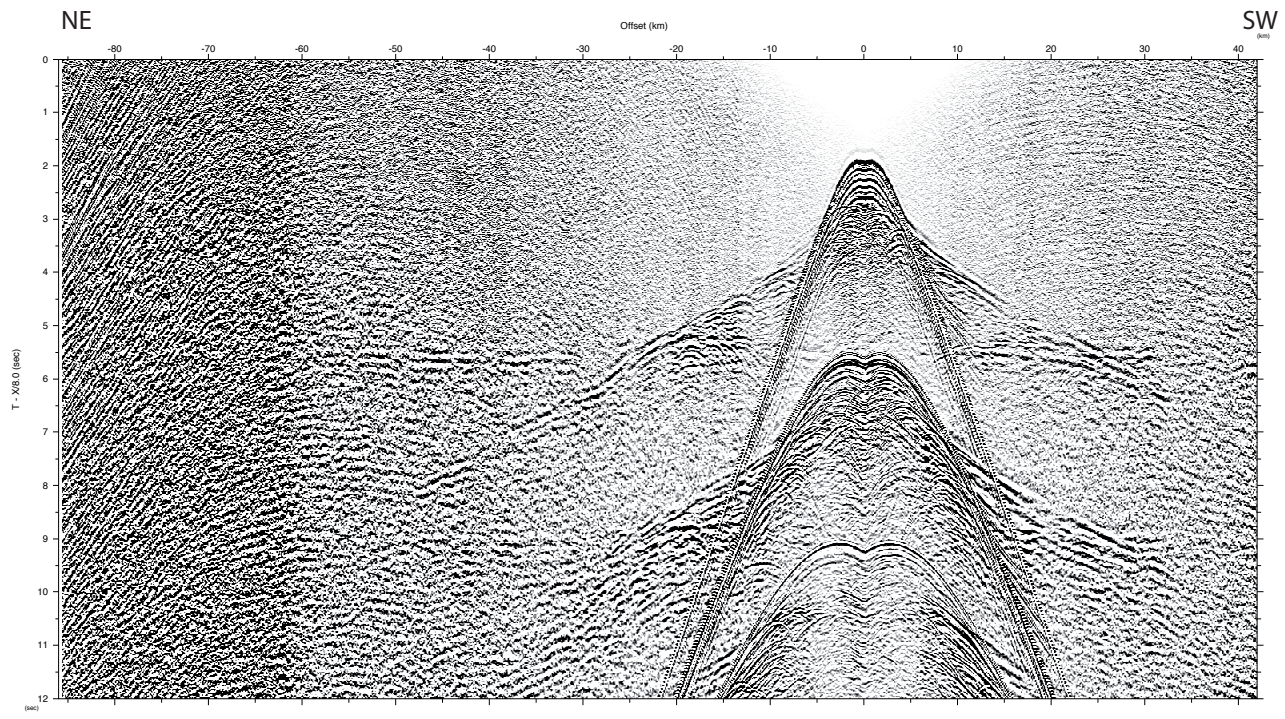




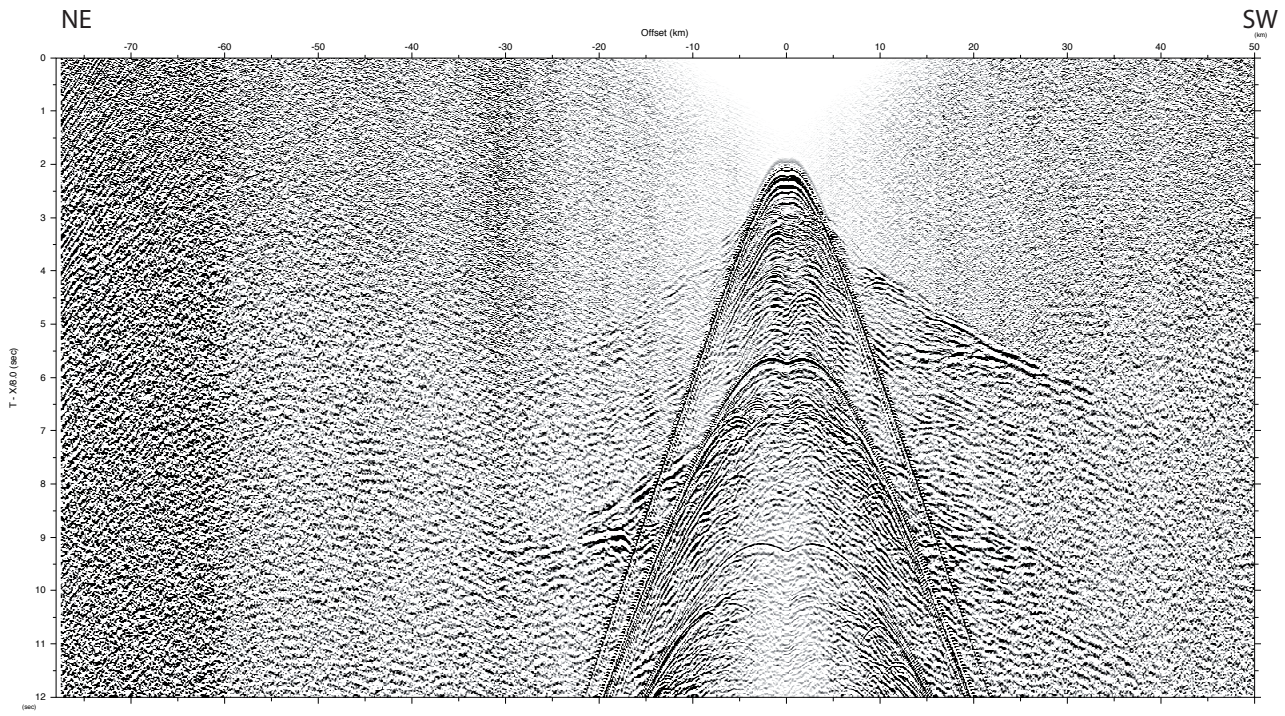
MSM 71 Profile P02 Record Section OBS203



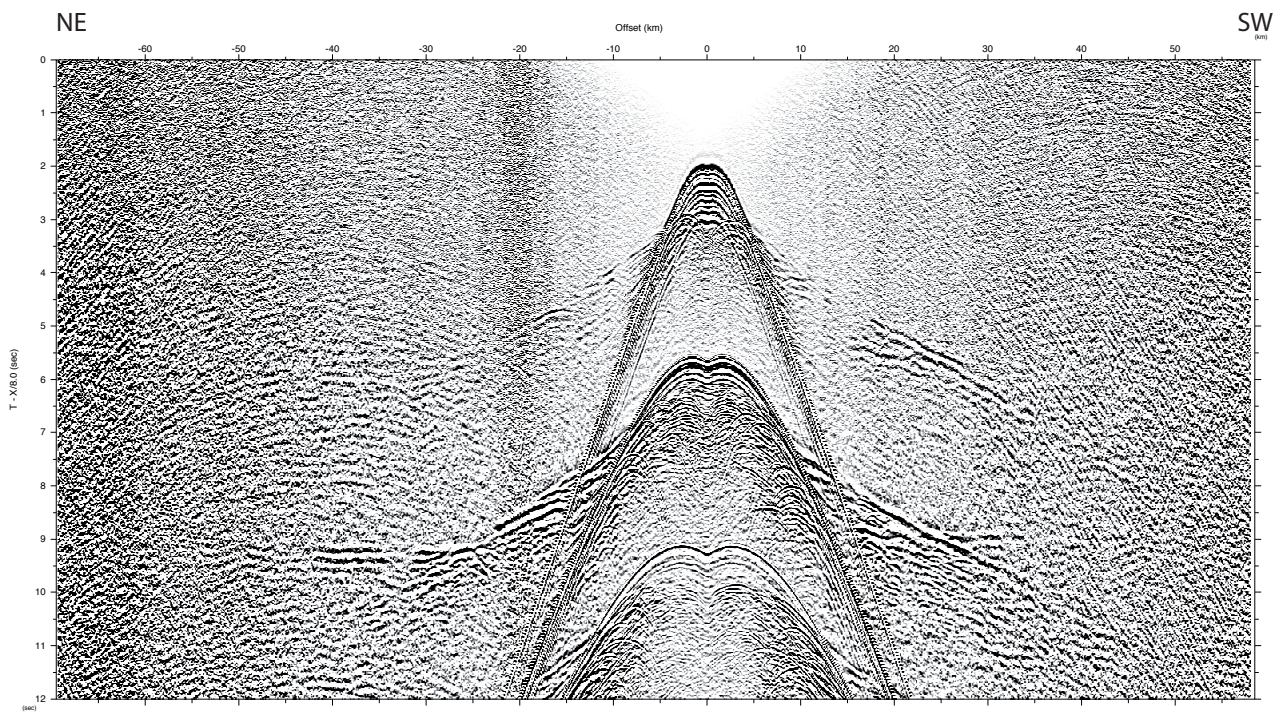
MSM 71 Profile P02 Record Section OBH204



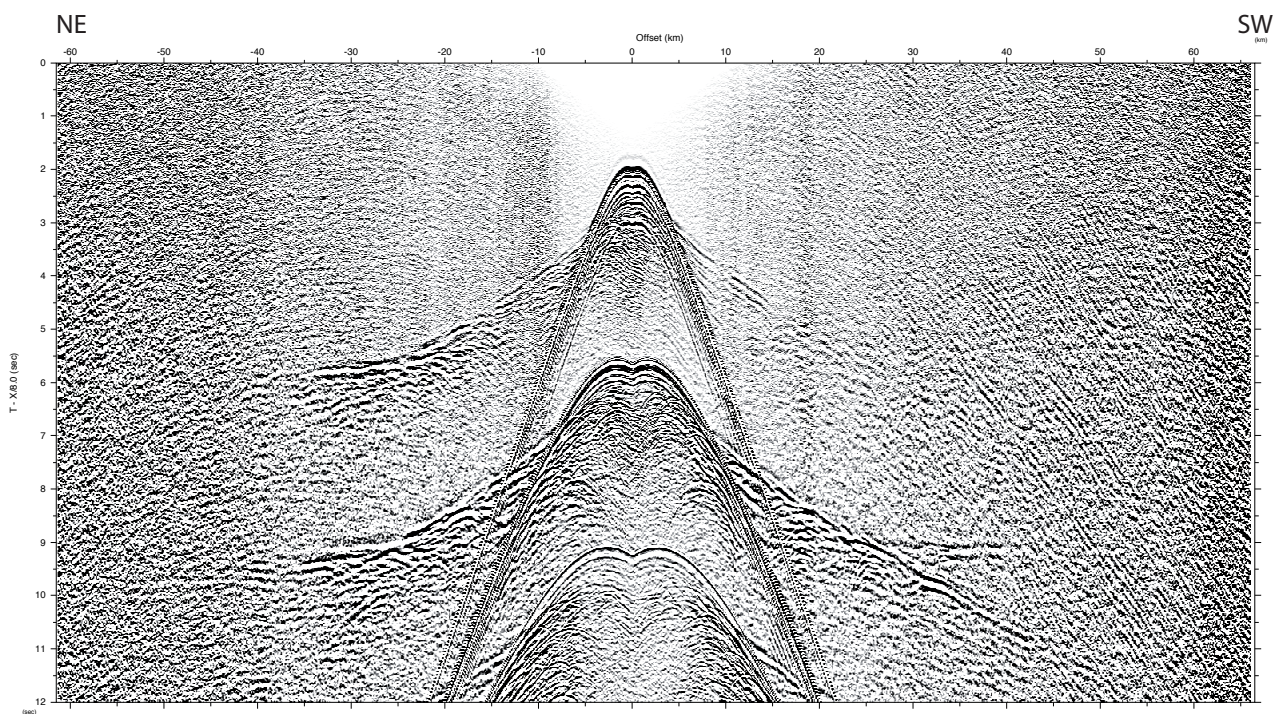
MSM 71 Profile P02 Record Section OBS205



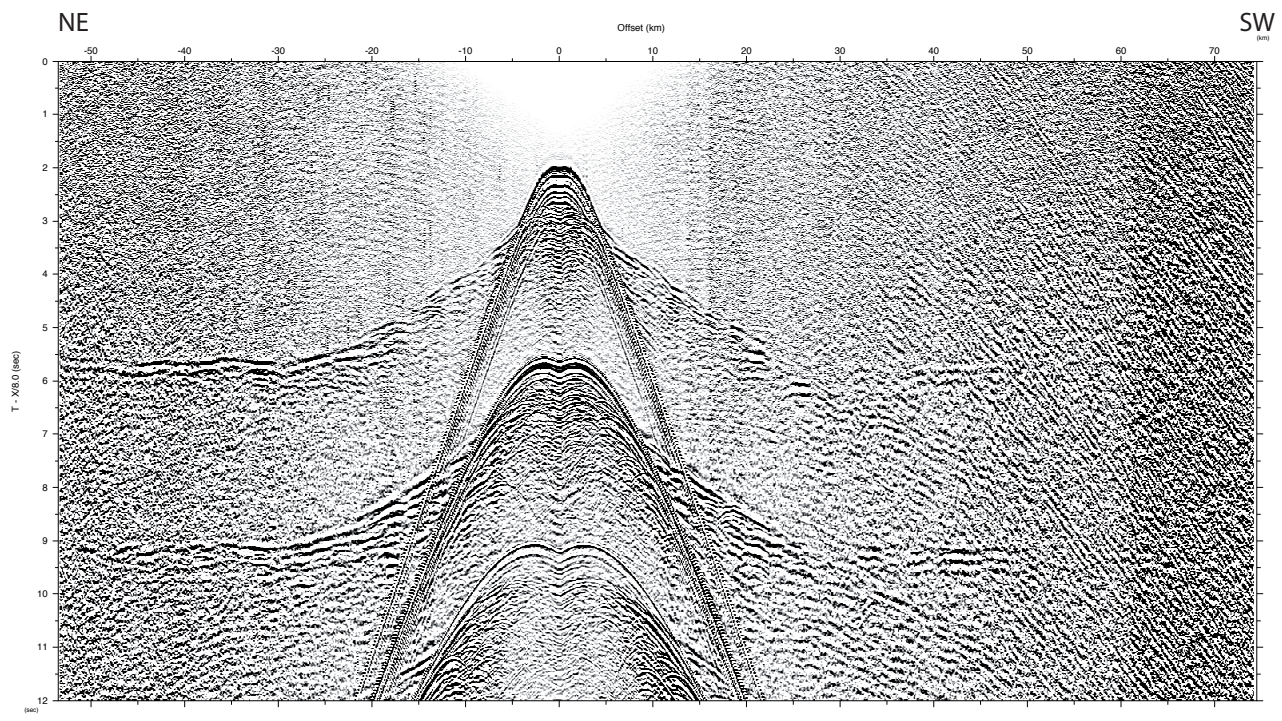
MSM 71 Profile P02 Record Section OBS206



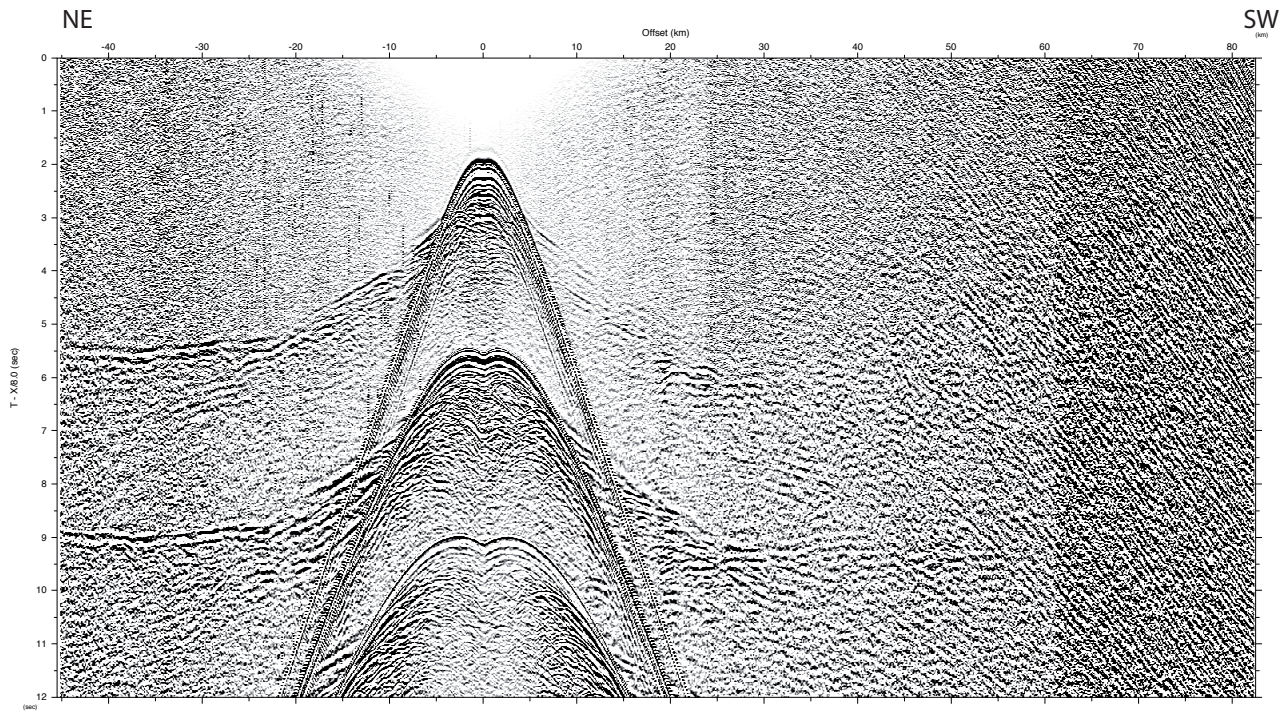
MSM 71 Profile P02 Record Section OBS207



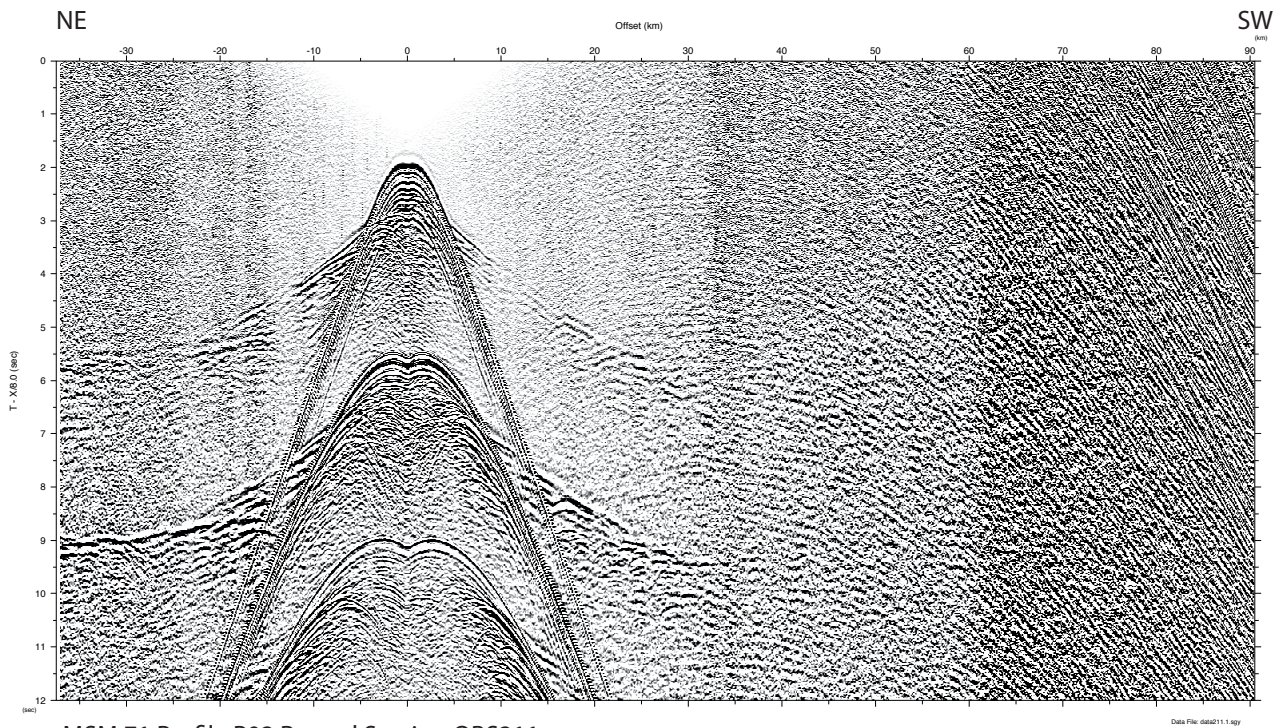
MSM 71 Profile P02 Record Section OBH208



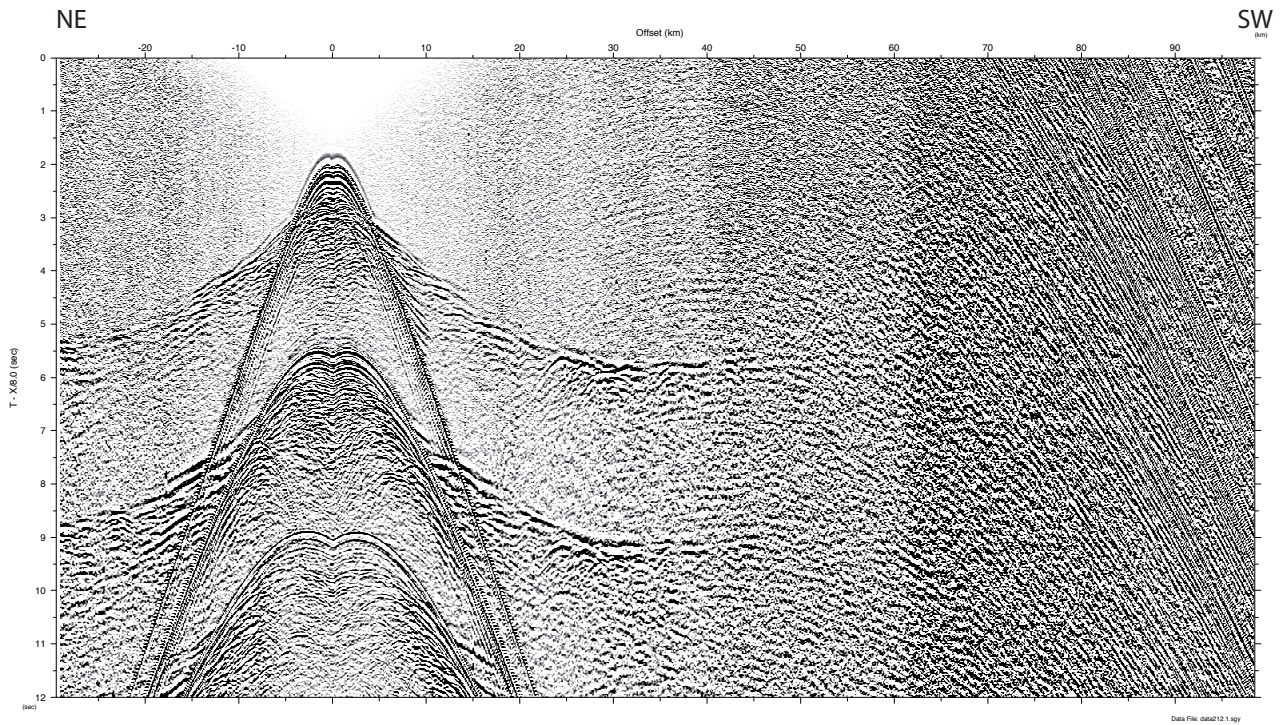
MSM 71 Profile P02 Record Section OBS209



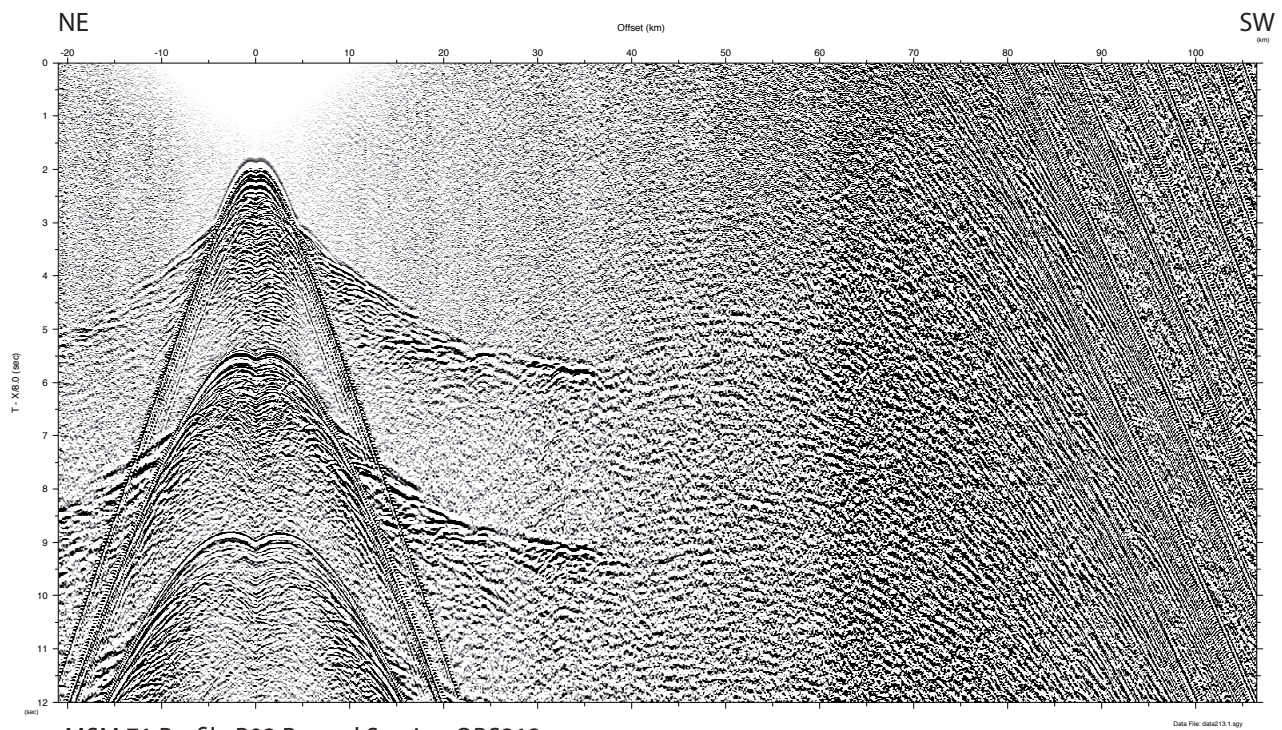
MSM 71 Profile P02 Record Section OBS210



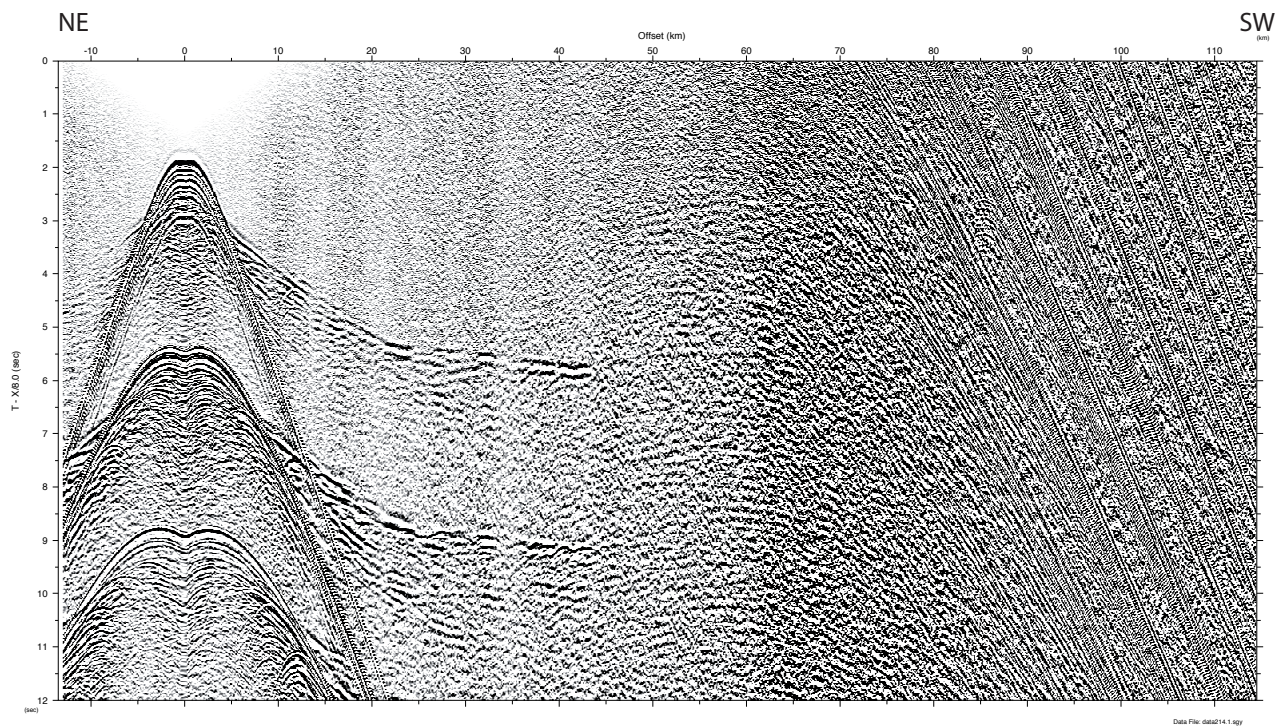
MSM 71 Profile P02 Record Section OBS211



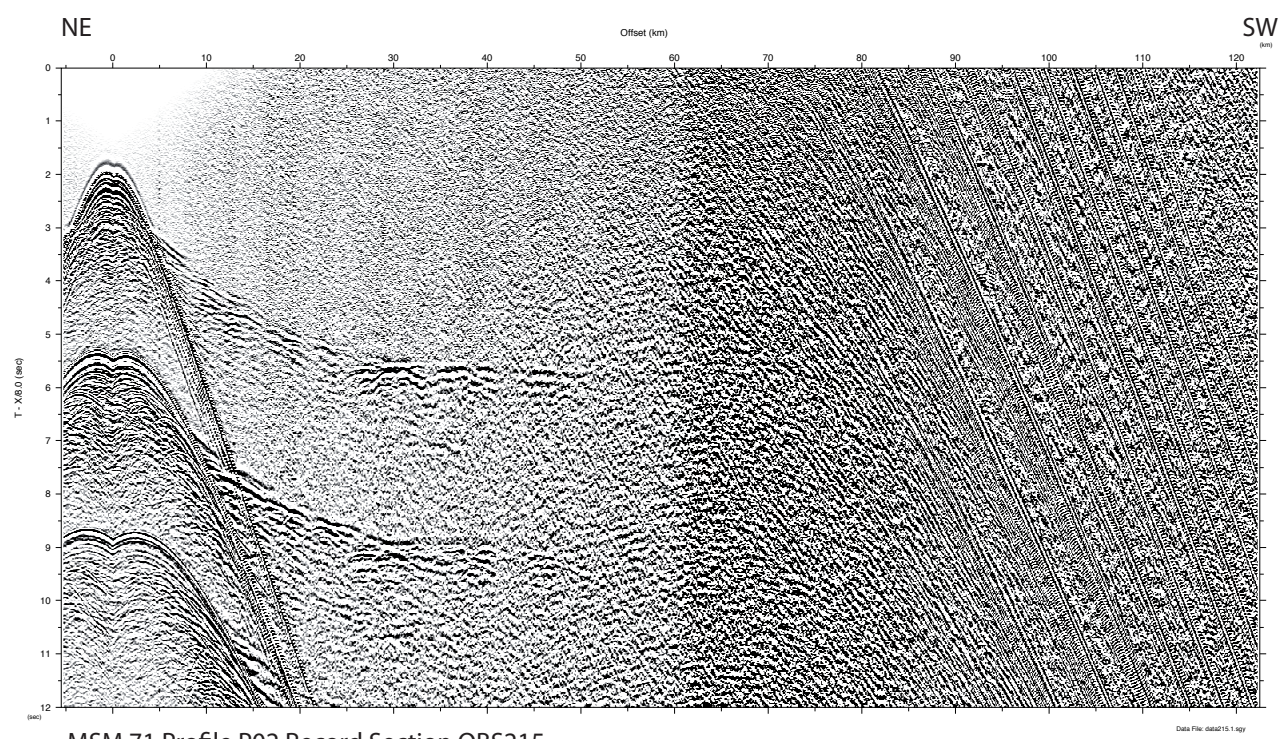
MSM 71 Profile P02 Record Section OBH212



MSM 71 Profile P02 Record Section OBS213



MSM 71 Profile P02 Record Section OBS214



MSM 71 Profile P02 Record Section OBS215



'Maria S. Merian' MSM 71 (27.02. - 27.02.2018)



Activity	Date / Time	Device	Action	Position	Position	Depth	Speed	Course	Wind Direction	Wind Velocity	Winch	Rope Length	Comment
No.	No.	[UTC]			Lat	Lon	[m]	kn	°]		m/s		m
MSM71_1-1	12.02.18 08:46	Seismic Ocean Bottom Receiver	released	41° 35,385' N	004° 44,923' E	0	1,4	169,4	355	28,4			A412A
MSM71_1-1	12.02.18 09:19	Seismic Ocean Bottom Receiver	at surface	41° 38,504' N	004° 45,053' E	0	1,3	323,2	7	24,2			
MSM71_1-1	12.02.18 09:35	Seismic Ocean Bottom Receiver	OBS on deck	41° 38,817' N	004° 45,132' E	0	1,9	115,8	358	23,9			
MSM71_2-1	12.02.18 16:19	Seismic Ocean Bottom Receiver	OBH deployed	42° 32,956' N	005° 30,012' E	2256,9	0,9	225,1	325	49			OBS 135
MSM71_4-1	12.02.18 17:04	Expandedable Sound Velocimeter	in the water	42° 32,448' N	005° 35,332' E	2287,2	0,4	186,5	324	44,9			
MSM71_3-1	12.02.18 17:07	Seismic Ocean Bottom Receiver	OBH deployed	42° 32,448' N	005° 35,335' E	2291	0,1	14	325	42,9			OBH 134
MSM71_4-1	12.02.18 17:10	Expandedable Sound Velocimeter	station end	42° 32,444' N	005° 35,337' E	2284,4	0,5	86,7	337	45,3			
MSM71_5-1	12.02.18 19:02	Seismic Ocean Bottom Receiver	OBH on deck	42° 31,896' N	005° 40,641' E	2369,5	0,2	146,2	328	37,9			OBH 133
MSM71_6-1	12.02.18 19:56	Seismic Ocean Bottom Receiver	OBH deployed	42° 31,311' N	005° 45,980' E	2403,2	0,7	329,2	325	35,7			OBH 132
MSM71_7-1	12.02.18 20:41	Seismic Ocean Bottom Receiver	OBH deployed	42° 30,739' N	005° 51,290' E	2468,5	0,2	23,9	329	32,1			OBH 131
MSM71_8-1	12.02.18 21:24	Seismic Ocean Bottom Receiver	OBH deployed	42° 30,095' N	005° 56,613' E	2491,7	0,1	312,8	325	24,2			OBH 130
MSM71_9-1	12.02.18 22:04	Seismic Ocean Bottom Receiver	OBS deployed	42° 29,624' N	006° 01,916' E	2524,7	0,1	95,4	328	23,4			OBs 129
MSM71_10-1	12.02.18 22:45	Seismic Ocean Bottom Receiver	OBH deployed	42° 29,048' N	006° 07,239' E	2532,4	0,2	6,5	312	20,4			OBH 128
MSM71_11-1	12.02.18 23:16	Seismic Ocean Bottom Receiver	OBS deployed	42° 28,478' N	006° 12,554' E	2551,8	0,2	219	305	16,6			OBS 127
MSM71_12-1	12.02.18 23:57	Seismic Ocean Bottom Receiver	OBH deployed	42° 27,886' N	006° 17,852' E	2558,8	0,2	114,4	314	15,1			OBH126
MSM71_13-1	13.02.18 00:28	Seismic Ocean Bottom Receiver	OBS deployed	42° 27,307' N	006° 23,150' E	2585,4	0,2	289,9	303	12,4			OBS 125
MSM71_14-1	13.02.18 01:01	Seismic Ocean Bottom Receiver	OBH deployed	42° 26,703' N	006° 28,486' E	2837,3	0,3	221,5	315	15			OBH 124
MSM71_15-1	13.02.18 01:31	Seismic Ocean Bottom Receiver	OBS deployed	42° 26,149' N	006° 33,768' E	2623,6	0,4	226,3	301	12,9			OBS 123
MSM71_16-1	13.02.18 02:07	Seismic Ocean Bottom Receiver	OBH deployed	42° 25,521' N	006° 39,066' E	2629,2	0,2	269,7	318	12,3			OBH 122
MSM71_17-1	13.02.18 02:40	Seismic Ocean Bottom Receiver	OBS deployed	42° 24,914' N	006° 44,376' E	2640,4	0,2	118	323	11,4			OBS 121
MSM71_18-1	13.02.18 03:18	Seismic Ocean Bottom Receiver	OBH deployed	42° 24,304' N	006° 49,644' E	2656,6	1	271	311	11,2			OBH 120
MSM71_19-1	13.02.18 03:48	Seismic Ocean Bottom Receiver	OBS deployed	42° 23,715' N	006° 54,954' E	2670,4	0,6	39	62	14,5			OBS 119
MSM71_20-1	13.02.18 04:21	Seismic Ocean Bottom Receiver	OBS deployed	42° 23,075' N	007° 00,251' E	0	0,8	57,4	57	25,1			OBS 118
MSM71_21-1	13.02.18 04:54	Seismic Ocean Bottom Receiver	OBS deployed	42° 22,474' N	007° 05,504' E	0	1,2	339,1	57	22,9			OBS 117
MSM71_22-1	13.02.18 05:28	Seismic Ocean Bottom Receiver	OBS deployed	42° 21,827' N	007° 10,852' E	3270,4	0,9	0,2	56	23			OBS 116
MSM71_23-1	13.02.18 05:58	Seismic Ocean Bottom Receiver	OBS deployed	42° 21,201' N	007° 16,111' E	2724,3	0,6	336,4	49	22,9			OBS 115
MSM71_24-1	13.02.18 06:26	Seismic Ocean Bottom Receiver	OBS deployed	42° 20,566' N	007° 21,417' E	2726,1	0,5	325,7	45	22			OBS 114
MSM71_25-1	13.02.18 06:54	Seismic Ocean Bottom Receiver	OBS deployed	42° 19,925' N	007° 26,688' E	2736,2	0,4	326,4	42	23,8			OBS 113
MSM71_26-1	13.02.18 07:23	Seismic Ocean Bottom Receiver	OBS deployed	42° 19,282' N	007° 31,974' E	0	0,2	10,3	41	22,6			OBS 112
MSM71_27-1	13.02.18 07:54	Seismic Ocean Bottom Receiver	OBS deployed	42° 18,626' N	007° 37,286' E	2978,4	0,3	237,8	34	26,8			OBS 111
MSM71_28-1	13.02.18 08:25	Seismic Ocean Bottom Receiver	OBS deployed	42° 18,006' N	007° 42,534' E	2736,8	0,2	353	49	23,8			OBS 110
MSM71_29-1	13.02.18 08:56	Seismic Ocean Bottom Receiver	OBS deployed	42° 17,342' N	007° 47,842' E	2975,9	0,1	79,1	25	21,7			OBS 109
MSM71_30-1	13.02.18 09:24	Seismic Ocean Bottom Receiver	OBS deployed	42° 16,695' N	007° 53,099' E	2733,9	0,3	42,2	35	19,6			OBS 108
MSM71_31-1	13.02.18 09:52	Seismic Ocean Bottom Receiver	OBS deployed	42° 16,055' N	007° 58,342' E	2970,4	0,2	191,7	22	16,4			OBS 107
MSM71_32-1	13.02.18 10:23	Seismic Ocean Bottom Receiver	OBS deployed	42° 15,372' N	008° 03,623' E	2725,1	0,1	83,5	17	16,6			OBS 106
MSM71_33-1	13.02.18 10:51	Seismic Ocean Bottom Receiver	OBS deployed	42° 14,708' N	008° 08,911' E	2706,2	0,1	33,4	12	17			OBS 105
MSM71_38-1	13.02.18 13:07	Seismic Source	Airgun in water	42° 08,984' N	008° 29,860' E	1287,3	13,8	190,2	343	16,4			Bb-Seite 40m
MSM71_38-1	13.02.18 13:57	Seismic Source	Airgun in water	42° 08,914' N	008° 30,814' E	1010,5	2	51,8	340	17,8			Stb-Seite 40m
MSM71_39-1	13.02.18 14:56	Parasound	profile start	42° 11,500' N	008° 33,682' E	54,1	4,5	294,2	359	10,6			rwk=278°, v=4,5kn
MSM71_38-1	13.02.18 14:56	Seismic Source	profile start	42° 11,509' N	008° 33,657' E	56,7	4,5	290,8	358	10,3			
MSM71_39-2	13.02.18 14:56	Deep-sea Multibeam Echosounder	profile start	42° 11,510' N	008° 33,654' E	63,7	4,4	295,3	358	10,2			rwk=278°, v=4,5kn
MSM71_38-1	13.02.18 14:56	Seismic Source	profile start	42° 11,520' N	008° 33,619' E	54,3	4,3	291,5	359	10,4			
MSM71_38-2	13.02.18 15:59	Seismic Towed Receiver	MCS in water	42° 12,339' N	008° 27,382' E	1591,1	4,6	277,7	325	8,2			280m
MSM71_38-2	14.02.18 22:01	Seismic Towed Receiver	MCS on deck	42° 33,267' N	005° 27,424' E	2268,9	4,5	278,9	291	12,1			
MSM71_38-1	14.02.18 22:07	Seismic Source	information	42° 33,325' N	005° 26,978' E	2261,7	2,4	281,2	280	11,1			Stb.-Seite Unterbrechung wg.
MSM71_38-1	14.02.18 22:29	Seismic Source	Airgun on deck	42° 33,443' N	005° 25,759' E	2243,8	2,3	276,6	292	10,7			Stb.-Array zur Reparatur
MSM71_38-1	14.02.18 23:03	Seismic Source	Airgun in water	42° 33,709' N	005° 23,304' E	2201,1	2,2	269,5	281	7,6			STb.-Array nach Reparatur
MSM71_38-1	14.02.18 23:04	Seismic Source	information	42° 33,709' N	005° 23,248' E	2206,1	2,3	269,3	282	8,6			Bb.-Seite Unterbrechung wg.
MSM71_38-1	14.02.18 23:16	Seismic Source	Airgun on deck	42° 33,786' N	005° 22,642' E	2194,9	2,4	282,6	272	9,1			Bb.-Array zur Reparatur
MSM71_38-1	14.02.18 23:40	Seismic Source	information	42° 33,990' N	005° 21,464' E	2178,8	2	286,7	263	8,9			Bb.-Array nach Reparatur
MSM71_39-2	15.02.18 05:05	Deep-sea Multibeam Echosounder	profile end	42° 08,803' N	005° 25,669' E	2354,8	5	167,1	278	11,9			
MSM71_39-1	15.02.18 05:05	Parasound	profile end	42° 08,791' N	005° 25,673' E	2352,4	5	165,4	278	12			
MSM71_38-1	15.02.18 08:05	Seismic Source	profile end	41° 54,076' N	005° 29,257' E	2358,6	5	170	299	5,8			
MSM71_38-1	15.02.18 08:05	Seismic Source	profile end	41° 54,027' N	005° 29,269' E	2356,2	5,1	170,4	298	6			
MSM71_38-1	15.02.18 08:24	Seismic Source	Airgun on deck	41° 53,028' N	005° 29,522' E	2364,4	2,6	165,7	296	5,6			Bb.-Array
MSM71_38-1	15.02.18 08:37	Seismic Source	Airgun on deck	41° 52,423' N	005° 29,680' E	2366,2	2,8	168,9	282	6,9			Stb.-Array
MSM71_40-1	15.02.18 09:59	Seismic Ocean Bottom Receiver	released	41° 44,143' N	005° 47,371' E	2508,9	0,5	51,1	259	10,4			A421A
MSM71_40-1	15.02.18 10:37	Seismic Ocean Bottom Receiver	at surface	41° 42,929' N	005° 50,497' E	0	0	57,8	287	9,6			
MSM71_40-1	15.02.18 10:47	Seismic Ocean Bottom Receiver	OBS on deck	41° 42,852' N	005° 50,942' E	0	0,9	169,5	290	9,9			
MSM71_41-1	15.02.18 12:46	Seismic Ocean Bottom Receiver	released	42° 07,838' N	005° 51,416' E	0	0,3	152,8	296	13,4			A414A
MSM71_41-1	15.02.18 13:27	Seismic Ocean Bottom Receiver	at surface	42° 10,610' N	005° 51,979' E	0	0,1	174,5	284	12,9			
MSM71_41-1	15.02.18 13:38	Seismic Ocean Bottom Receiver	OBS on deck	42° 10,483' N	005° 51,439' E	0	0,4	129,9	300	13,5			



'Maria S. Merian' MSM 71 (27.02. - 27.02.2018)



Activity	Date / Time	Device	Action	Position	Position	Depth	Speed	Course	Wind Direction	Wind Velocity	Winch	Rope Length	Comment
No.	No.	[UTC]			Lat	Lon	[m]	kn	°]		m/s		m
MSM71_42-1	15.02.18 15:41	Seismic Ocean Bottom Receiver	released	41° 58,002' N	005° 21,420' E	0	0,5	234,3	319	9			A413A
MSM71_42-1	15.02.18 16:50	Seismic Ocean Bottom Receiver	at surface	41° 56,097' N	005° 18,164' E	0	0	274,4	297	10,1			
MSM71_42-1	15.02.18 17:02	Seismic Ocean Bottom Receiver	OBS on deck	41° 56,146' N	005° 18,775' E	0	0,8	127,4	293	9,5			
MSM71_43-1	15.02.18 18:29	Seismic Ocean Bottom Receiver	released	42° 08,444' N	005° 03,836' E	0	0	51,7	314	6,4			A404A
MSM71_43-1	15.02.18 18:42	Seismic Ocean Bottom Receiver	at surface	42° 09,140' N	005° 02,845' E	2031,6	10,4	312	306	5,8			
MSM71_43-1	15.02.18 20:09	Seismic Ocean Bottom Receiver	OBS on deck	42° 10,450' N	005° 01,510' E	0	0,3	119,3	278	5,2			
MSM71_44-1	15.02.18 21:34	Seismic Ocean Bottom Receiver	released	42° 23,252' N	005° 16,300' E	0	0,5	358,1	295	8,1			A405A
MSM71_44-1	15.02.18 22:13	Seismic Ocean Bottom Receiver	at surface	42° 24,770' N	005° 17,791' E	0	0,4	106,2	272	6,2			
MSM71_44-1	15.02.18 22:23	Seismic Ocean Bottom Receiver	OBS on deck	42° 24,677' N	005° 18,361' E	0	0,6	127,9	270	7,1			
MSM71_45-1	16.02.18 00:01	Seismic Ocean Bottom Receiver	released	42° 37,548' N	005° 02,630' E	0	0,3	308,8	290	5			A401A
MSM71_45-1	16.02.18 00:54	Seismic Ocean Bottom Receiver	at surface	42° 38,910' N	005° 00,761' E	0	0,2	105,9	324	3,5			
MSM71_45-1	16.02.18 01:00	Seismic Ocean Bottom Receiver	OBS on deck	42° 38,918' N	005° 00,894' E	0	0,6	336,4	321	3,4			
MSM71_46-1	16.02.18 02:29	Seismic Ocean Bottom Receiver	released	42° 51,400' N	005° 16,312' E	0	0,3	269,9	325	5,2			A402A
MSM71_46-1	16.02.18 03:00	Seismic Ocean Bottom Receiver	at surface	42° 52,800' N	005° 17,544' E	0	0,1	198,3	348	6,1			
MSM71_46-1	16.02.18 03:13	Seismic Ocean Bottom Receiver	OBS on deck	42° 52,927' N	005° 18,090' E	0	0,3	138,8	346	6,8			
MSM71_47-1	16.02.18 04:52	Seismic Ocean Bottom Receiver	released	42° 38,683' N	005° 33,840' E	0	0,5	150,9	24	4,1			A406A
MSM71_47-1	16.02.18 06:33	Seismic Ocean Bottom Receiver	information	42° 36,725' N	005° 35,723' E	0	0	290,2	22	2			Position des OBS Falsch, neue
MSM71_47-1	16.02.18 07:40	Seismic Ocean Bottom Receiver	released	42° 36,958' N	005° 48,631' E	0	0,2	82	87	3,3			A406A
MSM71_47-1	16.02.18 10:30	Seismic Ocean Bottom Receiver	information	42° 37,111' N	005° 50,052' E	0	0,2	42,3	221	4,4			Station wird abgebrochen OBS
MSM71_48-1	16.02.18 12:37	Seismic Ocean Bottom Receiver	released	42° 25,494' N	006° 22,543' E	0	0,4	66,6	241	7,5			A415A
MSM71_48-1	16.02.18 13:19	Seismic Ocean Bottom Receiver	at surface	42° 24,863' N	006° 24,293' E	0	0,1	137,9	248	9,1			
MSM71_48-1	16.02.18 13:27	Seismic Ocean Bottom Receiver	OBS on deck	42° 24,639' N	006° 24,679' E	0	0,3	141,5	258	8,6			
MSM71_49-1	16.02.18 15:38	Seismic Ocean Bottom Receiver	released	42° 11,500' N	006° 55,605' E	0	0	2	234	4,7			A423A
MSM71_49-1	16.02.18 16:23	Seismic Ocean Bottom Receiver	at surface	42° 10,811' N	006° 57,513' E	0	0,2	110,9	228	3,8			
MSM71_49-1	16.02.18 16:34	Seismic Ocean Bottom Receiver	OBS on deck	42° 10,622' N	006° 58,095' E	0	0,6	89,8	213	4,7			
MSM71_50-1	16.02.18 19:51	Seismic Ocean Bottom Receiver	released	42° 10,757' N	007° 55,959' E	0	0,8	9,2	172	7,9			A430A
MSM71_50-1	16.02.18 20:32	Seismic Ocean Bottom Receiver	at surface	42° 10,871' N	007° 58,763' E	0	0	238,9	185	8,7			
MSM71_50-1	16.02.18 20:44	Seismic Ocean Bottom Receiver	OBS on deck	42° 10,642' N	007° 58,929' E	0	0,6	272,2	177	8,6			
MSM71_51-1	16.02.18 22:34	Seismic Ocean Bottom Receiver	released	42° 23,295' N	007° 33,359' E	0	0,3	156,1	183	3,8			A424A
MSM71_51-1	16.02.18 23:34	Seismic Ocean Bottom Receiver	at surface	42° 24,885' N	007° 30,987' E	0	0	60,9	168	3,8			
MSM71_51-1	16.02.18 23:42	Seismic Ocean Bottom Receiver	OBS on deck	42° 24,609' N	007° 31,114' E	0	0,5	295,1	190	4,3			
MSM71_52-1	17.02.18 01:54	Seismic Ocean Bottom Receiver	released	42° 37,853' N	007° 00,146' E	0	0,4	248,3	59	6,9			A416A
MSM71_52-1	17.02.18 03:12	Seismic Ocean Bottom Receiver	at surface	42° 38,672' N	006° 58,088' E	0	0	220,3	55	8,4			
MSM71_52-1	17.02.18 03:24	Seismic Ocean Bottom Receiver	OBS on deck	42° 38,865' N	006° 57,706' E	0	0	203,1	59	9,2			
MSM71_53-1	17.02.18 05:37	Seismic Ocean Bottom Receiver	released	43° 04,615' N	006° 57,863' E	0	0,1	236,9	76	15,2			A408A (keine Antwort)
MSM71_53-1	17.02.18 07:17	Seismic Ocean Bottom Receiver	information	43° 06,708' N	006° 57,403' E	0	0	150,2	96	13,2			Abbruch der Suche, keine Antwort
MSM71_54-1	17.02.18 09:40	Seismic Ocean Bottom Receiver	released	43° 19,807' N	007° 28,521' E	0	0,2	163,7	69	10,8			A409A
MSM71_54-1	17.02.18 10:09	Seismic Ocean Bottom Receiver	at surface	43° 20,741' N	007° 30,757' E	0	0	219,3	69	11,3			
MSM71_54-1	17.02.18 10:18	Seismic Ocean Bottom Receiver	OBS on deck	43° 20,804' N	007° 31,040' E	0	0,9	180,7	54	11,8			
MSM71_55-1	17.02.18 12:24	Seismic Ocean Bottom Receiver	released	42° 54,703' N	007° 31,052' E	0	0,4	260,6	82	6,3			A417A
MSM71_55-1	17.02.18 13:01	Seismic Ocean Bottom Receiver	at surface	42° 52,741' N	007° 30,726' E	0	0,1	338,6	190	4,2			
MSM71_55-1	17.02.18 13:10	Seismic Ocean Bottom Receiver	OBS on deck	42° 52,966' N	007° 31,165' E	0	0,6	323,9	199	5,6			
MSM71_56-1	17.02.18 15:05	Seismic Ocean Bottom Receiver	released	42° 59,471' N	008° 01,662' E	0	0,1	158,9	221	11,9			A418A
MSM71_56-1	17.02.18 15:47	Seismic Ocean Bottom Receiver	at surface	42° 59,817' N	008° 04,097' E	0	0	310,4	215	13,1			
MSM71_56-1	17.02.18 15:55	Seismic Ocean Bottom Receiver	OBS on deck	42° 59,979' N	008° 04,169' E	0	1,2	68,9	221	12,5			
MSM71_25-1	17.02.18 19:40	Seismic Ocean Bottom Receiver	released	42° 22,046' N	007° 28,659' E	0	0,4	143,5	272	11,9			
MSM71_25-1	17.02.18 20:17	Seismic Ocean Bottom Receiver	at surface	42° 19,887' N	007° 27,087' E	0	0	2,1	266	10,4			
MSM71_25-1	17.02.18 20:29	Seismic Ocean Bottom Receiver	OBS on deck	42° 19,608' N	007° 26,970' E	0	0,5	28,4	269	15,3			
MSM71_24-1	17.02.18 20:33	Seismic Ocean Bottom Receiver	released	42° 19,607' N	007° 26,968' E	0	0,1	157,3	272	13,1			
MSM71_24-1	17.02.18 21:12	Seismic Ocean Bottom Receiver	at surface	42° 20,477' N	007° 21,839' E	0	0	355	283	20,6			
MSM71_24-1	17.02.18 21:23	Seismic Ocean Bottom Receiver	OBS on deck	42° 20,323' N	007° 21,759' E	0	1,4	104,8	287	20,9			
MSM71_23-1	17.02.18 21:27	Seismic Ocean Bottom Receiver	released	42° 20,301' N	007° 21,883' E	0	0,2	285,7	288	19			
MSM71_23-1	17.02.18 22:04	Seismic Ocean Bottom Receiver	at surface	42° 20,958' N	007° 16,559' E	0	1,2	265,9	291	24,4			
MSM71_23-1	17.02.18 22:15	Seismic Ocean Bottom Receiver	OBS on deck	42° 20,975' N	007° 16,338' E	0	1,4	117,8	294	28,3			
MSM71_22-1	17.02.18 22:18	Seismic Ocean Bottom Receiver	released	42° 20,956' N	007° 16,387' E	0	0,5	118,5	290	26,4			
MSM71_22-1	17.02.18 22:59	Seismic Ocean Bottom Receiver	at surface	42° 21,636' N	007° 11,221' E	0	0	184,3	296	28,8			
MSM71_22-1	17.02.18 23:23	Seismic Ocean Bottom Receiver	OBS on deck	42° 21,931' N	007° 11,386' E	0	1,1	32,2	288	27,8			
MSM71_21-1	17.02.18 23:24	Seismic Ocean Bottom Receiver	released	42° 21,948' N	007° 11,394' E	0	0,6	31,4	292	29,3			Keine Antwort
MSM71_21-1	18.02.18 00:02	Seismic Ocean Bottom Receiver	at surface	42° 22,337' N	007° 05,695' E	0	0	293	283	29,5			
MSM71_21-1	18.02.18 00:12	Seismic Ocean Bottom Receiver	OBS on deck	42° 22,582' N	007° 05,721' E	0	0,7	30,9	274	29,5			
MSM71_20-1	18.02.18 00:14	Seismic Ocean Bottom Receiver	released	42° 22,588' N	007° 05,737' E	0	0,1	214	276	26			Keine Antwort
MSM71_20-1	18.02.18 00:54	Seismic Ocean Bottom Receiver	at surface	42° 23,031' N	007° 00,660' E	0	0,6	322,8	284	32,7			



'Maria S. Merian' MSM 71 (27.02. - 27.02.2018)



Activity	Date / Time	Device	Action	Position	Position	Depth	Speed	Course	Wind Direction	Wind Velocity	Winch	Rope Length	Comment
No.	No.	[UTC]			Lat	Lon	[m]	kn	°]		m/s		m
MSM71_20-1	18.02.18 01:08	Seismic Ocean Bottom Receiver	OBS on deck	42° 23,066' N	007° 00,496' E	0	1,8	77,9	284	34,3			
MSM71_19-1	18.02.18 01:16	Seismic Ocean Bottom Receiver	released	42° 23,085' N	007° 00,562' E	0	0	66,9	289	30			Keine Antwort
MSM71_19-1	18.02.18 01:51	Seismic Ocean Bottom Receiver	at surface	42° 23,624' N	006° 55,366' E	0	0,1	313,1	295	34,6			
MSM71_19-1	18.02.18 02:04	Seismic Ocean Bottom Receiver	OBS on deck	42° 23,463' N	006° 55,081' E	0	1,3	210,3	293	33,7			
MSM71_18-1	18.02.18 02:13	Seismic Ocean Bottom Receiver	released	42° 23,442' N	006° 55,064' E	0	0,5	14,8	297	34,1			keine Antwort
MSM71_18-1	18.02.18 02:50	Seismic Ocean Bottom Receiver	at surface	42° 24,287' N	006° 50,020' E	0	0,4	47,4	299	37,9			
MSM71_18-1	18.02.18 03:00	Seismic Ocean Bottom Receiver	OBH on deck	42° 24,256' N	006° 49,919' E	0	1,8	104,8	296	36,7			
MSM71_17-1	18.02.18 03:09	Seismic Ocean Bottom Receiver	released	42° 24,319' N	006° 50,070' E	0	0,1	290,5	300	35,9			
MSM71_17-1	18.02.18 03:40	Seismic Ocean Bottom Receiver	at surface	42° 24,827' N	006° 45,187' E	0	8	280	302	34,5			
MSM71_17-1	18.02.18 03:55	Seismic Ocean Bottom Receiver	information	42° 24,939' N	006° 44,613' E	0	1,2	62,2	301	37,2			
MSM71_16-1	18.02.18 04:02	Seismic Ocean Bottom Receiver	released	42° 24,952' N	006° 44,633' E	0	0,3	36,8	301	30,8			
MSM71_16-1	18.02.18 04:30	Seismic Ocean Bottom Receiver	at surface	42° 25,392' N	006° 40,226' E	0	8,8	280,6	309	33,8			
MSM71_16-1	18.02.18 04:39	Seismic Ocean Bottom Receiver	OBH on deck	42° 25,472' N	006° 39,270' E	0	0,7	58,1	306	34,5			
MSM71_15-1	18.02.18 04:46	Seismic Ocean Bottom Receiver	released	42° 25,472' N	006° 39,297' E	0	0	301,5	304	35,2			
MSM71_15-1	18.02.18 05:17	Seismic Ocean Bottom Receiver	at surface	42° 26,034' N	006° 34,545' E	0	8,6	279,5	313	34,4			
MSM71_15-1	18.02.18 05:27	Seismic Ocean Bottom Receiver	OBS on deck	42° 26,172' N	006° 33,957' E	0	0,2	74,6	302	33,2			
MSM71_14-1	18.02.18 05:32	Seismic Ocean Bottom Receiver	released	42° 26,181' N	006° 33,976' E	0	0,3	334	306	34,1			
MSM71_14-1	18.02.18 06:00	Seismic Ocean Bottom Receiver	at surface	42° 26,569' N	006° 29,813' E	0	8,7	279	312	31,2			
MSM71_14-1	18.02.18 06:11	Seismic Ocean Bottom Receiver	OBH on deck	42° 26,580' N	006° 28,610' E	0	0,4	215,6	309	29,2			
MSM71_13-1	18.02.18 06:15	Seismic Ocean Bottom Receiver	released	42° 26,575' N	006° 28,613' E	0	0,3	115	307	30,4			
MSM71_13-1	18.02.18 06:51	Seismic Ocean Bottom Receiver	at surface	42° 27,200' N	006° 23,293' E	0	0,7	282,3	306	28,7			
MSM71_13-1	18.02.18 07:00	Seismic Ocean Bottom Receiver	OBS on deck	42° 27,313' N	006° 23,388' E	0	1,4	125,3	319	28,2			
MSM71_12-1	18.02.18 07:03	Seismic Ocean Bottom Receiver	released	42° 27,245' N	006° 23,396' E	0	1,6	138,2	316	30,5			
MSM71_12-1	18.02.18 07:38	Seismic Ocean Bottom Receiver	at surface	42° 27,781' N	006° 18,511' E	0	6	265,7	315	29,3			
MSM71_12-1	18.02.18 07:50	Seismic Ocean Bottom Receiver	OBH on deck	42° 27,913' N	006° 17,918' E	0	0,4	234,9	320	28,3			
MSM71_11-1	18.02.18 07:54	Seismic Ocean Bottom Receiver	released	42° 27,914' N	006° 17,918' E	0	0,5	89,3	314	29,7			
MSM71_11-1	18.02.18 08:24	Seismic Ocean Bottom Receiver	at surface	42° 28,338' N	006° 12,976' E	0	4	264,4	315	30,5			
MSM71_11-1	18.02.18 08:35	Seismic Ocean Bottom Receiver	OBS on deck	42° 28,457' N	006° 12,649' E	0	0,7	169,8	318	31,8			
MSM71_10-1	18.02.18 08:44	Seismic Ocean Bottom Receiver	released	42° 28,347' N	006° 12,735' E	0	0,2	300,9	320	26,4			
MSM71_10-1	18.02.18 09:18	Seismic Ocean Bottom Receiver	at surface	42° 28,884' N	006° 07,657' E	0	4,3	273,5	319	33,4			
MSM71_10-1	18.02.18 09:27	Seismic Ocean Bottom Receiver	OBH on deck	42° 28,943' N	006° 07,258' E	0	0,9	104,4	322	28,3			
MSM71_9-1	18.02.18 09:36	Seismic Ocean Bottom Receiver	released	42° 28,902' N	006° 07,310' E	0	0,7	340,8	318	29,4			
MSM71_9-1	18.02.18 10:09	Seismic Ocean Bottom Receiver	at surface	42° 29,480' N	006° 02,361' E	0	6,1	275,7	318	32,6			
MSM71_9-1	18.02.18 10:18	Seismic Ocean Bottom Receiver	OBS on deck	42° 29,561' N	006° 01,931' E	0	0,8	103,4	307	33,6			
MSM71_8-1	18.02.18 10:24	Seismic Ocean Bottom Receiver	released	42° 29,550' N	006° 01,927' E	0	0,1	183,1	315	29,4			
MSM71_8-1	18.02.18 10:48	Seismic Ocean Bottom Receiver	at surface	42° 29,960' N	005° 57,880' E	0	9,9	278,3	324	31,5			
MSM71_8-1	18.02.18 11:03	Seismic Ocean Bottom Receiver	OBH on deck	42° 30,027' N	005° 56,616' E	0	1	79,2	320	31,3			
MSM71_7-1	18.02.18 11:08	Seismic Ocean Bottom Receiver	released	42° 30,016' N	005° 56,668' E	0	0,4	241,2	317	26,9			
MSM71_7-1	18.02.18 11:43	Seismic Ocean Bottom Receiver	at surface	42° 30,604' N	005° 51,567' E	0	2,2	235,4	322	33,9			
MSM71_7-1	18.02.18 11:51	Seismic Ocean Bottom Receiver	OBH on deck	42° 30,655' N	005° 51,190' E	0	0,7	41,6	317	34,8			
MSM71_6-1	18.02.18 11:53	Seismic Ocean Bottom Receiver	released	42° 30,648' N	005° 51,186' E	0	0,7	204	320	30,8			
MSM71_6-1	18.02.18 13:05	Seismic Ocean Bottom Receiver	at surface	42° 31,102' N	005° 46,226' E	0	0,7	305,8	318	35,2			
MSM71_6-1	18.02.18 13:14	Seismic Ocean Bottom Receiver	OBH on deck	42° 31,111' N	005° 45,936' E	0	0,6	93,2	310	35,3			
MSM71_5-1	18.02.18 13:15	Seismic Ocean Bottom Receiver	released	42° 31,118' N	005° 45,948' E	0	0,6	6,5	314	36,3			
MSM71_5-1	18.02.18 13:46	Seismic Ocean Bottom Receiver	at surface	42° 31,666' N	005° 40,876' E	0	3,8	306,7	313	32,4			
MSM71_5-1	18.02.18 13:51	Seismic Ocean Bottom Receiver	OBS on deck	42° 31,862' N	005° 40,675' E	0	0,6	54,9	321	31,1			
MSM71_3-1	18.02.18 13:53	Seismic Ocean Bottom Receiver	released	42° 31,858' N	005° 40,674' E	0	0,4	293,5	323	33,4			
MSM71_3-1	18.02.18 15:07	Seismic Ocean Bottom Receiver	information	42° 32,186' N	005° 35,399' E	0	0,2	142,8	325	35,4			Station abgebrochen, Auslöser
MSM71_2-1	18.02.18 15:08	Seismic Ocean Bottom Receiver	released	42° 32,185' N	005° 35,400' E	0	0,3	212,4	324	33,1			
MSM71_2-1	18.02.18 15:38	Seismic Ocean Bottom Receiver	at surface	42° 32,669' N	005° 30,991' E	0	7,9	277,1	332	35,4			
MSM71_2-1	18.02.18 15:50	Seismic Ocean Bottom Receiver	OBH on deck	42° 32,755' N	005° 30,207' E	0	0,2	85,9	329	34,6			
MSM71_57-1	19.02.18 04:08	Seismic Ocean Bottom Receiver	released	43° 16,318' N	008° 33,838' E	0	0,6	327,7	26	24,9			A419A
MSM71_57-1	19.02.18 05:46	Seismic Ocean Bottom Receiver	at surface	43° 17,105' N	008° 35,972' E	0	0,1	274,9	22	23,3			
MSM71_57-1	19.02.18 06:00	Seismic Ocean Bottom Receiver	OBS on deck	43° 17,503' N	008° 35,999' E	0	0,5	256,4	19	23,9			
MSM71_58-1	19.02.18 08:01	Seismic Ocean Bottom Receiver	released	43° 39,786' N	008° 38,755' E	0	0,3	283,8	10	26,7			A411A
MSM71_58-1	19.02.18 08:48	Seismic Ocean Bottom Receiver	at surface	43° 41,701' N	008° 39,036' E	0	0,1	132,5	2	27,8			
MSM71_58-1	19.02.18 08:59	Seismic Ocean Bottom Receiver	OBS on deck	43° 41,829' N	008° 38,976' E	0	2,9	83,5	9	31,4			
MSM71_59-1	19.02.18 11:14	Seismic Ocean Bottom Receiver	released	43° 50,143' N	009° 11,366' E	0	0,3	87	27	10,6			A434A
MSM71_59-1	19.02.18 11:29	Seismic Ocean Bottom Receiver	at surface	43° 50,704' N	009° 13,375' E	1148,7	7,3	73,8	13	14,8			
MSM71_59-1	19.02.18 11:38	Seismic Ocean Bottom Receiver	OBS on deck	43° 51,064' N	009° 13,860' E	1126,6	0,6	121,2	5	13,3			
MSM71_60-1	19.02.18 13:42	Seismic Ocean Bottom Receiver	released	43° 27,334' N	009° 11,331' E	0	0,1	359	12	12,5			A420A
MSM71_60-1	19.02.18 14:01	Seismic Ocean Bottom Receiver	at surface	43° 27,331' N	009° 11,389' E	0	0,2	102	13	9,9			



Activity	Date / Time	Device	Action	Position	Position	Depth	Speed	Course	Wind Direction	Wind Velocity	Winch	Rope Length	Comment
No.	No.	[UTC]			Lat	Lon	[m]	kn	°		m/s		m
MSM71_60-1	19.02.18 14:09	Seismic Ocean Bottom Receiver	OBS on deck	43° 27,294' N	009° 11,696' E	0	0,6	76,7	358	13			
MSM71_61-1	19.02.18 15:53	Seismic Ocean Bottom Receiver	released	43° 07,340' N	009° 11,626' E	0	0,5	245,7	31	7,3			A427A
MSM71_61-1	19.02.18 16:16	Seismic Ocean Bottom Receiver	at surface	43° 07,344' N	009° 11,605' E	0	0,1	19,6	20	6,4			
MSM71_61-1	19.02.18 16:24	Seismic Ocean Bottom Receiver	OBS on deck	43° 07,248' N	009° 11,572' E	0	0,5	233,1	30	6,9			
MSM71_62-1	19.02.18 19:45	Seismic Ocean Bottom Receiver	OBS deployed	43° 05,050' N	008° 11,803' E	2586	0,2	313,6	47	14,2			OBS 215
MSM71_63-1	19.02.18 20:19	Seismic Ocean Bottom Receiver	OBS deployed	43° 01,947' N	008° 07,753' E	2606,5	0	55,5	46	13,5			OBS 214
MSM71_64-1	19.02.18 20:49	Seismic Ocean Bottom Receiver	OBS deployed	42° 58,813' N	008° 03,659' E	2627,2	0	207,1	51	11,3			OBS 213
MSM71_65-1	19.02.18 21:22	Seismic Ocean Bottom Receiver	OBS deployed	42° 55,686' N	007° 59,540' E	2648,6	0	146,3	48	12,8			OBS 212
MSM71_66-1	19.02.18 21:55	Seismic Ocean Bottom Receiver	OBS deployed	42° 52,552' N	007° 55,461' E	2679,7	0,1	289,8	91	5,8			OBS 211
MSM71_67-1	19.02.18 22:26	Seismic Ocean Bottom Receiver	OBS deployed	42° 49,410' N	007° 51,390' E	2683,3	0,1	24,7	33	6,7			OBS 210
MSM71_68-1	19.02.18 22:58	Seismic Ocean Bottom Receiver	OBS deployed	42° 46,278' N	007° 47,322' E	2690,8	0,2	245,8	146	3,6			OBS 209
MSM71_69-1	19.02.18 23:30	Seismic Ocean Bottom Receiver	OBS deployed	42° 43,097' N	007° 43,277' E	2701,3	0,2	108	58	2,5			OBS 208
MSM71_70-1	20.02.18 00:01	Seismic Ocean Bottom Receiver	OBS deployed	42° 39,958' N	007° 39,206' E	2706,7	0,2	201,4	81	4,7			OBS 207
MSM71_71-1	20.02.18 00:32	Seismic Ocean Bottom Receiver	OBS deployed	42° 36,815' N	007° 35,151' E	2711,2	0,2	252,2	87	4,5			OBS 206
MSM71_72-1	20.02.18 01:04	Seismic Ocean Bottom Receiver	OBS deployed	42° 33,651' N	007° 31,111' E	2716,8	0,2	201,6	358	8,7			OBS 205
MSM71_73-1	20.02.18 01:34	Seismic Ocean Bottom Receiver	OBS deployed	42° 30,485' N	007° 27,072' E	2725	0,4	221,2	51	9,9			OBS 204
MSM71_74-1	20.02.18 02:03	Seismic Ocean Bottom Receiver	OBS deployed	42° 27,328' N	007° 23,066' E	2990,1	0,2	180,8	334	2,1			OBS 203
MSM71_75-1	20.02.18 02:36	Seismic Ocean Bottom Receiver	OBS deployed	42° 24,148' N	007° 19,049' E	2720,5	0,1	193,9	199	4,2			OBS 202
MSM71_76-1	20.02.18 03:07	Seismic Ocean Bottom Receiver	OBS deployed	42° 21,023' N	007° 15,009' E	2722,7	0,2	183,4	224	6,2			OBS 201
MSM71_77-1	20.02.18 05:47	Seismic Source	Airgun in water	42° 13,979' N	007° 14,825' E	0	2	306,4	9	7,5			Bb-Seite 40m
MSM71_77-1	20.02.18 05:59	Seismic Source	Airgun in water	42° 14,218' N	007° 14,364' E	0	2	307	31	8,9			Stb-Seite 40m
MSM71_77-2	20.02.18 06:31	Seismic Towed Receiver	MCS in water	42° 15,232' N	007° 12,402' E	0	4	305,3	16	11,2			280m
MSM71_77-4	20.02.18 07:17	Deep-sea Multibeam Echosounder	profile start	42° 17,490' N	007° 10,472' E	2715	4	46,5	35	11,4			rwk=044°, v=4,0 kn
MSM71_77-1	20.02.18 07:17	Seismic Source	profile start	42° 17,492' N	007° 10,475' E	2715	4,1	47,3	35	11,4			
MSM71_77-3	20.02.18 07:17	Parasound	profile start	42° 17,506' N	007° 10,494' E	2876	4	44	40	11,5			rwk=044°, v=4,0 kn
MSM71_77-4	21.02.18 00:29	Deep-sea Multibeam Echosounder	profile end	43° 07,390' N	008° 14,820' E	2576,2	4,3	39,8	36	23,5			
MSM71_77-3	21.02.18 00:29	Parasound	profile end	43° 07,398' N	008° 14,828' E	2578	4,3	41,5	36	24,1			
MSM71_77-2	21.02.18 00:45	Seismic Towed Receiver	MCS on deck	43° 07,954' N	008° 16,016' E	2575,5	3,6	63,6	24	24,3			
MSM71_77-1	21.02.18 00:59	Seismic Source	Airgun on deck	43° 08,169' N	008° 16,688' E	2815,1	2,2	71,6	24	22,8			Bb-Array
MSM71_77-1	21.02.18 01:13	Seismic Source	Airgun on deck	43° 08,354' N	008° 17,324' E	2583,1	2,4	64	24	22,8			Stb-Array
MSM71_78-1	21.02.18 03:40	Seismic Ocean Bottom Receiver	released	42° 40,745' N	008° 05,134' E	2618,5	0,9	204,7	44	28,4			A425A
MSM71_78-1	21.02.18 05:26	Seismic Ocean Bottom Receiver	at surface	42° 38,663' N	008° 03,958' E	2622,2	1,4	16,3	38	27,7			
MSM71_78-1	21.02.18 05:26	Seismic Ocean Bottom Receiver	OBS on deck	42° 38,665' N	008° 03,959' E	2621,8	1,3	16,6	38	27,7			
MSM71_79-1	21.02.18 07:57	Seismic Ocean Bottom Receiver	released	42° 51,743' N	008° 34,785' E	2472	1	201,3	44	21,2			A426A
MSM71_80-1	21.02.18 08:23	Expandedable Sound Velocimeter	in the water	42° 52,660' N	008° 36,940' E	0	0	322,4	53	22,1			
MSM71_80-1	21.02.18 08:30	Expandedable Sound Velocimeter	station end	42° 52,672' N	008° 36,927' E	0	0,1	338,5	71	22,7			
MSM71_79-1	21.02.18 08:43	Seismic Ocean Bottom Receiver	at surface	42° 52,697' N	008° 36,902' E	0	0,2	12,4	70	18			
MSM71_79-1	21.02.18 08:58	Seismic Ocean Bottom Receiver	OBS on deck	42° 52,999' N	008° 37,094' E	0	1,1	29	53	13,2			
MSM71_62-1	21.02.18 10:40	Seismic Ocean Bottom Receiver	released	43° 04,111' N	008° 14,197' E	0	0,9	246,5	43	23,7			
MSM71_62-1	21.02.18 11:11	Seismic Ocean Bottom Receiver	at surface	43° 04,855' N	008° 11,650' E	0	0,2	43,2	29	31,4			
MSM71_62-1	21.02.18 11:21	Seismic Ocean Bottom Receiver	OBS on deck	43° 05,045' N	008° 11,776' E	0	1,3	140,4	17	34,4			
MSM71_63-1	21.02.18 11:23	Seismic Ocean Bottom Receiver	released	43° 05,004' N	008° 11,776' E	0	0,3	230,9	33	34			
MSM71_63-1	21.02.18 12:02	Seismic Ocean Bottom Receiver	at surface	43° 01,778' N	008° 07,636' E	0	1,1	271,1	36	35,2			
MSM71_63-1	21.02.18 12:11	Seismic Ocean Bottom Receiver	OBS on deck	43° 01,938' N	008° 07,911' E	0	1,1	140,2	22	31,9			
MSM71_64-1	21.02.18 12:17	Seismic Ocean Bottom Receiver	released	43° 01,880' N	008° 07,981' E	0	0,3	126,4	27	32,6			
MSM71_64-1	21.02.18 12:51	Seismic Ocean Bottom Receiver	at surface	42° 58,643' N	008° 03,434' E	0	1,3	346,1	25	35			
MSM71_64-1	21.02.18 13:00	Seismic Ocean Bottom Receiver	OBS on deck	42° 58,851' N	008° 03,998' E	0	0,9	136,8	26	31,6			
MSM71_65-1	21.02.18 13:05	Seismic Ocean Bottom Receiver	released	42° 58,833' N	008° 03,997' E	0	0,1	305,6	36	34			
MSM71_65-1	21.02.18 13:35	Seismic Ocean Bottom Receiver	at surface	42° 55,477' N	007° 59,900' E	0	11,1	238,3	36	32,5			
MSM71_65-1	21.02.18 13:43	Seismic Ocean Bottom Receiver	OBS on deck	42° 55,795' N	007° 59,705' E	0	0,8	168	35	33,5			
MSM71_66-1	21.02.18 13:47	Seismic Ocean Bottom Receiver	released	42° 55,773' N	007° 59,742' E	0	0,2	157,6	30	33,2			
MSM71_66-1	21.02.18 14:20	Seismic Ocean Bottom Receiver	at surface	42° 52,470' N	007° 55,592' E	0	4,2	321,6	32	33,6			
MSM71_66-1	21.02.18 14:36	Seismic Ocean Bottom Receiver	OBS on deck	42° 52,637' N	007° 55,753' E	0	0,8	95	41	31,7			
MSM71_67-1	21.02.18 14:43	Seismic Ocean Bottom Receiver	released	42° 52,627' N	007° 55,752' E	0	0,5	131,9	32	30,9			
MSM71_67-1	21.02.18 15:02	Seismic Ocean Bottom Receiver	at surface	42° 50,789' N	007° 53,822' E	0	12,8	227,3	27	31,1			
MSM71_67-1	21.02.18 15:34	Seismic Ocean Bottom Receiver	OBS on deck	42° 49,401' N	007° 51,365' E	0	0,4	269,8	34	31,7			
MSM71_68-1	21.02.18 15:36	Seismic Ocean Bottom Receiver	released	42° 49,367' N	007° 51,353' E	0	0,9	131,9	31	33,8			
MSM71_68-1	21.02.18 16:12	Seismic Ocean Bottom Receiver	at surface	42° 46,035' N	007° 47,122' E	0	0,5	34,8	35	30,7			
MSM71_68-1	21.02.18 16:23	Seismic Ocean Bottom Receiver	OBS on deck	42° 46,363' N	007° 46,955' E	0	0,6	153,9	34	31,8			
MSM71_69-1	21.02.18 16:25	Seismic Ocean Bottom Receiver	released	42° 46,361' N	007° 46,961' E	0	0,3	357	34	30,5			
MSM71_69-1	21.02.18 16:53	Seismic Ocean Bottom Receiver	at surface	42° 43,269' N	007° 43,977' E	0	12,7	220,9	33	30			
MSM71_69-1	21.02.18 17:07	Seismic Ocean Bottom Receiver	OBS on deck	42° 43,056' N	007° 43,134' E	0	0,9	168,6	42	30,1			



'Maria S. Merian' MSM 71 (27.02. - 27.02.2018)



Activity	Date / Time	Device	Action	Position	Position	Depth	Speed	Course	Wind Direction	Wind Velocity	Winch	Rope Length	Comment
No.	No.	[UTC]			Lat	Lon	[m]	kn	°		m/s		m
MSM71_70-1	21.02.18 17:13	Seismic Ocean Bottom Receiver	released	42° 43,018' N	007° 43,174' E	0	0,6	138,4	45	29,1			
MSM71_70-1	21.02.18 17:48	Seismic Ocean Bottom Receiver	at surface	42° 39,722' N	007° 38,601' E	0	10,8	139,5	53	31,3			
MSM71_70-1	21.02.18 17:58	Seismic Ocean Bottom Receiver	OBS on deck	42° 39,968' N	007° 39,030' E	0	1,2	202,7	49	29,5			
MSM71_71-1	21.02.18 18:05	Seismic Ocean Bottom Receiver	released	42° 39,932' N	007° 39,068' E	0	1,5	164,7	36	30,4			
MSM71_71-1	21.02.18 18:40	Seismic Ocean Bottom Receiver	at surface	42° 36,690' N	007° 34,940' E	0	4	328,5	55	34,5			
MSM71_71-1	21.02.18 18:47	Seismic Ocean Bottom Receiver	OBS on deck	42° 36,731' N	007° 34,891' E	0	0,8	206,9	38	25,8			
MSM71_72-1	21.02.18 18:50	Seismic Ocean Bottom Receiver	released	42° 36,730' N	007° 34,882' E	0	0,6	311,4	47	30			
MSM71_72-1	21.02.18 19:28	Seismic Ocean Bottom Receiver	at surface	42° 33,742' N	007° 30,540' E	0	8,3	205,5	25	28,4			
MSM71_72-1	21.02.18 19:41	Seismic Ocean Bottom Receiver	OBS on deck	42° 33,303' N	007° 31,070' E	0	2,7	207,2	31	30			
MSM71_73-1	21.02.18 19:48	Seismic Ocean Bottom Receiver	released	42° 33,246' N	007° 31,079' E	0	0,6	137,5	37	28			
MSM71_73-1	21.02.18 20:16	Seismic Ocean Bottom Receiver	at surface	42° 30,760' N	007° 26,962' E	0	7,8	224,8	36	25,9			
MSM71_73-1	21.02.18 20:33	Seismic Ocean Bottom Receiver	OBS on deck	42° 30,233' N	007° 27,037' E	0	1,9	204,5	39	27,4			
MSM71_74-1	21.02.18 20:42	Seismic Ocean Bottom Receiver	released	42° 30,169' N	007° 27,008' E	0	0,2	82,4	33	24,4			
MSM71_74-1	21.02.18 21:13	Seismic Ocean Bottom Receiver	at surface	42° 27,254' N	007° 22,538' E	0	6,8	159,9	43	24,3			
MSM71_74-1	21.02.18 21:24	Seismic Ocean Bottom Receiver	OBS on deck	42° 27,223' N	007° 23,072' E	0	0,5	268,8	28	26,2			
MSM71_75-1	21.02.18 21:31	Seismic Ocean Bottom Receiver	released	42° 27,241' N	007° 22,990' E	0	0,8	301,3	39	26,4			
MSM71_75-1	21.02.18 22:04	Seismic Ocean Bottom Receiver	at surface	42° 23,995' N	007° 18,801' E	0	5,9	95,7	40	27,9			
MSM71_75-1	21.02.18 22:12	Seismic Ocean Bottom Receiver	OBS on deck	42° 24,040' N	007° 19,069' E	0	0,9	235,9	38	23,3			
MSM71_76-1	21.02.18 22:18	Seismic Ocean Bottom Receiver	released	42° 24,035' N	007° 19,066' E	0	0,2	35,4	38	23,8			
MSM71_76-1	21.02.18 22:53	Seismic Ocean Bottom Receiver	at surface	42° 20,872' N	007° 14,989' E	0	3,8	33,3	45	23,5			
MSM71_76-1	21.02.18 23:08	Seismic Ocean Bottom Receiver	OBS on deck	42° 21,079' N	007° 14,984' E	0	4,2	60,1	35	27,3			
MSM71_26-1	22.02.18 00:10	Seismic Ocean Bottom Receiver	released	42° 19,502' N	007° 29,317' E	0	1,3	143,9	25	26,3			
MSM71_26-1	22.02.18 00:51	Seismic Ocean Bottom Receiver	at surface	42° 19,056' N	007° 31,947' E	0	0,2	142,7	67	20,5			
MSM71_26-1	22.02.18 01:02	Seismic Ocean Bottom Receiver	OBS on deck	42° 18,959' N	007° 32,185' E	0	0,1	324,9	68	16,5			
MSM71_27-1	22.02.18 01:08	Seismic Ocean Bottom Receiver	released	42° 18,969' N	007° 32,116' E	0	0,2	301,3	56	15,9			
MSM71_27-1	22.02.18 02:21	Seismic Ocean Bottom Receiver	at surface	42° 18,474' N	007° 37,155' E	0	0,2	261,2	51	12,3			
MSM71_27-1	22.02.18 02:28	Seismic Ocean Bottom Receiver	OBS on deck	42° 18,459' N	007° 37,332' E	0	0,2	116,6	62	13,7			
MSM71_28-1	22.02.18 02:30	Seismic Ocean Bottom Receiver	released	42° 18,452' N	007° 37,338' E	0	0,5	195,1	57	12,4			
MSM71_28-1	22.02.18 03:09	Seismic Ocean Bottom Receiver	at surface	42° 17,832' N	007° 42,283' E	0	0,9	132,8	50	22,6			
MSM71_28-1	22.02.18 03:19	Seismic Ocean Bottom Receiver	OBS on deck	42° 17,934' N	007° 42,533' E	0	0,8	174,5	45	23,1			
MSM71_29-1	22.02.18 03:25	Seismic Ocean Bottom Receiver	released	42° 17,925' N	007° 42,557' E	0	0,2	135,4	41	19,9			
MSM71_29-1	22.02.18 04:03	Seismic Ocean Bottom Receiver	released	42° 17,205' N	007° 47,620' E	0	0,1	71,3	45	20,9			2. Versuch
MSM71_29-1	22.02.18 04:44	Seismic Ocean Bottom Receiver	at surface	42° 17,205' N	007° 47,623' E	0	0,1	163,5	45	23,2			
MSM71_29-1	22.02.18 04:52	Seismic Ocean Bottom Receiver	OBS on deck	42° 17,404' N	007° 47,808' E	0	0,5	318,2	35	24,9			
MSM71_30-1	22.02.18 04:58	Seismic Ocean Bottom Receiver	released	42° 17,382' N	007° 47,839' E	0	0,3	91,1	42	26,2			
MSM71_30-1	22.02.18 05:33	Seismic Ocean Bottom Receiver	at surface	42° 16,516' N	007° 53,002' E	0	1,6	215	33	21,5			
MSM71_30-1	22.02.18 05:43	Seismic Ocean Bottom Receiver	OBS on deck	42° 16,690' N	007° 53,042' E	0	0,2	313,8	53	21,9			
MSM71_31-1	22.02.18 05:50	Seismic Ocean Bottom Receiver	released	42° 16,645' N	007° 53,096' E	0	0,8	154,1	29	26,6			
MSM71_31-1	22.02.18 06:24	Seismic Ocean Bottom Receiver	at surface	42° 15,876' N	007° 58,249' E	0	0,1	64,4	49	21,6			
MSM71_31-1	22.02.18 06:33	Seismic Ocean Bottom Receiver	OBS on deck	42° 16,030' N	007° 58,310' E	0	0,7	254,3	61	23,6			
MSM71_32-1	22.02.18 06:40	Seismic Ocean Bottom Receiver	released	42° 16,014' N	007° 58,333' E	0	0,4	316,1	57	27,3			
MSM71_32-1	22.02.18 07:16	Seismic Ocean Bottom Receiver	at surface	42° 15,253' N	008° 03,432' E	0	0,2	185,9	50	25,1			
MSM71_32-1	22.02.18 07:31	Seismic Ocean Bottom Receiver	OBS on deck	42° 15,577' N	008° 03,521' E	0	0,2	310,1	44	26,2			
MSM71_33-1	22.02.18 07:37	Seismic Ocean Bottom Receiver	released	42° 15,582' N	008° 03,511' E	0	0,3	277,9	51	26,2			
MSM71_33-1	22.02.18 08:12	Seismic Ocean Bottom Receiver	at surface	42° 14,562' N	008° 08,742' E	0	0,3	144,6	45	23,9			
MSM71_33-1	22.02.18 08:25	Seismic Ocean Bottom Receiver	OBS on deck	42° 15,009' N	008° 08,812' E	0	0,6	281	39	24,9			
MSM71_34-1	22.02.18 08:36	Seismic Ocean Bottom Receiver	released	42° 15,156' N	008° 08,996' E	0	6,4	36,5	41	27,6			
MSM71_34-1	22.02.18 09:01	Seismic Ocean Bottom Receiver	at surface	42° 13,878' N	008° 13,983' E	0	0,1	55,8	39	21,6			
MSM71_34-1	22.02.18 09:12	Seismic Ocean Bottom Receiver	OBS on deck	42° 14,245' N	008° 14,127' E	0	0,7	174,4	43	21,4			
MSM71_35-1	22.02.18 09:19	Seismic Ocean Bottom Receiver	released	42° 14,238' N	008° 14,138' E	0	0,4	143,3	42	21,6			
MSM71_35-1	22.02.18 09:48	Seismic Ocean Bottom Receiver	at surface	42° 13,232' N	008° 19,336' E	0	0,1	320,6	31	18,3			
MSM71_35-1	22.02.18 09:58	Seismic Ocean Bottom Receiver	OBS on deck	42° 13,430' N	008° 19,361' E	0	0,4	153,8	30	19,1			
MSM71_36-1	22.02.18 10:02	Seismic Ocean Bottom Receiver	released	42° 13,414' N	008° 19,385' E	0	0,4	122,1	30	18,8			
MSM71_36-1	22.02.18 10:24	Seismic Ocean Bottom Receiver	at surface	42° 12,365' N	008° 24,224' E	0	9,6	101,3	21	17,8			
MSM71_36-1	22.02.18 10:34	Seismic Ocean Bottom Receiver	OBS on deck	42° 12,722' N	008° 24,744' E	0	0,4	173,2	24	16,2			
MSM71_37-1	22.02.18 11:03	Seismic Ocean Bottom Receiver	released	42° 11,852' N	008° 29,872' E	0	0,5	102,5	355	8,7			
MSM71_37-1	22.02.18 11:09	Seismic Ocean Bottom Receiver	at surface	42° 11,831' N	008° 29,958' E	0	0,6	95	356	13,5			
MSM71_37-1	22.02.18 11:16	Seismic Ocean Bottom Receiver	OBS on deck	42° 12,010' N	008° 30,053' E	0	0,3	80,5	357	10,7			
MSM71_81-1	22.02.18 14:16	Seismic Ocean Bottom Receiver	released	41° 44,163' N	008° 00,405' E	0	0,2	231,3	165	2,6			A431A
MSM71_81-1	22.02.18 14:52	Seismic Ocean Bottom Receiver	at surface	41° 42,390' N	007° 58,804' E	0	0,2	93,8	254	4,8			
MSM71_81-1	22.02.18 15:02	Seismic Ocean Bottom Receiver	OBS on deck	41° 42,496' N	007° 58,750' E	0	0,8	46,1	61	3,9			
MSM71_82-1	22.02.18 17:09	Seismic Ocean Bottom Receiver	released	41° 55,452' N	007° 33,513' E	0	0,4	214,9	36	28,8			A429A



## 'Maria S. Merian' MSM 71 (27.02. - 27.02.2018)



Activity	Date / Time	Device	Action	Position	Position	Depth	Speed	Course	Wind Direction	Wind Velocity	Winch	Rope Length	Comment
No.	No.	[UTC]			Lat	Lon	[m]	kn	°		m/s		m
MSM71_82-1	22.02.18 19:52	Seismic Ocean Bottom Receiver	at surface	41° 56,472' N	007° 30,809' E	0	0,3	0,4	36	31,2			
MSM71_82-1	22.02.18 20:07	Seismic Ocean Bottom Receiver	OBS on deck	41° 56,648' N	007° 30,520' E	0	1,8	203,7	30	27,5			
MSM71_83-1	23.02.18 00:15	Seismic Ocean Bottom Receiver	released	41° 56,633' N	006° 27,350' E	0	0	70,5	341	15,9			A422A
MSM71_83-1	23.02.18 01:37	Seismic Ocean Bottom Receiver	at surface	41° 56,414' N	006° 24,716' E	0	0,8	249,4	23	23,4			
MSM71_83-1	23.02.18 01:53	Seismic Ocean Bottom Receiver	OBS on deck	41° 56,319' N	006° 24,939' E	0	1,7	157,9	2	25,4			
MSM71_84-1	23.02.18 05:36	Seismic Ocean Bottom Receiver	released	41° 42,573' N	006° 57,810' E	0	0,9	286,4	8	22,7			A428A
MSM71_84-1	23.02.18 06:16	Seismic Ocean Bottom Receiver	at surface	41° 42,418' N	006° 57,674' E	0	0,1	266,6	27	19,1			
MSM71_84-1	23.02.18 06:25	Seismic Ocean Bottom Receiver	OBS on deck	41° 42,565' N	006° 57,527' E	0	1,2	152,1	19	22,4			
MSM71_84-1	23.02.18 06:25	Seismic Ocean Bottom Receiver	information	41° 42,565' N	006° 57,527' E	0	1,1	189,8	19	22,4			
MSM71_85-1	25.02.18 00:34	Geodesy Station	recording start	37° 32,388' N	015° 15,562' E	0	0,1	294,8	247	10,8			
MSM71_85-1	25.02.18 04:12	Geodesy Station	recording end	37° 31,796' N	015° 15,778' E	0	9,7	141,8	1	10,7			

Geräte-Einsätze		Gesamt:
Anzahl:	86	



'Maria S. Merian' MSM 71 (27.02. - 27.02.2018)





'Maria S. Merian' MSM 71 (27.02. - 27.02.2018)





'Maria S. Merian' MSM 71 (27.02. - 27.02.2018)





'Maria S. Merian' MSM 71 (27.02. - 27.02.2018)





'Maria S. Merian' MSM 71 (27.02. - 27.02.2018)





'Maria S. Merian' MSM 71 (27.02. - 27.02.2018)

INST.	LAT (N)	LON (E)	DEPLOY.	RECOV.	RECOV.	DEPTH	RELEASER CODE	ENABLE CODE	TIME RELEASE	ANT.	FREQ	RECORDER	REC.	CYLIND.	SKEW	SENSORS	Hydrophone
	D:M	D:M	DATE	DATE	TIME	(m)			UTC	CH.	MHz	NO.	NO.	NO.	(ms)		
DEPAS	1 A402A	42° 52.76	5° 18.03	20.06.17	16.02.18	02:29:00	1632	644421	656454	01.10.2018 09:00	C	160,725	6D6	61607097	87	Trillium 000155	984007
	2 A404A	42° 10.695	5° 01.156	20.06.17	15.02.18	18:29:00	2013	534037	516253	01.10.2018 10:30	C	160,725	6D6	61607095	80	Trillium 000141	984003
	3 A405A	42° 24.694	5° 18.219	16.06.17	15.02.18	21:34:00	2192	231104	213614	01.10.2018 13:00	C	160,725	6D6	61607086	Trim	Trillium 000151	700049
	4 A406A	42° 38.8	5° 51.4	22.06.17	-	-	2399	534224	516742	01.10.2018 08:30	B	159,480	6D6	61607098	78	Trillium 1608-218	583004
	5 A408A	43° 6.805	6° 57.820	18.06.17	-	-	2249	650727	670435	01.10.2018 19:00	C	160,725	6D6	61607096	Teiran	Trillium 000142	312180
	6 A409A	43° 20.891	7° 31.003	18.06.17	17.02.18	09:40:00	1981	650761	670544	01.10.2018 12:30	D	160,785	6D6	61607093	Till	Trillium 000139	700043
	7 A411A	43° 42.023	8° 39.070	19.06.17	19.02.18	08:01:00	2550	534123	516517	01.10.2018 16:30	A	159,585	MTS	050818	69	Güralp T4N61	-
	8 A412A	41° 38.855	4° 44.690	16.06.17	12.02.18	08:42:00	2519	231203	214047	01.10.2018 13:30	B	159,480	6D6	61607085	0912-139	Trillium 000152	700065
	9 A414A	42° 10.696	5° 51.499	15.06.17	15.02.18	12:46:00	2463	334750	336502	01.10.2018 14:30	D	160,785	6D6	61607088		Trillium 000122	700054
	10 A415A	42° 24.714	6° 24.656	15.06.17	16.02.18	12:37:00	2595	334735	336450	01.10.2018 15:00	C	160,725	6D6	61607087	Trubert	Trillium 000146	700047
	11 A417A	42° 52.777	7° 31.069	17.06.17	17.02.18	12:24:00	2677	445036	462304	01.10.2018 18:30	D	160,785	6D6	61607092	Tedrich	Trillium 000158	700053
	12 A418A	42° 59.995	8° 04.254	19.06.17	17.02.18	15:05:00	2632	533770	516131	01.10.2018 17:30	B	159,480	6D6	61607099	79	Trillium 000156	984004
	13 A420A	43° 27.224	9° 11.729	24.06.17	19.02.19	13:42:00	1354	534165	516633	01.10.2018 11:30	A	159,585	6D6	61607100	40	Trillium 000157	31201902
	14 A421A	41° 42.918	5° 50.998	17.06.17	15.02.18	09:59:00	2525	445717	464353	01.10.2018 14:00	B	159,480	6D6	63667089	Tarik	Trillium 000154	700042
	15 A423A	42° 10.704	6° 57.843	18.06.17	16.02.18	15:38:00	2706	430462	412606	01.10.2018 19:30	D	160,785	6D6	61607094	0912-137	Trillium 000144	700050
	16 A424A	42° 24.669	7° 30.920	18.06.17	16.02.18	22:34:00	2746	533736	516006	01.10.2018 08:00	D	160,785	MTS	050814	25	Güralp T4N26	-
	17 A426A	42° 52.805	8° 37.289	19.06.17	21.02.18	07:57:00	2564	533664	515660	01.10.2018 09:30	A	159,585	MTS	050808	6	Güralp T4N25	-
	18 A427A	43° 07.139	9° 11.680	19.06.17	19.02.18	15:53:00	1357	534071	516364	01.10.2018 10:00	C	160,725	MTS	050812	39	Güralp T4R07	-
	19 A428A	41° 42.614	6° 57.833	17.06.17	23.02.18	05:36:00	2734	446460	466147	01.10.2018 12:00	D	160,785	6D6	61607090	0912-138	Trillium 000143	700048
	20 A430A	42° 10.674	7° 58.855	17.06.17	16.02.18	19:51:00	2752	231056	213462	01.10.2018 20:00	D	160,785	6D6	61607091	Tohbert	Trillium 000138	700045
	21 A431A	41° 42.58	7° 58.831	17.06.17	22.02.18	14:16:00	2666	334773	336544	01.10.2018 15:30	C	160,725	MCS	060740	Tabby	Güralp 1205-005	700044
	22 A434A	43° 51.019	9° 13.792	24.06.17	19.02.18	11:14:00	1133	451241	471533	01.10.2018 17:00	D	160,785	6D6	61607067	34	Trillium 000153	984002
IPGP	1 A401A	42° 38.828	5° 01.145	21.06.17	16.02.18	00:01:00	1613.5			C	160,725	SIO				Trillium 240	
	2 A413A	41° 56.583	5° 18.213	22.06.17	15.02.18	15:41:00	2278			C	160,725	SIO				Trillium 240	
	3 A416A	42° 38.805	6° 57.807	25.06.17	17.02.18	01:54:00	2757			C	160,725	SIO				Trillium 240	
	4 A419A	43° 17.426	8° 36.053	23.06.17	19.02.18	04:08:00	2588			C	160,725	SIO				Trillium 240	
	5 A422A	41° 56.602	6° 24.607	22.06.17	23.02.18	00:15:00	2542.8			C	160,725	SIO				Trillium 240	
	6 A425A	42° 38.828	8° 4.218	23.06.17	21.01.18	03:40:00	2713			C	160,725	SIO				Trillium 240	
	7 A429A	41° 56.608	7° 31.004	23.06.17	22.02.18	17:09:00	2773			C	160,725	SIO				Trillium 240	

# OBS-Deployment

**MSM71 - LOBSTER** - Februar 2018 Profile R1

Station	Latitude	Longitude	Depth	Ch.	Freq./MHz	Release	Enable	Disable	Deployment date/time	Release date/time	Recorder	Hydrophone	Geophone				
OBH135	42.54928	N	5.50022	E	2257	C	160.725	431606	415711	415732	12.02.2018	16:19:00	23.02.2018	11:00	Geolog-014	HTI-43	
OBH134	42.54078	N	5.58887	E	2285	C	160.725	647077	664247	664264	12.02.2018	17:06:00	23.02.2018	11:20	Geolog-019	HTI-28	
OBH133	42.53160	N	5.67735	E	2366	B	159.480	450253	467130	467155	12.02.2018	19:03:00	23.02.2018	11:40	Geolog-001	OAS-46	
OBH132	42.52178	N	5.76640	E	2404	no antenna		427524	410310	410333	12.02.2018	19:55:00	23.02.2018	12:00	Geolog-003	HTI-37	
OBH131	42.51232	N	5.85482	E	2467	A	154.585	447756	466147	466164	12.02.2018	20:41:00	23.02.2018	12:20	Geolog-009	HTI-302	
OBH130	42.50517	N	5.94357	E	2492	D	160.785	133525	117432	117457	12.02.2018	21:23:00	23.02.2018	12:40	Geolog-002	HTI-81	
OBS129	42.49385	N	6.03187	E	2523	A	154.585	134071	120527	120542	12.02.2018	22:05:00	23.02.2018	13:00	Geolog-022	HTI-11	
OBH128	42.48410	N	6.12065	E	2531	D	160.785	646574	663316	663335	12.02.2018	22:44:00	23.02.2018	13:20	Geolog-004	HTI-113	
OBS127	42.47464	N	6.20923	E	2553	B	159.480	433477	417644	417667	12.02.2018	23:17:00	23.02.2018	13:40	Geolog-013	OAS-26	1001-113
OBH126	42.46477	N	6.29753	E	2560	A	154.585	451146	471277	471306	12.02.2018	23:57:00	23.02.2018	14:00	Geolog-021	HTI-32	
OBS125	42.45512	N	6.38588	E	2587	D	160.785	450215	467007	467024	13.02.2018	0:30:00	23.02.2018	14:20	Geolog-017	OAS-44	Owen-0509-072
OBH124	42.44513	N	6.47473	E	2594	B	159.480	433622	420225	420263	13.02.2018	1:00:00	23.02.2018	14:40	Geolog-016	HTI-102	
OBS123	42.43587	N	6.56285	E	2622	D	160.785	647031	664125	664140	13.02.2018	1:31:00	23.02.2018	15:00	Geolog-012	OAS-27	Owen-0205-026
OBH122	42.42537	N	6.65112	E	2631	C	160.725	430135	411537	411552	13.02.2018	2:06:00	23.02.2018	15:20	Geolog-008	HTI-119	
OBS121	42.41525	N	6.73960	E	2915	D	160.785	451207	471707	471427	13.02.2018	2:39:00	23.02.2018	15:40	Geolog-010	OAS-11	0309-046
OBH120	42.40502	N	6.82765	E	2660	C	160.725	427623	410540	410563	13.02.2018	3:17:00	23.02.2018	16:00	Geolog-020	HTI-26	
OBS119	42.39520	N	6.91582	E	2668	D	160.785	435610	440126	440143	13.02.2018	3:48:00	23.02.2018	16:40	Geolog-011	HTI-58	Owen-0708-101
OBS118	42.38452	N	7.00412	E	2675	B	159.480	133770	120263	120312	13.02.2018	4:20:00	23.02.2018	17:00	Geolog-005	HTI-90	Owen-0807-102
OBS117	42.37448	N	7.09180	E	2708	D	160.785	647125	664370	664417	13.02.2018	4:54:00	23.02.2018	17:20	Geolog-015	HTI-73	Owen-0708-099
OBS116	42.36363	N	7.18095	E	2709	B	159.480	433166	416704	416727	13.02.2018	5:27:00	23.02.2018	17:40	Geolog-018	HTI-984005	Owen-1205-126
OBS115	42.35328	N	7.26853	E	2724	A	154.585	447503	465324	465341	13.02.2018	5:58:00	23.02.2018	18:00	6D6-61607128	HTI-39	Owen-0403-057
OBS114	42.34265	N	7.35702	E	2967	A	154.585	444674	461737	461752	13.02.2018	6:25:00	23.02.2018	18:20	?6D6-61067127	HTI-27	Owen-1001-119
OBS113	42.33203	N	7.44492	E	2973	D	160.785	427737	411005	411026	13.02.2018	6:54:00	23.02.2018	18:40	6D6-61607124	HTI-984006	Owen-0807-097
OBS112	42.32135	N	7.53290	E	2737	D	160.785	250177	237153	237170	13.02.2018	7:23:00	23.02.2018	19:00	6D6-61607126	HTI-33	Owen-1205-131
OBS111	42.31027	N	7.62143	E	2740	D	160.785	433227	417037	417052	13.02.2018	7:53:00	23.02.2018	19:20	6D6-61607123	HTI-47	Owen-0509-076
OBS110	42.30010	N	7.70892	E	2978	B	159.480	430424	412470	412501	13.02.2018	8:25:00	23.02.2018	19:40	6D6-61607122	HTI-84	Owen-0510-078
OBS109	42.28903	N	7.79737	E	2740	B	159.480	427260	407463	407512	13.02.2018	8:56:00	23.02.2018	20:00	6D6-61607125	HTI-68	Owen-1609-128
OBS108	42.27825	N	7.88498	E	2732	A	154.585	145331	160061	160110	13.02.2018	9:24:00	23.02.2018	20:20	6D6-61607118	HTI-53	Owen-0205-031
OBS107	42.26758	N	7.97237	E	2732	A	154.585	427430	410051	410072	13.02.2018	9:52:00	23.02.2018	20:40	6D6-61607117	HTI-984009	Owen-0403-054
OBS106	42.25620	N	8.06038	E	2726	D	160.785	442205	440755	440776	13.02.2018	10:23:00	23.02.2018	21:00	6D6-61607119	HTI-50	Owen-0307-210
OBS105	42.24513	N	8.14852	E	2714	B	159.480	433375	417411	417432	13.02.2018	10:51:00	23.02.2018	21:20	6D6-61607120	HTI-40	Owen-0701-086
OBS104	42.23415	N	8.23650	E	2654	C	160.725	450445	467632	467657	13.02.2018	11:21:00	23.02.2018	21:40	6D6-61607116	HTI-46	Owen-1205-132
OBS103	42.22280	N	8.32440	E	2500	no antenna		143272	141117	141134	13.02.2018	11:49:00	23.02.2018	22:00	6D6-61607115	HTI-111	Owen-1205-125
OBS102	42.21162	N	8.41232	E	1954	C	160.725	450742	470567	470605	13.02.2018	12:17:00	23.02.2018	22:20	6D6-61607114	HTI-67	Owen-1205-129
OBS101	42.20010	N	8.50030	E	609	no antenna		646532	663160	663202	13.02.2018	12:48:00	23.02.2018	22:40	6D6-61607113	HTI-48	Owen-1609-131

**OBS-Deployment**

MSM71 - LOBSTER - Februar 2018

Profile R2

Station	Latitude	Longitude	Depth	Ch.	Freq./MHz	Release	Enable	Disable	Deployment date/time	Release date/time	Recorder	Hydrophone	Geophone				
OBS201	42.35038	N	7.25015	E	2720	D	160.785	427737	411005	411026	20.02.2018	3:07:00	23.02.18	18:40	Geolog-014	HTI-43	Owen-0807-097
OBS202	42.40247	N	7.31748	E	2721	A	154.585	444674	461737	461752	20.02.2018	2:36:00	23.02.18	18:20	Geolog-004	???-102	Owen-1001-119
OBS203	42.45548	N	7.38443	E	2960	A	154.585	447503	465324	465341	20.02.2018	2:03:00	23.02.18	18:00	Geolog-003	HTI-37	Owen-0403-057
OBH204	42.50810	N	7.45120	E	2725	B	159.480	450253	467130	467155	20.02.2018	1:34:00	23.02.18	11:40	Geolog-002	HTI-81	
OBS205	42.56087	N	7.51852	E	2722	B	159.480	433166	416704	416727	20.02.2018	1:04:00	23.02.18	17:40	Geolog-018	HTI-984005	Owen-1205-126
OBS206	42.61358	N	7.58588	E	2715	D	160.785	647125	664370	664417	20.02.2018	0:32:00	23.02.18	17:20	Geolog-015	HTI-73	Owen-0708-099
OBS207	42.66598	N	7.65343	E	2707	B	159.480	133770	120263	120312	20.02.2018	0:01:00	23.02.18	17:00	Geolog-005	HTI-90	Owen-0807-102
OBH208	42.71828	N	7.72128	E	2700	C	160.725	447756	466147	466164	19.02.2018	23:30:00	23.02.18	12:20	Geolog-009	HTI-302	
OBS209	42.77118	N	7.78852	E	2693	A	154.585	134071	120527	120542	19.02.2018	22:56:00	23.02.18	13:00	Geolog-022	HTI-11	Owen-1001-117
OBS210	42.82350	N	7.85648	E	2683	D	160.785	435610	440126	440143	19.02.2018	22:26:00	23.02.18	16:40	Geolog-011	HTI-58	Owen-0708-101
OBS211	42.87587	N	7.92435	E	2670	D	160.785	451207	471404	471427	19.02.2018	21:55:00	23.02.18	15:40	Geolog-010	OAS-11	Owen-0309-046
OBH212	42.92810	N	7.99233	E	2647	D	160.785	133525	117432	117457	19.02.2018	21:21:00	23.02.18	12:40	Geolog-001	OAS-46	
OBS213	42.98022	N	8.06098	E	2627	D	160.785	647031	664125	664140	19.02.2018	20:50:00	23.02.18	15:00	Geolog-012	OAS-27	Owen-0209-026
OBS214	43.03245	N	8.12583	E	2606	D	160.785	450215	467007	467024	19.02.2018	20:19:00	23.02.18	14:20	Geolog-017	OAS-44	Owen-0509-072
OBS215	43.08417	N	8.19672	E	2586	B	159.480	433477	417644	417667	19.02.2018	19:45:00	23.02.18	13:40	Geolog-013	OAS-26	Owen-1001-113

### **GEOMAR Reports**

No.	Title
1	FS POSEIDON Fahrtbericht / Cruise Report POS421, 08. – 18.11.2011, Kiel - Las Palmas, Ed.: T.J. Müller, 26 pp, DOI: 10.3289/GEOMAR_REP_NS_1_2012
2	Nitrous Oxide Time Series Measurements off Peru – A Collaboration between SFB 754 and IMARPE -, Annual Report 2011, Eds.: Baustian, T., M. Graco, H.W. Bange, G. Flores, J. Ledesma, M. Sarmiento, V. Leon, C. Robles, O. Moron, 20 pp, DOI: 10.3289/GEOMAR_REP_NS_2_2012
3	FS POSEIDON Fahrtbericht / Cruise Report POS427 – Fluid emissions from mud volcanoes, cold seeps and fluid circulation at the Don- _Kuban deep sea fan (Kerch peninsula, Crimea, Black Sea) – 23.02. – 19.03.2012, Burgas, Bulgaria - Heraklion, Greece, Ed.: J. Bialas, 32 pp, DOI: 10.3289/GEOMAR_REP_NS_3_2012
4	RV CELTIC EXPLORER EUROFLEETS Cruise Report, CE12010 – ECO2@NorthSea, 20.07. – 06.08.2012, Bremerhaven – Hamburg, Eds.: P. Linke et al., 65 pp, DOI: 10.3289/GEOMAR_REP_NS_4_2012
5	RV PELAGIA Fahrtbericht / Cruise Report 64PE350/64PE351 – JEDDAH-TRANSECT -, 08.03. – 05.04.2012, Jeddah – Jeddah, 06.04 - 22.04.2012, Jeddah – Duba, Eds.: M. Schmidt, R. Al-Farawati, A. Al-Aidaroos, B. Kürten and the shipboard scientific party, 154 pp, DOI: 10.3289/GEOMAR_REP_NS_5_2013
6	RV SONNE Fahrtbericht / Cruise Report SO225 - MANIHIKI II Leg 2 The Manihiki Plateau - Origin, Structure and Effects of Oceanic Plateaus and Pleistocene Dynamic of the West Pacific Warm Water Pool, 19.11.2012 - 06.01.2013 Suva / Fiji – Auckland / New Zealand, Eds.: R. Werner, D. Nürnberg, and F. Hauff and the shipboard scientific party, 176 pp, DOI: 10.3289/GEOMAR_REP_NS_6_2013
7	RV SONNE Fahrtbericht / Cruise Report SO226 – CHRIMP CHatham RIse Methane Pockmarks, 07.01. - 06.02.2013 / Auckland – Lyttleton & 07.02. – 01.03.2013 / Lyttleton – Wellington, Eds.: Jörg Bialas / Ingo Klaucke / Jasmin Mögeltönder, 126 pp, DOI: 10.3289/GEOMAR_REP_NS_7_2013
8	The SUGAR Toolbox - A library of numerical algorithms and data for modelling of gas hydrate systems and marine environments, Eds.: Elke Kossel, Nikolaus Bigalke, Elena Piñero, Matthias Haeckel, 168 pp, DOI: 10.3289/GEOMAR_REP_NS_8_2013
9	RV ALKOR Fahrtbericht / Cruise Report AL412, 22.03.-08.04.2013, Kiel – Kiel. Eds: Peter Linke and the shipboard scientific party, 38 pp, DOI: 10.3289/GEOMAR_REP_NS_9_2013
10	Literaturrecherche, Aus- und Bewertung der Datenbasis zur Meerforelle ( <i>Salmo trutta trutta</i> L.) Grundlage für ein Projekt zur Optimierung des Meerforellenmanagements in Schleswig-Holstein. Eds.: Christoph Petereit, Thorsten Reusch, Jan Dierking, Albrecht Hahn, 158 pp, DOI: 10.3289/GEOMAR_REP_NS_10_2013
11	RV SONNE Fahrtbericht / Cruise Report SO227 TAIFLUX, 02.04. – 02.05.2013, Kaohsiung – Kaohsiung (Taiwan), Christian Berndt, 105 pp, DOI: 10.3289/GEOMAR_REP_NS_11_2013
12	RV SONNE Fahrtbericht / Cruise Report SO218 SHIVA (Stratospheric Ozone: Halogens in a Varying Atmosphere), 15.-29.11.2011, Singapore - Manila, Philippines, Part 1: SO218- SHIVA Summary Report (in German), Part 2: SO218- SHIVA English reports of participating groups, Eds.: Birgit Quack & Kirstin Krüger, 119 pp, DOI: 10.3289/GEOMAR_REP_NS_12_2013
13	KIEL276 Time Series Data from Moored Current Meters. Madeira Abyssal Plain, 33°N, 22°W, 5285 m water depth, March 1980 – April 2011. Background Information and Data Compilation. Eds.: Thomas J. Müller and Joanna J. Waniek, 239 pp, DOI: 10.3289/GEOMAR_REP_NS_13_2013

### GEOMAR Reports

No.	Title
14	RV POSEIDON Fahrtbericht / Cruise Report POS457: ICELAND HAZARDS Volcanic Risks from Iceland and Climate Change: The Late Quaternary to Anthropogene Development Reykjavík / Iceland – Galway / Ireland, 7.-22. August 2013. Eds.: Reinhard Werner, Dirk Nürnberg and the shipboard scientific party, 88 pp, DOI: 10.3289/GEOMAR_REP_NS_14_2014
15	RV MARIA S. MERIAN Fahrtbericht / Cruise Report MSM-34 / 1 & 2, SUGAR Site, Varna – Varna, 06.12.13 – 16.01.14. Eds: Jörg Bialas, Ingo Klaucke, Matthias Haeckel, 111 pp, DOI: 10.3289/GEOMAR_REP_NS_15_2014
16	RV POSEIDON Fahrtbericht / Cruise Report POS 442, "AUVinTYS" High-resolution geological investigations of hydrothermal sites in the Tyrrhenian Sea using the AUV "Abyss", 31.10. – 09.11.12, Messina – Messina, Ed.: Sven Petersen, 32 pp, DOI: 10.3289/GEOMAR_REP_NS_16_2014
17	RV SONNE, Fahrtbericht / Cruise Report, SO 234/1, "SPACES": Science or the Assessment of Complex Earth System Processes, 22.06. – 06.07.2014, Walvis Bay / Namibia - Durban / South Africa, Eds.: Reinhard Werner and Hans-Joachim Wagner and the shipbord scientific party, 44 pp, DOI: 10.3289/GEOMAR_REP_NS_17_2014
18	RV POSEIDON Fahrtbericht / Cruise Report POS 453 & 458, "COMM3D", Crustal Structure and Ocean Mixing observed with 3D Seismic Measurements, 20.05. – 12.06.2013 (POS453), Galway, Ireland – Vigo, Portugal, 24.09. – 17.10.2013 (POS458), Vigo, Portugal – Vigo, Portugal, Eds.: Cord Papenberg and Dirk Klaeschen, 66 pp, DOI: 10.3289/GEOMAR_REP_NS_18_2014
19	RV POSEIDON, Fahrtbericht / Cruise Report, POS469, "PANAREA", 02. – 22.05.2014, (Bari, Italy – Malaga, Spain) & Panarea shallow-water diving campaign, 10. – 19.05.2014, Ed.: Peter Linke, 55 pp, DOI: 10.3289/GEOMAR_REP_NS_19_2014
20	RV SONNE Fahrtbericht / Cruise Report SO234-2, 08.-20.07.2014, Durban, -South Africa - Port Louis, Mauritius, Eds.: Kirstin Krüger, Birgit Quack and Christa Marandino, 95 pp, DOI: 10.3289/GEOMAR_REP_NS_20_2014
21	RV SONNE Fahrtbericht / Cruise Report SO235, 23.07.-07.08.2014, Port Louis, Mauritius to Malé, Maldives, Eds.: Kirstin Krüger, Birgit Quack and Christa Marandino, 76 pp, DOI: 10.3289/GEOMAR_REP_NS_21_2014
22	RV SONNE Fahrtbericht / Cruise Report SO233 WALVIS II, 14.05-21.06.2014, Cape Town, South Africa - Walvis Bay, Namibia, Eds.: Kaj Hoernle, Reinhard Werner, and Carsten Lüter, 153 pp, DOI: 10.3289/GEOMAR_REP_NS_22_2014
23	RV SONNE Fahrtbericht / Cruise Report SO237 Vema-TRANSIT Bathymetry of the Vema-Fracture Zone and Puerto Rico TRench and Abyssal AtlaNtic BiodiverSITY Study, Las Palmas (Spain) - Santo Domingo (Dom. Rep.) 14.12.14 - 26.01.15, Ed.: Colin W. Devey, 130 pp, DOI: 10.3289/GEOMAR_REP_NS_23_2015
24	RV POSEIDON Fahrtbericht / Cruise Report POS430, POS440, POS460 & POS467 Seismic Hazards to the Southwest of Portugal; POS430 - La-Seyne-sur-Mer - Portimao (7.4. - 14.4.2012), POS440 - Lisbon - Faro (12.10. - 19.10.2012), POS460 - Funchal - Portimao (5.10. - 14.10.2013), POS467 - Funchal - Portimao (21.3. - 27.3.2014), Ed.: Ingo Grevemeyer, 43 pp, DOI: 10.3289/GEOMAR_REP_NS_24_2015
25	RV SONNE Fahrtbericht / Cruise Report SO239, EcoResponse Assessing the Ecology, Connectivity and Resilience of Polymetallic Nodule Field Systems, Balboa (Panama) – Manzanillo (Mexico), 11.03. -30.04.2015, Eds.: Pedro Martínez Arbizu and Matthias Haeckel, 204 pp, DOI: 10.3289/GEOMAR_REP_NS_25_2015

### GEOMAR Reports

- | <b>No.</b> | <b>Title</b>   |
|------------|--|
| 26         | RV SONNE Fahrtbericht / Cruise Report SO242-1, JPI OCEANS Ecological Aspects of Deep-Sea Mining, DISCOL Revisited, Guayaquil - Guayaquil (Ecuador), 29.07.-25.08.2015, Ed.: Jens Greinert, 290 pp, DOI: 10.3289/GEOMAR_REP_NS_26_2015  |
| 27         | RV SONNE Fahrtbericht / Cruise Report SO242-2, JPI OCEANS Ecological Aspects of Deep-Sea Mining DISCOL Revisited, Guayaquil - Guayaquil (Ecuador), 28.08.-01.10.2015, Ed.: Antje Boetius, 552 pp, DOI: 10.3289/GEOMAR_REP_NS_27_2015   |
| 28         | RV POSEIDON Fahrtbericht / Cruise Report POS493, AUV DEDAVE Test Cruise, Las Palmas - Las Palmas (Spain), 26.01.-01.02.2016, Ed.: Klas Lackschewitz, 17 pp, DOI: 10.3289/GEOMAR_REP_NS_28_2016   |
| 29         | Integrated German Indian Ocean Study (IGIOS) - From the seafloor to the atmosphere - A possible German contribution to the International Indian Ocean Expedition 2 (IIOE-2) programme – A Science Prospectus, Eds.: Bange, H.W. , E.P. Achterberg, W. Bach, C. Beier, C. Berndt, A. Biastoch, G. Bohrmann, R. Czeschel, M. Dengler, B. Gaye, K. Haase, H. Herrmann, J. Lelieveld, M. Mohtadi, T. Rixen, R. Schneider, U. Schwarz-Schampera, J. Segschneider, M. Visbeck, M. Voß, and J. Williams, 77pp, DOI: 10.3289/GEOMAR_REP_NS_29_2016 |
| 30         | RV SONNE Fahrtbericht / Cruise Report SO249, BERING – Origin and Evolution of the Bering Sea: An Integrated Geochronological, Volcanological, Petrological and Geochemical Approach, Leg 1: Dutch Harbor (U.S.A.) - Petropavlovsk-Kamchatsky (Russia), 05.06.2016-15.07.2016, Leg 2: Petropavlovsk-Kamchatsky (Russia) - Tomakomai (Japan), 16.07.2016-14.08.2016, Eds.: Reinhard Werner, et al., DOI: 10.3289/GEOMAR_REP_NS_30_2016   |
| 31         | RV POSEIDON Fahrtbericht/ Cruise Report POS494/2, HIERROSEIS Leg 2: Assessment of the Ongoing Magmatic-Hydrothermal Discharge of the El Hierro Submarine Volcano, Canary Islands by the Submersible JAGO, Valverde – Las Palmas (Spain), 07.02.-15.02.2016, Eds.: Hannington, M.D. and Shipboard Scientific Party, DOI: 10.3289/GEOMAR_REP_NS_31_2016  |
| 32         | RV METEOR Fahrtbericht/ Cruise Report M127, Extended Version, Metal fluxes and Resource Potential at the Slow-spreading TAG Mid-ocean Ridge Segment (26°N, MAR) – Blue Mining@Sea, Bridgetown (Barbados) – Ponta Delgada (Portugal) 25.05.-28.06.2016, Eds.: Petersen, S. and Shipboard Scientific Party, DOI: 10.3289/GEOMAR_REP_NS_32_2016   |
| 33         | RV SONNE Fahrtbericht/Cruise Report SO244/1, GeoSEA: Geodetic Earthquake Observatory on the Seafloor, Antofagasta (Chile) – Antofagasta (Chile), 31.10.-24.11.2015, Eds.: Jan Behrmann, Ingo Klaucke, Michal Stipp, Jacob Geersen and Scientific Crew SO244/1, DOI: 10.3289/GEOMAR_REP_NS_33_2016  |
| 34         | RV SONNE Fahrtbericht/Cruise Report SO244/2, GeoSEA: Geodetic Earthquake Observatory on the Seafloor, Antofagasta (Chile) – Antofagasta (Chile), 27.11.-13.12.2015, Eds.: Heidrun Kopp, Dietrich Lange, Katrin Hannemann, Anne Krabbenhoeft, Florian Petersen, Anina Timmermann and Scientific Crew SO244/2, DOI: 10.3289/GEOMAR_REP_NS_34_2016  |
| 35         | RV SONNE Fahrtbericht/Cruise Report SO255, VITIAZ – The Life Cycle of the Vitiaz-Kermadec Arc / Backarc System: from Arc Initiation to Splitting and Backarc Basin Formation, Auckland (New Zealand) - Auckland (New Zealand), 02.03.-14.04.2017, Eds.: Kaj Hoernle, Folkmar Hauff, and Reinhard Werner with contributions from cruise participants, DOI: 10.3289/GEOMAR_REP_NS_35_2017  |

### GEOMAR Reports

No.	Title
36	RV POSEIDON Fahrtbericht/Cruise Report POS515, CALVADOS - CALabrian arc mud VolcAnoes: Deep Origin and internal Structure, Dubrovnik (Croatia) – Catania (Italy), 18.06.-13.07.2017, Eds.: M. Riedel, J. Bialas, A. Krabbenhoeft, V. Bähre, F. Beeck, O. Candoni, M. Kühn, S. Muff, J. Rindfleisch, N. Stange, DOI: 10.3289/GEOMAR_REPORT_NS_36_2017
37	RV MARIA S. MERIAN Fahrtbericht/Cruise Report MSM63, PERMO, Southampton – Southampton (U.K.), 29.04.-25.05.2017, Eds.: Christian Berndt and Judith Elger with contributions from cruise participants C. Böttner, R. Gehrmann, J. Karstens, S. Muff, B. Pitcairn, B. Schramm, A. Lichtschlag, A.-M. Völsch, DOI: 10.3289/GEOMAR_REPORT_NS_37_2017
38	RV SONNE Fahrtbericht/Cruise Report SO258/1, INGON: The Indian - Antarctic Break-up Engima, Fremantle (Australia) - Colombo (Sri Lanka), 07.06.-09.07.2017, 29.04.-25.05.2017, Eds.: Reinhard Werner, Hans-Joachim Wagner, and Folkmar Hauff with contributions from cruise participants, DOI: 10.3289/GEOMAR_REPORT_NS_38_2017
39	RV POSEIDON Fahrtbericht/Cruise Report POS509, ElectroPal 2: Geophysical investigations of sediment hosted massive sulfide deposits on the Palinuro Volcanic Complex in the Tyrrhenian Sea, Malaga (Spain) – Catania (Italy), 15.02.-03.03.2017, Ed.: Sebastian Hölz, DOI: 10.3289/GEOMAR_REPORT_NS_39_2017
40	RV POSEIDON Fahrtbericht/Cruise Report POS518, Baseline Study for the Environmental Monitoring of Subseafloor CO <sub>2</sub> Storage Operations, Leg 1: Bremerhaven – Bremerhaven (Germany), 25.09.-11.10.2017, Leg 2: Bremerhaven – Kiel (Germany), 12.10.-28.10.2017, Eds.: Peter Linke and Matthias Haeckel, DOI: 10.3289/GEOMAR_REPORT_NS_40_2018
41	RV MARIA S. MERIAN Fahrtbericht/Cruise Report MSM71, LOBSTER: Ligurian Ocean Bottom Seismology and Tectonics Research, Las Palmas (Spain) – Heraklion (Greece), 07.02.-27.02.2018, Eds.: H. Kopp, D. Lange, M. Thorwart, A. Paul, A. Dannowski, F. Petersen, C. Aubert, F. Beek, A. Beniest, S. Besançon, A. Brotzer, G. Caielli, W. Crawford, M. Deen, C. Lehmann, K. Marquardt, M. Neckel, L. Papanagnou, B. Schramm, P. Schröder, K.-P. Steffen, F. Wolf, Y. Xia, DOI: 10.3289/GEOMAR_REPORT_NS_41_2018

For GEOMAR Reports, please visit:

[https://oceanrep.geomar.de/view/series/GEOMAR\\_Report.html](https://oceanrep.geomar.de/view/series/GEOMAR_Report.html)

Reports of the former IFM-GEOMAR series can be found under:

[https://oceanrep.geomar.de/view/series/IFM-GEOMAR\\_Report.html](https://oceanrep.geomar.de/view/series/IFM-GEOMAR_Report.html)

Das GEOMAR Helmholtz-Zentrum für Ozeanforschung Kiel  
ist Mitglied der Helmholtz-Gemeinschaft  
Deutscher Forschungszentren e.V.

The GEOMAR Helmholtz Centre for Ocean Research Kiel  
is a member of the Helmholtz Association of  
German Research Centres

**Helmholtz-Zentrum für Ozeanforschung Kiel / Helmholtz Centre for Ocean Research Kiel**  
GEOMAR  
Dienstgebäude Westufer / West Shore Building  
Düsternbrooker Weg 20  
D-24105 Kiel  
Germany

**Helmholtz-Zentrum für Ozeanforschung Kiel / Helmholtz Centre for Ocean Research Kiel**  
GEOMAR  
Dienstgebäude Ostufer / East Shore Building  
Wischhofstr. 1-3  
D-24148 Kiel  
Germany

Tel.: +49 431 600-0  
Fax: +49 431 600-2805  
[www.geomar.de](http://www.geomar.de)